Doctoral Dissertation

Dynamics for Epitaxial Growth Model under Dirichlet Conditions

By

SOMAYYEH AZIZI

Department of Applied Physics

Quantum Engineering Design Course

Graduate School of Engineering

Osaka University

December 2015

Preface

This dissertation is devoted to studying the dynamics of crystal surface grown by molecular beam epitaxy from the aspect of theoretical understanding of its mechanism. The molecular beam epitaxy (MBE) is regarded as one of useful techniques that enable us to grow structures with very high precision in the vertical direction in spite of difficulty of controlling instability of growing surface caused from roughening tendency that it naturally possesses.

We will use a nonlinear diffusion model which has been presented by Johnson-Orme-Hunt-Graff-Sudijono-Sauder-Orr in 1994 to describe the growing process of crystal surface by MBE. The model equation is a fourth order parabolic equation containing two terms describing surface diffusion and roughening effect caused from the Schwoebel barrier. Equipping the homogeneous Dirichlet boundary conditions, we study the model equation analytically and numerically. After proving global existing of solutions, we construct a dynamical system and show that the dynamical system possesses a Lyapunov function, i.e., a real valued function whose values decreases monotonously along any trajectory. Furthermore, using the Lyapunov function, it is proved that every trajectory converges asymptotically to a stationary state which is a critical point of the Lyapunov function and in which the roughening effect is completely balanced with the surface diffusion. Finally, stability of the flat surface is investigated. It is indeed shown that, if the roughening coefficient is suitably smaller than the coefficient of surface diffusion, then the flat state is stable; meanwhile, if it is contrary, then the flat state becomes unstable. It is also shown that slenderness of the substrate domain enhances flatting effect of the surface against roughening.

In order to study profiles of solutions, we perform numerical computations. We are mainly interested in stationary solutions to which every trajectory converges. It is observed that all non-flat stationary states have a number of ridges. It is also observed that, as the roughening coefficient increases, the number of columns of ridges increase and similarly the number of ridges in a column increase.

Contents

Listing of Figures

1

Introduction

Molecular beam epitaxy (MBE) is one of useful techniques that enable us to grow structures with very high precision in the vertical direction, such as monolayer-thin interfaces or atomically flat surfaces. But there still remains the major challenge of growing surfaces which are structured laterally. A theoretical contribution in order to control the unstable growth may then lie in understanding its basic mechanisms.

In the present study, we are concerned with the initial-boundary value problem for a nonlinear parabolic equation of fourth order

$$\begin{cases} \dfrac{\partial u}{\partial t} = -a\Delta^2 u - \mu\nabla\cdot\left[\dfrac{\nabla u}{1+|\nabla u|^2}\right] & \text{in } \Omega\times(0,\infty), \\ u = \dfrac{\partial u}{\partial n} = 0 & \text{on } \partial\Omega\times(0,\infty), \\ u(x,y,0) = u_0(x,y) & \text{in } \Omega, \end{cases} \tag{1.1}$$

in a two-dimensional bounded domain $\Omega \subset R^2$, Ω being a substrate domain. We assume that Ω is convex or of $\mathcal{C}^2$class. Such a problem has been presented by Johonson-Orme-Hunt-Graff-Sudijono-Sauder-Orr [8], in order to describe the process of growing crystal surface under MBE. Here, $u = u(x,y,t)$ denotes a height of surface at position $(x,y) \in \Omega$ and at time t. The term $-a\Delta^2 u$ in the equation of (1.1) denotes a surface diffusion which is caused by the difference of the chemical potential which is proportional to the curvature of the surface. Therefore, the adatoms have a tendency to migrate from the positions of large curvature to those of small one. In the meantime, the term $-\mu\nabla.\left[\frac{\nabla u}{1+|\nabla u|^2}\right]$ denotes the effect of surface roughening, μ being a positive constant called the surface roughening coefficient. Such roughening is caused by the Schwoebel barrier. In Chapter 2, we shall review the two effects, surface diffusion and roughening, together with somewhat detailed derivations of the forth-order parabolic equation in (1.1).

To solve the parabolic equation, it is naturally necessary to impose suitable boundary conditions on the unknown function $u(x,y,t)$. In this study, we choose the homogeneous Dirichlet boundary conditions on $\partial\Omega$ which mean that we assume that the surface height is always

controlled at a constant level, $u = 0$, on $\partial\Omega$ together with vanishing normal derivatives, $\frac{\partial u}{\partial n} = 0$.

In the papers Fujimura et al. [4,5,6], Neumann like boundary conditions $\frac{\partial}{\partial n}\Delta u = 0$ were assumed by some mathematical reasons. But it seems very difficult to give any physical meaning to such boundary conditions.

We shall study the problem (1.1) analytically and numerically. After constructing a global solution to (1.1) for any initial state $u_0(x, y)$, we construct a dynamical system generated by the problem in the Hilbert space $L_2(\Omega)$. We then show that the dynamical system has a Lyapunov function $\Phi(u)$, namely, a real valued function defined for all state functions $u(x, y)$ whose values decline monotonously as $t \to \infty$ for any trajectory. So, the function plays a role of dynamical energy such that the trajectory proceeds every time to a direction in which the energy decreases. And a state $\bar{u}(x, y)$ is stationary if and only if $\bar{u}(x, y)$ is a critical value of the function, i.e., $\Phi'(\bar{u}) = 0$. On account of this function, we can furthermore prove that every trajectory $u(x, y, t)$ converges as $t \to \infty$ to a stationary state $\bar{u}(x, y)$. Clearly, $\bar{u}(x, y)$ satisfies $\Phi'(\bar{u}) = 0$ and $a\Delta^2\bar{u} = -\mu\nabla \cdot \left[\frac{\nabla\bar{u}}{1+|\nabla\bar{u}|^2}\right]$, and so $\bar{u}(x, y)$ is a state that the roughening is balanced against a surface diffusion. Analytical study is finally devoted to investigating stability of the stationary state $\bar{u}(x, y) \equiv 0$, the completely flat surface. In fact, we can show that there exists a crucial constant C such that, if $a > C\mu$, then the flat state is stable, meanwhile if $a < C\mu$, then the roughening becomes a dominator and destabilizes the flat growing surface. Furthermore, C is seen to be estimated by the band length of the substrate domain Ω. Slenderer is Ω, smaller is C, that is, slenderness of Ω can enhance flatting effect of the surface against roughening.

Under those analytical results, we shall investigate profiles of solutions by numerical methods. As the equation is of fourth order, any usual scheme is not readily available. We must build up some scheme for fourth order parabolic equation which adapts to the homogeneous Dirichlet boundary conditions. We are mainly interested in the question of how profiles of stationary state change as the roughening coefficient μ increases. Indeed, it is observed that all non-flat stationary solutions have a number of ridges. As μ increases, the number of columns of ridges increases. Similarly, the number of ridge in a column also increases. We perform numerical computations in rectangular domains Ω whose areas are fixed, say, as 1, starting with an initial state of slight perturbation of $u_0 \equiv 0$. When Ω is square, the trajectory converges to a non-flat stationary state, but when Ω is slender enough, the trajectory goes back to the flat state. The critical value of C (i.e., $a < C\mu$) agrees well to the analytically expected one.

The remainder of this thesis is separated into 5 chapters. The summery of description and details

of mathematical models that lead to construct of equation (1.1) is given in chapter 2. The construct of dynamical system and also the Lyapunov function of the dynamical system are express in third chapter. The fourth chapter is devoted to showing longtime convergence of trajectories to some stationary solution of problem. The fifth chapter is related to prove stability and instability of the null solution under Dirichlet boundary condition which is a unique homogeneous stationary solution. Indeed, we shall prove that, when surface diffusion effects are stronger than roughening effects then, the null solution is globally stable, and in the meantime, when the roughening effects are stronger than surface diffusion effects, the null solution is unstable. Finally the numerical results for the problem of (1.1) based on finite difference scheme are given in the last chapter.

2

Mathematical Models of Epitaxial Growth

In this chapter we introduce the mathematical models of main physical effects for describing the process of growing crystal surface under MBE. These physical effects are surface diffusion and roughening.

2.1 MOLECULAR BEAM EPITAXY

Molecular beam epitaxy is a technique for epitaxial growth via the interaction of one or several molecular or atomic beams that occurs on a surface of a heated crystalline substrate. Epitaxial growth deposition grows a single crystal film over a substrate by rearranging the atoms on top of the substrate and also can be categorized as either homoepitaxial or heteroepitaxial depending on the type of material grown on the substrate. A homoepitaxial growth has a film of the same material as the substrate (i.e., Si on Si growth). A heteroepitaxial growth, on the other hand, has a film of different material than the substrate (i.e., AlAs on GaAs or GaAs on Si growth). This property of heteroepitaxy is used as an advantage on optoelectronic and band gap engineering applications. Using beam epitaxy, it is possible to grow structures with very high precision in the vertical direction, such as monolayer- thin interface or atomically flat surfaces. After irradiation, crystal surface will grow in some function of *t*. Figure 2.1.1 shows the mechanism of MBE.

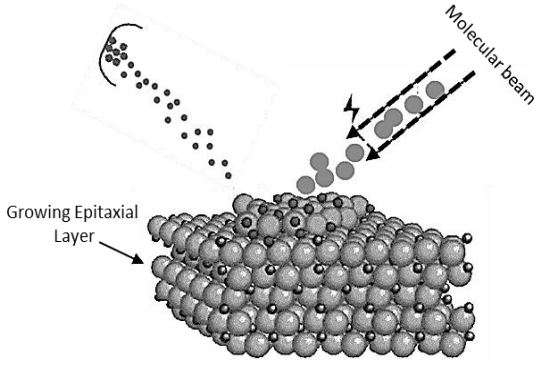

Figure 2.1: MBE growth mechanism

After irradiation molecular beam epitaxy, two physical effects on crystal surface are observed, one is a surface diffusion and the other is roughening. The following summary explains the most important features of these processes.

2.2 SURFACE DIFFUSION

Surface diffusion (SD) is a really common phenomenon playing a highly important part in the field of science and technology. The effect of SD is to move surface atoms, molecules and clusters and allows them to assemble into some desirable configurations or, vice versa, to destroy the configurations that have been purposely created. (cf. [21]).

Surface diffusion rates and mechanisms are affected by a variety of factors like of chemical potential gradients proportional to the curvature of surface. In the effect of chemical potential proportional to the curvature of surface, the atoms have tendency to migrate form the positions of large curvature to those of small one.

2.2.1 Types of surface diffusion

There are two different general schemes in which diffusion may take place [68], tracer diffusion, and chemical diffusion.

. *Tracer diffusion or low diffusion* describes the motion of individual ad particles on a surface at relatively low coverage levels. The single atom diffusing in Figure 2.2 (b) is a nice example of tracer diffusion. Notice that the low diffusion is stable. See Figure 2.2 (a)

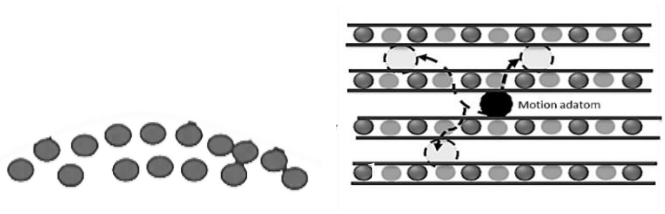

(a) Stable surface (b) Low diffusion

Figure 2.2: Model of tracer diffusion

. *Chemical diffusion or high diffusion* describes the process at higher level of coverage where the effects of attraction. In a crude way, figure 2.3 (b) serves to show how adatoms may interact at higher coverage levels. The adatoms have no "choice" but to move to the right at first, and adjacent adatoms may block adsorption sites from one another. The high diffusion is unstable. See Figure 2.3(a)

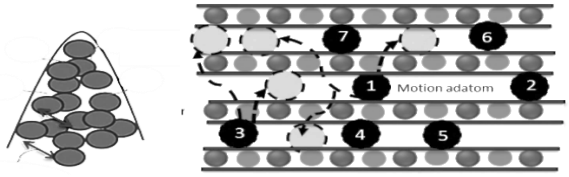

(a) UnStable surface (b) High diffusion

Figure 2.3: Model of chemical diffusion

2.2.2 Adatom diffusion

Diffusion of adatoms may occur by a variety of mechanisms. The following is a summary of the most important of these processes: [65].

. ***Hopping or jumping*** is conceptually the most basic mechanism for diffusion of adatoms. In this model, the adatoms reside on adsorption sites on the surface lattice. Motion occurs through successive jumps to adjacent sites, the number of which depends on the nature of the surface lattice. As shown in Figure 2.4.

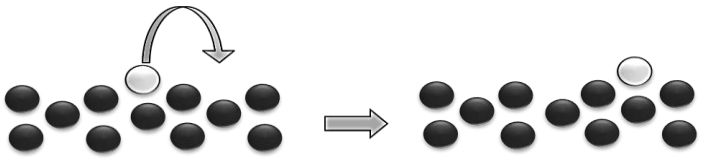

Figure 2.4 Model of an atomic hopping mechanism.

. ***Atomic exchange*** involves exchange between an adatom and an adjacent atom within the surface lattice, as shown in Figure 2.5

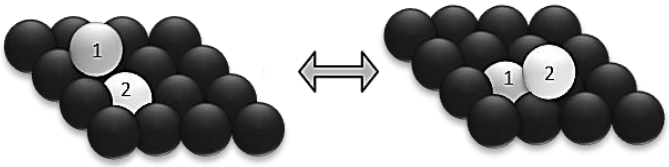

Figure 2.5 .Model of an atomic exchange mechanism occurring between an adatom (1) and surface atom (2) at a square surface lattice (black).

. ***Vacancy diffusion*** can occur as the predominant method of surface diffusion at high coverage levels approaching complete coverage. It is very difficult to directly observe vacancy diffusion due to the typically high diffusion rates and low vacancy concentration: [67]. Figure 2.6 shows the basic theme of this mechanism.

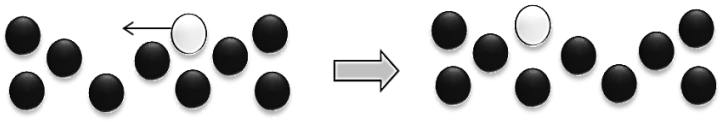

Figure 2.6 Model of vacancy diffusion mechanism.

. ***Long-range atomic exchange*** is a process involving an adatom inserting into the surface as in the normal atomic exchange mechanism, but instead of a nearest-neighbor atom it is an atom some distance further from the initial adatom that emerges. Shown in figure 2.7, this process has only been observed in molecular dynamics simulations and has yet to be confirmed experimentally.

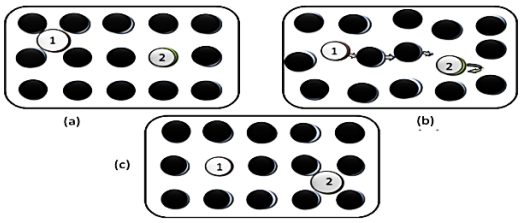

Figure 2.7.Model of Long-range atomic exchange mechanism at a square lattice. Adatom (1), resting at surface (a), inserts into lattice disturbing neighboring atoms (b), ultimately causing one of the original substrate atoms emerge as an adatom (2) (c). Not to scale.

2.2.3 Thermal grooving due to surface diffusion

. *The phenomenon.* A polished polycrystal has a flat surface. At room temperature, the surface remains flat for a long time. At an elevated temperature atoms move. The surface grows grooves along triple junctions, where the surface meet grain boundaries. Atoms may move in many ways. They may diffuse in the lattice, diffuse on the surface, or evaporate into the vapor phase. Here we will only consider surface diffusion. Atoms diffuse on the surface away from the triple junction, making a dent along the junction, and piling two bumps nearby. The process conserves the total mass. The process of grooving was modeled by Mullins (1957). See Figure 2.8.

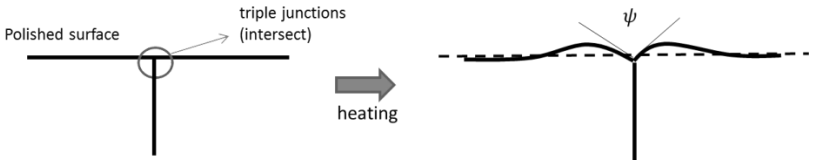

Figure2.8. Section showing profile of ideal thermal groove

. *Grain boundary energy and surface energy.* Development of groove is resultant of the two surface tension and the one grain tension along the line of intersection**.** Let γ_s be the surface energy per unit area, and be γ_b the grain boundary energy per unit area, see Fig 2.9. The free energy of the system is the sum of the surface energy and the grain boundary energy:

$$G = \gamma_s A_s + \gamma_b A_b.$$

As the groove grows, the grain boundary area decreases, but the surface area increases. The net free energy must decrease.

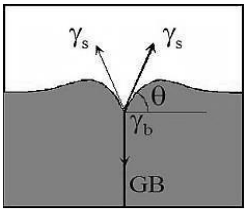

Figure 2.9 Surface energy and grain boundary energy

L. Klinger and E. Rabkin, 2001

. *Local equilibrium and the dihedral angle.* During the motion of the surface, the triple junction maintains local equilibrium. Local equilibrium at the triple junction implies that the surface tensions balance one another, giving the angle, θ,

$$2\gamma_s sin\,\theta = \gamma_b.$$

. *Differential geometry of a curve in a plane.* For example, we can prescribe the coordinates of a point on the curve, *x* and *y*, as functions of the curve length *s*. The functions and *x*(*s*) and *y*(*s*) describe a set of points that trace the curve. We have adopted a sign convention. The solid is beneath the surface. The curvature is positive when the solid is convex. *K=+1/R* for a cylindrical solid of radius *R*, and *K=−1/R* for a cylindrical hole of radius *R*. When the surface evolves with time, we represent the family of curves by a function of two variables:$h(x,t)$ is the height of the surface at location *x* and time *t*. At a given time, the curve has the length, the tangent angle, and the curvature. In the above expressions, the differential becomes the partial differential $\partial h/\partial x$ with time fixed.

. *Atomic flux.* The adatoms have tendency to flow on the surface from positions of large curvature to those of lower one. According to Nernst-Einstein low, the mean velocity *V* of adatom's flow along the surface is 1D case known as

$$V = -\frac{D_s\gamma\Omega}{kT}\frac{\partial K}{\partial s}.$$

Here, D_s is a surface diffusion constant, γ is a surface energy per unit area, Ω is a volume of molecule, k is the Boltzmann constant, and *T* is temperature. Thereby, the flux of flow is given by

$$J = -Vv = -\frac{D_s\gamma\Omega v}{kT}\frac{\partial K}{\partial s},$$

where v is a number of adatoms per unit area.

. *Mass conservation.* Consider the motion of a surface element *dx*. When the time goes from *t* to $+\Delta t$, $J(x)\Delta t$, number of atoms flow into the element, $J(x+dx,t)\Delta t$, number of atoms flow out of the element, and the surface height changes from $h(x,t)$ to $h(x,t+\Delta t)$. Mass conservation requires that

$$\frac{\partial h}{\partial t} = -\Omega^{-1}\frac{\partial J}{\partial x}.$$

2.2.4 Mathematical model of surface diffusion

Let us derive an equation satisfied by the surface curve following the methods due to Mullins [10]. The normal component of growing velocity of surface can now be describe by

$$r_n = -\Omega^{\frac{1}{3}} \frac{\partial J}{\partial s} = \frac{D_s \gamma \Omega^{\frac{4}{3}} v}{kT} \frac{\partial^2 K}{\partial s^2}.$$

Since $s = \int \sqrt{1 + h_x^2} dx,$ it follows that

$$\frac{\partial}{\partial s} = \frac{\partial x}{\partial s} \frac{\partial}{\partial x} = \frac{1}{\sqrt{1 + h_x^2}} \frac{\partial}{\partial x}.$$

Furthermore,

$$\frac{\partial^2}{\partial s^2} = \left(\frac{1}{\sqrt{1 + h_x^2}} \frac{\partial}{\partial x} \right)^2.$$

Meanwhile, the curvature is equal to $K = -\frac{h_{xx}}{(1+h_x^2)^{\frac{3}{2}}}.$ Therefore, we obtain that

$$r_n = -B \left(\frac{1}{\sqrt{1 + h_x^2}} \frac{\partial}{\partial x} \right)^2 \left(\frac{h_{xx}}{(1 + h_x^2)^{\frac{3}{2}}} \right)$$

with a constant $B = \frac{D_s \gamma \Omega^{4/3} v}{KT}.$

On the other hand, we have

$$r_n = \frac{1}{\sqrt{1 + h_x^2}} \frac{\partial h}{\partial t}.$$

Combing these two equations, we arrive at

$$\frac{\partial h}{\partial t} = -B \frac{\partial}{\partial x} \left[\frac{1}{\sqrt{1 + h_x^2}} \frac{\partial}{\partial x} \left(\frac{h_{xx}}{(1 + h_x^2)^{\frac{3}{2}}} \right) \right].$$

In this study, we are concerned with the case when the gradient of the curve is sufficiently small, i.e., $h_x \approx 0,$ thereby

$$\frac{\partial h}{\partial t} = -B \frac{\partial^4 h}{\partial x^4}.$$

These arguments can be extended into two- dimensional case by analogous arguments. The two-dimensional equation of surface diffusion is indeed given by

$$\begin{aligned} \frac{\partial u}{\partial t} &= -B \left(\frac{\partial^2}{\partial x^2} + \frac{\partial^2}{\partial y^2} \right)^2 u \\ &= -B \Delta^2 u, \end{aligned}$$

where $u(x, y, t)$ denotes a displacement of surface from the standard level at position (x, y) of substrate and at time t.

2.3 ROUGHENING

During the film production by MBE, the surface may follow distinct growth regimes: [60]. The so-called kinetic roughening, where is caused by Schwoebel barriers [3; 10] (cf. also [14]). The step edge barriers prevent adatoms from hopping down from the upper terraces to lower ones. See Figure 2.10.

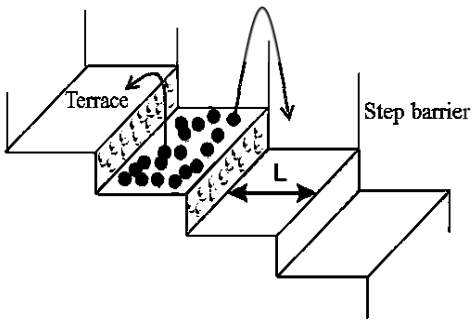

Figure 2.10. Step barrier mechanism

As a consequence, diffusing adatoms preferably attach to steps from the terrace below rather than from above and non-equilibrium uphill currents are induced [3; 11]. See Figure 2.11.

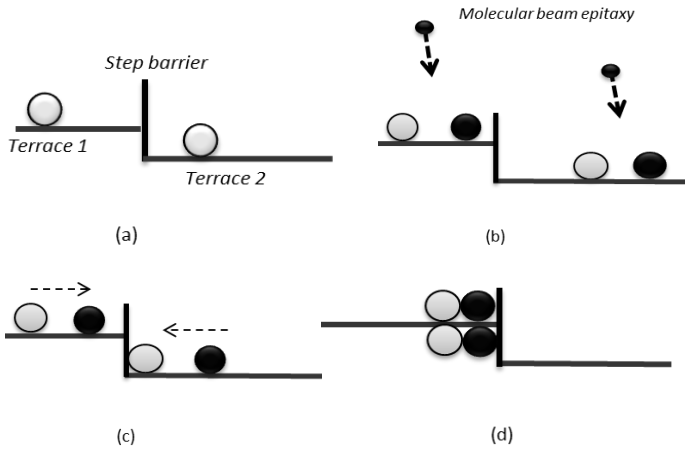

Figure 2.11. Processes of roughening due to step barriers; (a) step barrier between up and down terrace; (b) injection of new molecules; (c) tendency of old and new molecules toward step barrier; (d) growth of terrace 1 to end of new molecules in terrace 2.

2.3.1 Mathematical model of Roughening

A mathematical model of surface roughening was presented by Rost [26]. He assumed that the surface evolves according to an equation

$$\frac{\partial h}{\partial t} = -B\Delta^2 h - \nabla . J_{NE} + F,$$

where the first term on the right hand side denotes smoothing due to the surface diffusion, J_{NE} is the uphill non-equilibrium mass current induced by the step edge barriers, and F is the deposition rate. Under the assumption of in-plane isotropy the current is directed along the local tilt ∇h, and it can be written as

$$J_{NE} = \emptyset(|\nabla h|)\nabla h.$$

A calculation in [65] in the framework of Burton-Cabrera-Frank (BCF) theory [23] yields that

$$\emptyset(|\nabla h|) = F\tilde{l}_D^2 f(l_D|\nabla h|),$$

where l_D is the diffusion length or terrace size on the singular surface: [15], $\tilde{l}_D$ is the effective diffusion length which is obtained by some modifications on l_D, and $f(s)$ is a dimensionless shape function. There are several possibilities for choosing this function. Johnson [8] proposed in 1994 a form

$$f(s) = \frac{1}{1+s^2},$$

by interpolating the facts that, as $s \to 0$, $f(s) \approx 1$, and as $s \to \infty$, $f(s) \approx \frac{1}{s^2}$. Following this idea, we obtain that

$$\frac{\partial h}{\partial t} = -B\Delta^2 h - F\tilde{l}_D^2 \nabla . \left(\frac{\nabla h}{1 + l_D^2 |\nabla h|^2} \right) + F.$$

Replacing $h(x,y,t)$ by $u(x,y,t) = h(x,y,t) - Ft$ as before, we arrive at the equation

$$\frac{\partial u}{\partial t} = -B\Delta^2 u - F\tilde{l}_D^2 \nabla . \left(\frac{\nabla u}{1 + l_D^2 |\nabla u|^2} \right).$$

3

Dynamical System for Epitaxial Growth Model under Dirichlet Conditions

In this chapter we construct a dynamical system generated by the initial value problem (1.1) for the Dirichlet boundary conditions and we verify that the dynamical system has a finite-dimensional attractor. Also this chapter is devoted to presenting a Lyapunov function of the dynamical system whose values are monotonously decreasing along trajectories.

3.1 ABSTRACT FORMULATION

In order to employ the theory of abstract parabolic equations, let us formulate (1.1) as the Cauchy problem for an abstract evolution equation. We first define a realization of the operator $a\Delta^2$ under the conditions $u = \frac{\partial u}{\partial n} = 0$. For this purpose, we consider a symmetric sesquilinear form

$$a(u, v) = a \int_{\Omega} \Delta u \cdot \Delta \overline{v}\, dx, \qquad u, v \in H_0^2(\Omega),$$

defined on $H_0^2(\Omega)$. Since $\nabla u \in H_0^1(\Omega)$ if $u \in H_0^2(\Omega)$, $u \in H_0^2(\Omega)$ satisfies $\frac{\partial u}{\partial n} = 0$ on $\partial\Omega$. Of course, $u \in H_0^2(\Omega)$ satisfies $u = 0$ on $\partial\Omega$. Therefore $u \in H_0^2(\Omega)$ satisfies the homogeneous Dirichlet boundary conditions. Furthermore, as Ω is convex or of class $\mathcal{C}^2$, in either case, the elliptic estimates yield that

(3.1.a) $$\|u\|_{H_2} \leq C\|u\|_{L_2}, \qquad u \in H^2(\Omega) \cap H_0^1(\Omega).$$

This then implies the coercive estimate

$$a(u, v) \geq \delta \|u\|_{H_2}^2 \qquad \text{for all } u \in H_0^2(\Omega),$$

with some constant $\delta > 0$. As a consequence, we see that $a(u, v)$ determines a linear operator A from $H_0^2(\Omega)$ into $H^{-2}(\Omega)$ by a formula $a(u, v) = \langle Au, v \rangle_{H^{-2} \times H_0^2}$, see, [2]. Here, $H^{-2}(\Omega)$ is the dual space of $H_0^2(\Omega)$ and these spaces compose a triplet

(3.1.b) $$H_0^2(\Omega) \subset L_2(\Omega) \subset H^{-2}(\Omega).$$

The operator A thus defined is considered as a realization of $a\Delta^2$ under the homogenous Dirichlet boundary conditions which is a densely defined, closed operator in $H^{-2}(\Omega)$ whose spectrum is contained in the positive real line (0, ∞). (Note that the part of A in $L_2(\Omega)$ is a

positive definite self-adjoint operator of $L_2(\Omega).$) For $0 \le \theta \le 1$, A^θ denotes the fractional power of A with exponent θ. Of course, $A^0 = I$ (identity operator on $H^{-2}(\Omega)$) and $A^1 = A$. As a general result (cf. [15, Theorem 2.35]), it follows from (3.1.b) that $\mathcal{D}\left(A^{\frac{1}{2}}\right) = L_2(\Omega)$ with norm equivalence. From this fact it is further deduced that, for $\frac{1}{2} \le \theta \le 1$,

(3.1.c) $$\mathcal{D}(A^\theta) = [\mathcal{D}\left(A^{\frac{1}{2}}\right), \mathcal{D}(A)]_{2\theta-1} = [L_2(\Omega), H_0^2(\Omega)]_{2\theta-1} \subset H^{4\theta-2}(\Omega).$$

As well, (3.1.a) can be extended for $\frac{1}{2} \le \theta \le 1$,

$$\|u\|_{H^{4\theta-2}} \le C \left\|A^{\theta-\frac{1}{2}}u\right\|_{L_2}, \qquad \mathcal{D}(A^\theta).$$

We next define a realization of a nonlinear operator $-\mu\nabla \cdot \left(\frac{\nabla u}{1+|\nabla u|^2}\right)$ in the framework of (3.1.b). Since ∇ is a bounded operator from $L_2(\Omega)$ into $H^{-1}(\Omega)$, if $\frac{\nabla u}{1+|\nabla u|^2}$ is in $L_2(\Omega)$, then we see that $\nabla \cdot \left(\frac{\nabla u}{1+|\nabla u|^2}\right) \in H^{-1}(\Omega) \subset H^{-2}(\Omega)$. So, it is natural to set

(3.1.d) $$f(u) = -\mu\nabla \cdot \left(\frac{\nabla u}{1+|\nabla u|^2}\right), \qquad u \in H^1(\Omega).$$

In view of (3.1.c), $\mathcal{D}\left(A^{\frac{3}{4}}\right) \subset H^1(\Omega)$. This shows that f is defined on the domain $\mathcal{D}\left(A^{\frac{3}{4}}\right)$ and can be regarded as a subordinate operator to A. We thus arrive at an abstract formulation of (1.1) which is written as

(3.1.e) $$\begin{cases} \frac{du}{dt} + Au = f(u), & 0 < t < \infty, \\ u(0) = u_0, \end{cases}$$

in the underlying space $H^{-2}(\Omega)$. It is now possible to apply the various results of the theory of semilinear abstract parabolic equations.

3.2 CONSTRUCTION OF SOLUTIONS

We begin with constructing local solutions to (3.1.e) by using [15, Theorem 4.4]. To this end, it suffices to verify a suitable Lipschitz condition for $f(u)$. In fact, for $u, v \in H^1(\Omega)$,

$$\begin{aligned} \frac{\nabla u}{1+|\nabla u|^2} - \frac{\nabla v}{1+|\nabla v|^2} &= \frac{(1+|\nabla v|^2)\nabla(u-v) - (|\nabla u|^2 - |\nabla v|^2)\nabla v}{(1+|\nabla u|^2)(1+|\nabla v|^2)} \\ &= \frac{\nabla(u-v)}{1+|\nabla u|^2} - \frac{(|\nabla u| - |\nabla v|)(|\nabla u| + |\nabla v|)\nabla v}{(1+|\nabla u|^2)(1+|\nabla v|^2)}. \end{aligned}$$

Therefore,

$$\left\| \frac{\nabla u}{1+|\nabla u|^2} - \frac{\nabla v}{1+|\nabla v|^2} \right\|_{L_2} \le \mathrm{C}\|u-v\|_{H^1}.$$

This then yields that

$$\|f(u)-f(v)\|_{H^{-1}} \le C \left\| A^{\frac{3}{4}}(u-v) \right\|_{H^{-2}}, \qquad u,v \in \mathcal{D}\left(A^{\frac{3}{4}}\right),$$

i.e., *f* fulfills [15, (4.21)] with $\eta = \frac{3}{4}$.

As a direct consequence of [15, Theorem 4.4], for any $u_0 \in H^{-2}(\Omega)$, there exists a unique local solution to (3.1.e) in the function space:

(3.2.a) $$u \in \mathcal{C}\left([0,T_{u_0}];H^{-2}(\Omega)\right) \cap \mathcal{C}^1\left((0,T_{u_0}];H^{-2}(\Omega)\right) \cap \mathcal{C}\left((0,T_{u_0}];H_0^2(\Omega)\right).$$

The local solution *u* satisfies the estimate

(3.2.b) $$t\|u(t)\|_{H^2} + t^{\frac{3}{4}}\|u(t)\|_{H^1} + \|u(t)\|_{H^{-2}} \le C_{u_0}, \qquad 0 < t \le T_{u_0}.$$

The time $T_{u_0} > 0$ and constant C_{u_0} are determined by the norm $\|u_0\|_{H^{-2}}$ alone.

For constructing global solution, the essential thing is to establish the *a priori* estimates for global solution, cf. [15, Corollary 4.3]. By the smoothing effect of solution seen by (3.2.a) we have $u(t) \in H^2(\Omega)$ for any $t > 0$. So in proving the *a priori* estimates (and hence constructing a global solution to (3.1.e)), there is no loss of generality to assume that $u_0 \in L_2(\Omega) = \mathcal{D}(A^{\frac{1}{2}})$. Under this assumption, let *u* denote any local solution to (3.1.e) in the space:

(3.2.c) $$u \in \mathcal{C}([0,T_u];L_2(\Omega)) \cap \mathcal{C}^1((0,T_u];H^{-2}(\Omega)) \cap \mathcal{C}((0,T_u];H_0^2(\Omega)).$$

Proposition 3.1. *There exists a constant $C > 0$ such that the estimate*

$$\|u(t)\|_{L^2} \le C\left(\|u_0\|_{L_2} + 1\right), \qquad 0 \le t \le T_u,$$

holds true for any local solution u lying in (3.2.c), *C being independent of the interval* $[0,T_u]$.

Proof. Take a scalar product of the equation of (3.1.e) and $\bar{u}$. Noting that $\|u(t)\|_{L^2}^2$ is differentiable for $t > 0$ with derivative $\frac{d}{dt}\|u(t)\|_{L^2}^2 = 2Re\,\langle \frac{du}{dt}(t), u(t)\rangle_{H^{-2},H_0^2}$ and that $\langle Au(t), u(t)\rangle_{H^{-2},H_0^2} = a\left(u(t),u(t)\right)$, we have

$$\frac{1}{2}\frac{d}{dt}\int_\Omega |u|^2 dx + a\int_\Omega |\Delta u|^2 dx = \mu \int_\Omega \frac{|\nabla u^2|}{1+|\nabla u|^2}\, dx \le \mu|\Omega|.$$

By (3.1.a) there exists a constant $\delta > 0$ such that

$$\frac{1}{2}\frac{d}{dt}\int_\Omega |u|^2 dx + \delta\int_\Omega |u|^2 dx \le \mu|\Omega|.$$

Solving this integral inequality, we obtain that

$$\|u(t)\|_{L^2}^2 \le e^{-2\delta t}\|u_0\|_{L^2}^2 + \mu\delta^{-1}|\Omega|, \qquad 0 \le t \le T_u.$$

Proposition 3.1 shows that the norm $\|u(t)\|_{L_2}$ remains uniformly bounded for any interval

$[0, T_u]$. This then means that one can always extend any local solution with a uniform time interval to obtain a global solution in the space:

(3.2.d) $$u \in \mathcal{C}([0,\infty]; L_2(\Omega)) \cap \mathcal{C}^1((0,\infty]; H^{-2}(\Omega)) \cap \mathcal{C}((0,\infty]; H_0^2(\Omega)).$$

Of course, the global solution satisfies the similar estimate

(3.2.e) $$\|u(t)\|_{L^2}^2 \le e^{-2\delta t}\|u_0\|_{L^2}^2 + \mu\delta^{-1}|\Omega|, \qquad 0 \le t \le \infty.$$

Finally, let us remark that, if the initial function u_0 is real, then the solution $u(t)$ with $u(0) = u_0$ is also real for every time $t > 0$. In fact, we notice that the complex conjugate $\bar{u}$ of the solution u to (3.1.e) satisfies the same evolution equation for every *t*. So, $\bar{u}$ is a solution satisfying an initial condition $\overline{u(0)} = \overline{u_0}$. If u_0 is real, i.e., $u_0 = \overline{u_0}$, then uniqueness of solution implies $u(t) = \overline{u(t)}$ and $u(t)$ must be real for every *t*.

3.3 DYNAMICAL SYSTEM

The next step is to observe that the problem (3.1.e) generates a dynamical system. For this purpose, we can again follow the general procedure for semilinear abstract parabolic equations; see [15, Section 6.5].

For $u_0 \in H^{-2}(\Omega)$, let $u(t; u_0)$ denote the global solution of (3.1.e), and set

$$S(t)u_0 = u(t; u_0), \qquad 0 \le t \le \infty.$$

Then, $S(t)$ is a nonlinear semigroup acting on $H^{-2}(\Omega)$, i.e., $S(0) = I$ and $S(t+s) = S(t)S(s)$ for $0 \le s, t < \infty$. Furthermore, $S(t)$ is seen to be continuous in the sense that $(t, u_0) \mapsto S(t)u_0$ is continuous from $[0,\infty) \times H^{-2}(\Omega)$ into $H^{-2}(\Omega)$. Whence, $S(t)$ defines a dynamical system in $H^{-2}(\Omega)$ which is denoted by $(S(t), H^{-2}(\Omega))$. We can see from the dissipative estimate (3.2.e) that $(S(t), H^{-2}(\Omega))$ has an exponential attractor.

Remember that a set $\mathcal{M}$ satisfying the following conditions is called the exponential attractor:

1. $\mathcal{M}$ is a compact subset of $H^{-2}(\Omega)$ with finite fractal dimension.
2. $\mathcal{M}$ is a positively invariant set of $S(t)$, i.e., $S(t)\mathcal{M} \subset \mathcal{M}$ for any $0 \le t \le \infty$.
3. There exists an exponent $k > 0$ such that, for any bounded subset *B* of $H^{-2}(\Omega)$, it holds true that

$$h(S(t)B, \mathcal{M} \le C_{B^{e^{-kt}}}, \qquad 0 < t < \infty,$$

with a constant $C_B > 0$.

Here, $h(B_1, B_2) = \sup_{f \in B_1} \inf_{g \in B_2} \|f - g\|_{H^{-2}}$ is a semi-distance of two bounded B_1 and B_2.

As explained in [15, Section 6.4], the compact smoothing property

(3.3.a) $$\|S(t^*)u_0 - S(t^*)v_0\|_{L_2} \le C\|u_0 - v_0\|_{H^{-2}}, \qquad u_0, v_0 \in \mathcal{B},$$

of $S(t)$ provides existence of exponential attractors, where $\mathcal{B}$ is an attractive, positively invariant, compact subset of $H^{-2}(\Omega)$ and where $t^* > 0$ is a fixed time. But, this property is also easily verified from the known estimates (3.2.b) and (3.2.e). In fact, let *B* be any bounded subset of $H^{-2}(\Omega)$. Then, it follows from (3.2.b) that there exist a bounded ball B_2 of $L_2(\Omega)$ and time $t_B > 0$ both depending on *B* such that $S(T_B)B \subset B_{2,B}$. In addition, (3.2.e) yields that,

for any $u_0 \in \mathcal{B}$,

$$\|S(t)u_0\|_{L_2}^2 = \|S(t-T_B)S(T_B)u_0\|_{L_2}^2 \le e^{-2\delta(t-T_B)}R_{2,B} + \mu\delta^{-1}|\Omega|, \quad \forall t \ge T_B,$$

where $R_{2,B}$ is the radius of $B_{2,B}$. This shows that the ball $B(0;\sqrt{1+\mu\delta^{-1}|\Omega|})$ of $L_2(\Omega)$ is an absorbing set. Let $\mathcal{B}$ be the collection of all trajectories starting from this ball. Obviously, $\mathcal{B}$ is an absorbing and invariant set. Finally, the desired Lipschitz condition (3.3.a) can be verified by using the standard techniques described in [15, Subsection 6.5.3]. In this way, we verify that our dynamical system admits an exponential attractor.

Finally, let us notice that $S(t)$ defines a dynamical system even in the space $L_2(\Omega)$ and the restricted dynamical system denoted by $\big(S(t),\ L_2(\Omega)\big)$ also admits an exponential attractor. In fact, as seen in (3.2.d), $S(t)$maps $L_2(\Omega)$ into itself. In addition, it is proved that $S(t)$is continues from $L_2(\Omega)$ into itself. Therefore, (3.1.e) generates a dynamical system in $L_2(\Omega)$, too. Furthermore, the exponential attractor $\mathcal{M}$ in $H^{-2}(\Omega)$ constructed above is obviously a bounded subset of $\mathcal{D}(A)\ \big(=\mathrm{H}_0^2(\Omega)\big)$, and remains to be an exponential attractor of $\big(S(t),\ L_2(\Omega)\big)$.

3.4 LYAPUNOV FUNCTION

Multiply the equation of (1.1) by $-\frac{\partial\bar{u}}{\partial t}$ and integrate the product in Ω. By somewhat formal computations, its real part is given by

$$-\int_\Omega \left|\frac{\partial u}{\partial t}\right|^2 dx = a\mathrm{Re}\int_\Omega \Delta u\frac{\partial}{\partial t}\Delta\bar{u}dx \ - \mu\mathrm{Re}\int_\Omega \left[\frac{\nabla u}{1+|\nabla u|^2}\right]\cdot\frac{\partial}{\partial t}\nabla\bar{u}dx$$

$$= \frac{1}{2}\frac{d}{dt}\int_\Omega [-\mu\log(1+|\nabla u|^2)]dx.$$

These computations then suggest that the functional

(3.4.a) $$\Phi(u) = \tfrac{1}{2}\textstyle\int_\Omega [a|\Delta u|^2 - \mu\log(1+|\nabla u|^2)]dx, \qquad u_0 \in H_0^2(\Omega),$$

becomes a Lyapunov function of the dynamical system.

In order to justify this, however, we need a higher regularity of solution to (3.1.e) belonging to

(3.4.b) $$u \in \mathcal{C}^1\big((0,\infty];L_2(\Omega)\big) \quad \text{and} \quad \Delta^2 u \in \mathcal{C}\big((0,\infty];L_2(\Omega)\big).$$

It is clear that

$$\begin{aligned}&\|\Delta u(t+h)\|_{L_2}^2 - \|\Delta u(t)\|_{L_2}^2\\ &= \big(\Delta[u(t+h)-u(t)], \Delta^2 u(t+h)\big) + (\Delta u(t), \Delta u[u(t+h)-u(t)])\\ &= \big(u(t+h)-u(t), \Delta u(t+h)\big) + \big(\Delta^2 u(t), u(t+h)-u(t)\big).\end{aligned}$$

In view of (3.4.b), it is observed that

$$\frac{d}{dt}\|\Delta u(t)\|_{L_2}^2 = \left(\frac{du}{dt}(t), \Delta^2 u(t)\right) + \left(\Delta^2 u(t), \frac{du}{dt}(t)\right)$$
$$= 2\mathrm{Re}\left(\frac{du}{dt}(t), \Delta^2 u(t)\right).$$

In the meantime, for $u, v \in H_0^2(\Omega)$, consider

$$\int_\Omega [\log(1+|\nabla v|^2) - \log(1+|\nabla u|^2)]dx$$

For a.e. $x \in \Omega$, we have

$$\log[1+|\nabla v(x)|^2] - \log[1+|\nabla u(x)|^2] = \int_0^1 \frac{d}{d\theta}\log\{1+|\nabla[\theta v(x)+(1-\theta)u(x)]|^2\}\,d\theta$$

$$= \int_0^1 \frac{2\mathrm{Re}\nabla[v(x)-u(x)]\cdot\nabla\bar{u}(x) + 2\theta|\nabla[v(x)-u(x)]|^2}{1+|\nabla[\theta v(x)+(1-\theta)u(x)]|^2}\,d\theta.$$

Moreover, since

$$\frac{1}{1+|\nabla[\theta v(x)+(1-\theta)u(x)]|^2}$$
$$= \frac{1}{1+|\nabla u(x)|^2} - \frac{2\theta\mathrm{Re}\nabla[v(x)-u(x)]\cdot\nabla\bar{u}(x) + \theta^2|\nabla[v(x)-u(x)]|^2}{\{1+|\nabla[\theta v(x)+(1-\theta)u(x)]|^2\}(1+|\nabla u(x)|^2)},$$

we have

$$\left|\log[1+|\nabla v(x)|^2] - \log[1+|\nabla u(x)|^2] - \frac{2\mathrm{Re}\nabla[v(x)-u(x)]\cdot\nabla\bar{u}(x)}{1+|\nabla u(x)|^2}\right|$$
$$\le C\{|\nabla[v(x)-u(x)]|^2 + |\nabla[v(x)-u(x)]|^4\}.$$

Therefore, integration in Ω yields that

$$\left|\int_\Omega \left[\log(1+|\nabla v|^2) - \log[1+|\nabla u|^2] - \frac{2\mathrm{Re}\nabla[u-v]\cdot\nabla\bar{u}}{1+|\nabla u|^2}\right]dx\right|$$
$$\le C\left\{\|\nabla(v-u)\|_{L_2}^2 + \|\nabla(v-u)\|_{L_4}^4\right\}.$$

We have to use Galiardo- Nirenberg's inequality ([15, Theorem 1.37]) to obtain that

$$\|\nabla(v-u)\|_{L_4} \le C\|\nabla(v-u)\|_{L_2}^{\frac{1}{2}}\|\nabla(v-u)\|_{H^1}^{\frac{1}{2}} \le C\|v-u\|_{H^1}^{\frac{1}{2}}\|v-u\|_{H^2}^{\frac{1}{2}}$$

$$\le C\|v-u\|_{L_2}^{\frac{1}{4}} C\|v-u\|_{H^2}^{\frac{3}{4}}.$$

Then,

$$\left|\int_\Omega \left\{\log(1+|\nabla v|^2) - \log[1+|\nabla u|^2] + 2\mathrm{Re}\left[\nabla\cdot\frac{\nabla u}{1+|\nabla u|^2}(\bar{v}-\bar{u})\right]dx\right\}\right|$$
$$\le C\|v-u\|_{L_2} + \left(\|v-u\|_{H^2} + \|v-u\|_{H^2}^3\right).$$

Let us apply this estimate with $v = u(t+h)$ and $u = u(t)$, where u is the solution mentioned

above. Then, since $\|u(t+h)-u(t)\|_{H^2} \to 0$ as $h \to 0$, it is easily verified that

$$\frac{d}{dt}\int_\Omega \log[1+|\nabla u(t)|^2]dx = -2\mathrm{Re}\int_\Omega \nabla\cdot\left(\frac{\nabla u(t)}{1+|\nabla u(t)|^2}\right)\frac{d\bar{u}}{dt}(t)dx.$$

We have thus proved that, for any solution lying in (3.4.b), the function $\Phi\big(u(t)\big)$ is differentiable with derivative

(3.4.c) $$\frac{d}{dt}\Phi\big(u(t)\big) = \left\|-\frac{du}{dt}(t)\right\|_{L_2}^2, \qquad 0 \le t \le \infty.$$

4

Longtime Convergence for Epitaxial Growth Model under Dirichlet Conditions

This chapter is devoted to showing longtime convergence of trajectory. We shall prove that every trajectory converges to some stationary solution as $t \to \infty$.
In this chapter, we assume that Ω is a rectangular domain or $\mathcal{C}^4$ domain.

4.1 DYNAMICAL SYSTEM

4.1.1 Abstract formulation. We rewrite (1.1) into the form

$$\begin{cases} \frac{du}{dt} + Au = f(u), & 0 < t < \infty, \\ u(0) = u_0, \end{cases} \tag{4.1.a}$$

in the underlying space $X = L_2(\Omega)$. Here, A is a realization of $a\Delta^2$ in $L_2(\Omega)$ under the Dirichlet boundary conditions. In fact, A is defined in the following way. Consider the symmetric sesquilinear from

$$a(u, v) = \int_\Omega \Delta u \cdot \Delta \overline{v}\, dx, \qquad u, v \in H_0^2(\Omega).$$

Here, $H_0^2(\Omega)$ is the closure of $\mathcal{C}_0^\infty(\Omega)$ (space of infinitely differentiable function in Ω with compact support) in $H^{\,2}(\Omega)$. If $u \in H_0^2(\Omega)$, then $\nabla u \in H_0^1(\Omega)$; consequently, u satisfies $\frac{\partial u}{\partial n} = 0$ on $\partial\Omega$. Since it is clear that $u = 0$ on $\partial\Omega$, $u \in H_0^2(\Omega)$ implies that u satisfies the Dirichlet boundary conditions in (1.1). Furthermore, the convexity of Ω when Ω is rectangular, or the $\mathcal{C}^4$ regularity of $\partial\Omega$ in the alternative case yields that

$$\|u\|_{H_2} \le C\|u\|_{L_2}, \qquad u \in H^2(\Omega) \cap H_0^1(\Omega).$$

This shows that the form $a(u, v)$ is coercive on $H_0^2(\Omega)$. Consequently, $a(u, v)$ determines a linear operator $\mathcal{A}$ from $H_0^2(\Omega)$ into $H^{-2}(\Omega)$ by the formula $a(u, v) = \langle \mathcal{A}u, v \rangle_{H^{-2} \times H_0^2}$, where $H^{-2}(\Omega)$ denotes the dual space of $H_0^2(\Omega)$ and these space compose a triple $H_0^2(\Omega) \subset L_2(\Omega) \subset H^{-2}(\Omega)$. The operator $\mathcal{A}$ thus defined is considered as a realization of $a\Delta^2$ in $H^{-2}(\Omega)$ under the Dirichlet boundary conditions which is a densely defined, closed operator in $H^{-2}(\Omega)$ with the domain $\mathcal{D}(\mathcal{A}) = H_0^2(\Omega)$. Furthermore, its part in $L_2(\Omega)$ denoted by $A\big(= \mathcal{A}_{|L_2}\big)$ is defined by

(4.1.b)
$$\begin{cases} \mathcal{D}(A) = \{u \in H_0^2(\Omega);\ \mathcal{A}u \in L_2(\Omega)\}, \\ Au = \mathcal{A}u. \end{cases}$$

Whence, A is a realization of $a\Delta^2$ in $L_2(\Omega)$ under the Dirichlet boundary conditions. It is easily seen that A is a positive definite self-adjoint operator of $L_2(\Omega)$.

Proposition 4.1. *The domain of A given by* (4.1.b) *can actually be characterized as* $\mathcal{D}(A) = H^4(\Omega) \cap H_0^2(\Omega)$. *Furthermore,*

(4.1.c) $$\|u\|_{H^4} \le C\|u\|_{L_2}, \qquad u \in \mathcal{D}(A).$$

Proof. If $u \in H^4(\Omega) \cap H_0^2(\Omega)$, then $a(u,v) = (a\Delta^2 u, v)$ for any $v \in H_0^2(\Omega)$. Therefore, $u \in \mathcal{D}(A)$. This shows that it is the case in general that $H^4(\Omega) \cap H_0^2(\Omega) \subset \mathcal{D}(A)$. So what we have to prove is the converse inclusion

$$H^4(\Omega) \cap H_0^2(\Omega) \supset \mathcal{D}(A).$$

Let us first prove this in the case where $\Omega = (0, l_1) \times (0, l_2)$ is rectangular. We use the Fourier expansion for the function of $L_2(\Omega)$. Any function $u \in L_2(\Omega)$ can be expanded as a series

$$u = \sum_{m,n=1}^{\infty} u_{mn} \sin\frac{m\pi}{l_1}x \cdot \sin\frac{n\pi}{l_2}y$$

with Fourier coefficients u_{mn} satisfying $\sum_{m,n}|u_{mn}|^2 < \infty$.

Then,

$$\Delta^2 u = \sum_{m,n=1}^{\infty} u_{mn}\left[\left(\frac{m\pi}{l_1}\right)^2 + \left(\frac{n\pi}{l_2}\right)^2\right]^2 \sin\frac{m\pi}{l_1}x \,.\, \sin\frac{n\pi}{l_2}y$$

in the distribution sense. So, if $\Delta^2 u \in L_2(\Omega)$, then there exists a double sequence f_{mn} satisfying $\sum_{m,n}|f_{mn}|^2 < \infty$ such that

$$u_{mn} = \left[\left(\frac{m\pi}{l_1}\right)^2 + \left(\frac{n\pi}{l_2}\right)^2\right]^{-2} f_{mn}, \qquad 1 \le m, n < \infty.$$

This yields that for $k = 0,1,2,3,4$, $D_x^k D_y^{4-k} u \in L_2(\Omega)$ as may be evident for $k = 0,2,4$. For $k = 1,3$, say $k = 1$, we have

$$D_x D_y^3 u = -\sum_{m,n=1}^{\infty} u_{mn}\frac{m\pi}{l_1}\left(\frac{n\pi}{l_2}\right)^3 \cos\frac{m\pi}{l_1}x \cdot \cos\frac{n\pi}{l_2}y.$$

So, since $\cos\frac{m\pi}{l_1}x \cdot \cos\frac{n\pi}{l_2}y$ are mutually orthogonal in Ω, it is seen that

$$\left\|D_x D_y^3 u\right\|_{L_2}^2 = \frac{l_1 l_2}{4}\sum_{m,n=1}^{\infty}\left\{\frac{m\pi}{l_1}\left(\frac{n\pi}{l_2}\right)^3\left[\left(\frac{m\pi}{l_1}\right)^2 + \left(\frac{n\pi}{l_2}\right)^2\right]^{-2}\right\}^2 |f_{mn}|^2 < \infty.$$

Furthermore, $\left\|D_x D_y^3 u\right\|_{L_2}^2 \leq c\sum_{m,n=1}^{\infty}|f_{mn}|^2 \leq c\|\Delta^2 u\|_{L_2}^2$.

Hence, $\Delta^2 u \in L_2(\Omega)$ implies $u \in H^2(\Omega)$.

Second, let us consider the case where Ω is a $\mathcal{C}^4$ bounded domain. In this case, we have to appeal to existence result for the higher order elliptic operators. Among other, the arguments due to Tanabe [12, Section 3.8] are very comprehensible (cf. also [17, Section 5.2]). It is then asserted that for any $f \in L_2(\Omega)$, there exists a unique global solution $u \in H^4(\Omega)$ for which it holds that $\Delta^2 u = f$ in Ω and $u = \frac{\partial u}{\partial n} = 0$ on $\partial\Omega$ together with $\|u\|_{\mathrm{H}^4} \leq C\|f\|_{L_2}, C >$ 0 being some constant. Furthermore, since $u = \frac{\partial u}{\partial n} = 0$ on $\partial\Omega$ implies $u \in H_0^2(\Omega)$, we see that $u \in H^4(\Omega) \cap H_0^2(\Omega) \subset (\mathcal{D}(A))$ and $Au = f$. Then, since A is one-to-one from $\mathcal{D}(A)$ onto $L_2(\Omega), \mathcal{D}(A)$ must coincide with $H^4(\Omega) \cap H_0^2(\Omega)$.

Proposition4.2. *For the square root $A^{\frac{1}{2}}$ of A, it holds true that $\mathcal{D}\left(A^{\frac{1}{2}}\right) = H_0^2(\Omega)$ together with the estimate*

(4.1.d) $$\|u\|_{\mathrm{H}^2} \leq C\left\|A^{\frac{1}{2}}u\right\|_{L_2}, \quad u \in \mathcal{D}\left(A^{\frac{1}{2}}\right).$$

Proof. Note that $a(u, v)$ is symmetric. It is then kown (cf. [15, Chapter 16]) that for $\frac{1}{2} \leq \theta \leq 1$,

(4.1.e) $$\mathcal{D}(A^{\theta}) \subset H^{4\theta}(\Omega) \cap H_0^2(\Omega).$$

And, for $0 \leq \theta \leq \frac{1}{2}$,

$$\mathcal{D}(A^{\theta}) \subset H^{4\theta}(\Omega).$$

It also holds true that for any $0 \leq \theta \leq 1$,

(4.1.f) $$\|u\|_{\mathrm{H}^{4\theta}} \leq C\left\|A^{\theta}u\right\|_{L_2}, \quad u \in \mathcal{D}(A^{\theta}).$$

The nonlinear operator $f(u)$ is defined by

$$f(u) = -\mu\nabla \cdot \frac{\nabla u}{1 + |\nabla u|^2}$$

$$= -\mu\left[\frac{\Delta u}{1 + |\nabla u|^2} + \frac{\nabla|\nabla u|^2 . \nabla u}{(1 + |\nabla u|^2)^2}\right].$$

By direct calculations (as in the proof of [7, Proposition 2]), we observe that

$$\|f(u) - f(v)\|_{L_2} \leq C[\|u - v\|_{H^2} + (\|u\|_{\mathcal{C}^2} + \|v\|_{\mathcal{C}^2})\|u - v\|_{H^1}].$$

In view of the inequality (4.1.f) (with $\theta = \frac{1}{4}$ and $\theta = \frac{7}{8}$) and the embedding $H^{\frac{7}{2}}(\Omega) \subset \mathcal{C}^2(\overline{\Omega})$, it

is verified that

(4.1.g) $$\|f(u)-f(v)\|_{L_2} \le C\left[\left\|A^{\frac{1}{2}}(u-v)\right\|_{L_2} + \left(\left\|A^{\frac{7}{8}}u\right\|_{L_2} + \left\|A^{\frac{7}{8}}v\right\|_{L_2}\right)\left\|A^{\frac{1}{4}}(u-v)\right\|_{L_2}\right].$$

By the theory of abstract semilinear parabolic equations (see [15, Theorem 4.1]), we can state that, for any $u_0 \in \mathcal{D}\left(A^{\frac{1}{4}}\right) \subset H^1(\Omega)$, there exists a unique local solution to (4.1.a) in the space:

$$u \in \mathcal{C}([0,T_{u_0}];\mathcal{D}(A^{\frac{1}{4}})) \cap \mathcal{C}^1((0,T_{u_0}];L_2(\Omega)) \cap \mathcal{C}((0,T_{u_0}];\mathcal{D}(A)),$$

$T_{u_0} > 0$ being determined by the norm $\left\|A^{\frac{1}{4}}u_0\right\|_{L_2}$ alone.

4.1.2. Global Solution. In order to extend the local solution constructed above to a global solution, we show *a priori* estimate for the local solutions of (4.1.a). Consider a local solution u which is defined on interval $[0,T_u]$:

(4.1.h) $$u \in \mathcal{C}([0,T_u];\mathcal{D}(A^{\frac{1}{4}})) \cap \mathcal{C}^1((0,T_u];L_2(\Omega)) \cap \mathcal{C}((0,T_u];\mathcal{D}(A)).$$

We can then prove the following estimates.

Proposition4.3. *There exist positive constant* δ *and* C such that, *for any local solution* u *in the space* (4.1.h), *it holds true that*

(4.1.i) $$\left\|A^{\frac{1}{4}}u(t)\right\|_{L_2} \le e^{-\delta t}\left\|A^{\frac{1}{4}}u_0\right\|_{L_2} + C, \qquad 0 \le t \le T_u.$$

Here, δ *and* C *are independent of the interval* $[0,T_u]$ *on which u is defined.*

Proof. Consider the inner product of the equation of (4.1.a) and $A^{\frac{1}{2}}u(t)$. Then, since $\frac{\partial u}{\partial n} = 0$ on $\partial\Omega$, it follows that

$$\begin{aligned}\frac{d}{dt}\left\|A^{\frac{1}{4}}u(t)\right\|_{L_2}^2 + \left\|A^{\frac{3}{4}}u(t)\right\|_{L_2}^2 &= -\mu\int_\Omega\left[\nabla\cdot\left(\frac{\nabla u}{1+|\nabla u|^2}\right)\right]A^{\frac{1}{2}}u(t)dx \\ &= \mu\int_\Omega\left(\frac{\nabla u}{1+|\nabla u|^2}\right).\nabla A^{\frac{1}{2}}u(t)dx \\ &\le \frac{\mu}{2}\left\|\nabla A^{\frac{1}{2}}u(t)\right\|_{L_2}.\end{aligned}$$

Noting that $\left\|\nabla A^{\frac{1}{2}}u(t)\right\|_{L_2} \le C\left\|A^{\frac{3}{4}}u(t)\right\|_{L_2}$ and $\left\|\nabla A^{\frac{1}{4}}u(t)\right\|_{L_2} \le C\left\|A^{\frac{3}{4}}u(t)\right\|_{L_2}$, we conclude that

$$\frac{d}{dt}\left\|A^{\frac{1}{4}}u(t)\right\|_{L_2}^2 + \delta\left\|A^{\frac{1}{4}}u(t)\right\|_{L_2}^2 \le C$$

with some constant $\delta > 0$. Solving this differential inequality, we obtain (4.1.i).

By the standard arguments we can then construct for any $u_0 \in \mathcal{D}\left(\mathrm{A}^{\frac{1}{4}}\right)$, a unique global solution to (4.1.a) in the function space:

$$u \in \mathcal{C}([0,\infty); \mathcal{D}(A^{\frac{1}{4}})) \cap \mathcal{C}^1((0,\infty); L_2(\Omega)) \cap \mathcal{C}((0,\infty); H^4(\Omega) \cap H_0^2(\Omega)).$$

The global solution u as well satisfies the same estimates

(4.1.j) $$\left\|\mathrm{A}^{\frac{1}{4}} u(t)\right\|_{L_2} \leq e^{-\delta t} \left\|\mathrm{A}^{\frac{1}{4}} u_0\right\|_{L_2} + C \qquad 0 \leq t < \infty,$$

(4.1.k) $$\|A\, u(t)\|_{L_2} \leq C\, \left(t^{-\frac{3}{4}} + 1\right) \|A\, u_0\|_{L_2}\ , \qquad 0 \leq t < \infty.$$

As shown in chapter 3, however, there is a local solution u to (4.1.a) for any initial value $u_0 \in L_2(\Omega)$. Then, since a smoothing property of the u implies that $u(t_1) \in \mathcal{D}\left(A^{\frac{1}{4}}\right)$ for any $t_1 > 0$, we can extend this local solution to a global one by considering the problem (4.1.a) replacing the initial condition by $u(0) = u_1$, where $u_1 = u(t_1)$. Ultimately, we arrive at the following existence result. For any initial function $u_0 \in L_2(\Omega)$, (4.1.a) possesses a unique global solution in the function space:

(4.1.*l*) $u \in \mathcal{C}([0,\infty); L_2(\Omega)) \cap \mathcal{C}^1((0,\infty); L_2(\Omega)) \cap \mathcal{C}((0,\infty); H^4(\Omega) \cap H_0^2(\Omega))$.

For $0 \leq t < \infty$, set $S(t)u_0 = u(t; u_0)$,where $u(t; u_0)$ is the global solution of (4.1.a) for initial value $u_0 \in L_2(\Omega)$. Then, $S(t)$ defines a family of nonlinear operators acting on $L_2(\Omega)$ with the semigroup property $S(t+s) = S(t)S(s)$ and $S(0) = I$. Moreover, the mapping $G: [0,\infty) \times L_2(\Omega) \longrightarrow L_2(\Omega)$ defined by $G(t, u_0) = S(t)u_0$ is continuous, i.e., $S(t)$ is a continuous semigroup on $L_2(\Omega)$. In this way, (4.1.k) generates a dynamical system $\left(S(t), L_2(\Omega)\right)$. Let $u_0 \in L_2(\Omega)$. In view of (4.1.k), the trajectory $\{S(t)u_0; 1 \leq t < \infty\}$ is a bounded subset of $H^4(\Omega)$. Consequently, it is

relatively compact subset of $L_2(\Omega)$. In particular, its ω-limit set

$$\omega(u_0) = \{\bar{u}; \exists t_n \uparrow \infty \text{ such that } \mathrm{S}(t_n)u_0 \longrightarrow \bar{u} \text{ in } L_2(\Omega)\}$$

is a nonempty set. In addition, if $S(t)u_0 \longrightarrow \bar{u}$ in $L_2(\Omega)$, then it automatically observed that

(4.1.*m*) $$\mathrm{S}(t_n)u_0 \longrightarrow \bar{u} \text{ in } H^s(\Omega)$$

for any $0 \leq s \leq 4$.

As verified in [16], $\left(S(t), L_2(\Omega)\right)$ has furthermore a finite-dimensional attractor which attracts every trajectory at an exponential rate (c.f, [1, 13, and 15]).

4.2 LYAPUNOV FUNCTION

It is already proved in chapter 3, that the following function

(4.2.a) $$\Phi(u) = \frac{1}{2}\int_\Omega [a|\Delta u|^2 - \mu \log(1 + |\nabla u|^2)]dx, \qquad u_0 \in H_0^2(\Omega),$$

becomes a Lyapunov function of our dynamical system $\big(S(t), L_2(\Omega)\big)$.

In what follows, we will consider Φ to be a function from $H_0^2(\Omega)$ to $\mathbb{R}$ (although Φ may be defined on the whole space $H^2(\Omega)$). And we handle it in the triplet

(4.2.b) $$H_0^2(\Omega) \subset L_2(\Omega) \subset H^{-2}(\Omega) = H_0^2(\Omega)',$$

this section is then devoted to verifying various properties of the derivatives $\Phi'(u) \in \mathcal{L}(H_0^2(\Omega), \mathbb{R}) = H^{-2}(\Omega)$ and $\Phi''(u) \in \mathcal{L}\big(H^2(\Omega), H^{-2}(\Omega)\big)$.

4.2.1 Differentiability of $\boldsymbol{\Phi(u)}$. Let us begin with showing differentiability of $\Phi(u)$.

Proposition4.4. Φ: $H_0^2(\Omega) \longrightarrow \mathbb{R}$ *is differentiability with the derivative* $\Phi'(u) = \mathcal{A}u - \mathcal{F}(u) \in H^{-2}(\Omega)$ *for* $u \in H_0^2(\Omega)$. *Here,* $\mathcal{F}(\mathrm{u}) = -\mu\nabla \cdot \left(\frac{\nabla u}{1+|\nabla u|^2}\right)$ *is a nonlinear operator from* $H_0^2(\Omega)$ *into* $H^{-2}(\Omega)$.

Proof. For $u, h \in H_0^2(\Omega)$, we have

$$\|\Delta(u+h)\|_{L_2}^2 - \|\Delta u\|_{L_2}^2 = 2(\Delta u, \Delta h).$$

Therefore,

(4.2.c) $$\|\Delta(u+h)\|_{L_2}^2 - \|\Delta u\|_{L_2}^2 - 2\langle \Delta^2 u, h\rangle_{H^{-2}\times H_0^2} = \|\Delta h\|_{L_2}^2.$$

In the meantime, for a,e $x \in \Omega$, we have

$$\log\{1 + |\nabla[u(x)+h(x)]|^2\} - \log\{1+|\nabla u(x)|^2\}$$
$$= \int_0^1 \frac{d}{d\theta}\log\{1+|\nabla[u(x)+\theta h(x)]|^2\}\,d\theta$$
$$= \int_0^1 \frac{2\nabla u(x).\nabla h(x) + 2\theta|\nabla h(x)|^2}{1+|\nabla[u(x)+\theta h(x)]|^2}d\theta.$$

Moreover, since

$$\frac{1}{1+|\nabla[u(x)+\theta h(x)]|^2} = \frac{1}{1+|\nabla u(x)|^2} - \frac{2\theta\nabla u(x)\cdot\nabla h(x) + \theta^2|\nabla h(x)|^2}{\{1+|\nabla[u(x)+\theta h(x)]|^2\}(1+|\nabla u(x)|^2)},$$

it follows that

$$\left|\log\{1+|\nabla[u(x)+h(x)]|^2\} - \log\{1+|\nabla u(x)|^2\} - \frac{2\nabla u(x)\cdot\nabla h(x)}{1+|\nabla u(x)|^2}\right|$$
$$\le C\{|\nabla h(x)|^2 + |\nabla h(x)|^4\}.$$

We have to use Galrardo- Nireberge's inequality ([15, Theorem 1.37]) to obtain that

$$\|\nabla h\|_4 \le C\|\nabla h\|_{L_2}^{\frac{1}{2}}\|\nabla h\|_{H_1}^{\frac{1}{2}} \le C\|h\|_{H_1}^{\frac{1}{2}}\|h\|_{H_2}^{\frac{1}{2}} \le C\|h\|_{L_2}^{\frac{1}{4}}\|h\|_{H_2}^{\frac{3}{4}}.$$

Hence, (4.2.d)

$$\left|\int_\Omega \log\{1+|\nabla(u+h)|^2\} - \log\{1+|\nabla u|^2\}dx + 2\left\langle\nabla\cdot\left(\frac{\nabla u}{1+|\nabla u|^2}\right), h\right\rangle_{H^{-1}\times H_0^1}\right|$$
$$\le C\|h\|_{L_2}\big(\|h\|_{H^2} + \|h\|_{H^{-2}}^3\big).$$

Combining (4.2.c) and (4.2.d), we conclude that

$$\left|\Phi(u+h)-\Phi(u)-\langle \mathcal{A}u-\mathcal{F}(u),h\rangle_{H^{-2}\times H_0^2}\right| \le C\left[\|\Delta h\|_{L_2}^2+\|h\|_{L_2}\left(\|h\|_{H^2}+\|h\|_{H^{-2}}^3\right)\right].$$

This shows that $\Phi(u)$ is differentiable and the derivative is given by $\Phi'(u)=\mathcal{A}u-\mathcal{F}(u)$ for any $u\in H_0^2(\Omega)$. On the domain $\mathcal{D}(A)\left(\subset H^4(\Omega)\right)$, however, it is possible to observe that $\Phi(u)$ is differentiable in somewhat weak topology.

Proposition 4.5. *If* $u\in\mathcal{D}(A)$, *then* $\Phi(u)=Au-fu\in L_2(\Omega)$. In additions, when the variable *h also runs only in* $\mathcal{D}(A)$, *it holds true that*

(4.2.e) $|\Phi(u+h)-\Phi(u)-\langle \mathcal{A}u-\mathcal{F}(u),h\rangle| \le C\,\|h\|_{L_2}\left(\|h\|_{H^4}+\|h\|_{H^2}+\|h\|_{H^{-2}}^3\right)$.

Proof. Since $u\in\mathcal{D}(A)$ implies $\mathcal{A}u-\mathcal{F}(u)=Au-f(u)$, that first assertions are obvious. In addition, for $h\in\mathcal{D}(A)$, we observe that

$\|\Delta h\|_{L_2}^2=(\Delta h,\Delta h)=\langle\Delta^2 h,h\rangle_{H^{-2}\times H_0^2}=(\Delta^2 h,h)\le\|h\|_{H^4}\|h\|_{L_2}$.

Hence, (4.2.e) is also verified.

Let $u_0\in L_2(\Omega)$. Let $\{u(t);0\le t<\infty\}$ be the trajectory starting from u_0 and $\omega(u_0)$ be its ω-limit set. As an immediate consequence of (4.2.e), we observe that $\Phi(u(\mathrm{t}))$ is differentiable for $t>0$ with the derivative

(4.2.f) $$\frac{d}{dt}\Phi\big(u(\mathrm{t})\big)=-\|Au(t)-fu(t))\|_{L_2}^2$$

Indeed we apply (4.2.e) with $u=u(t)$ and $h=u(t+\Delta t)-u(t)$. Then,

$$\left|\frac{\Phi(u(t+\Delta t))-\Phi(u(t))}{\Delta t}-\left(Au(t)-f(u(t)),\frac{u(t+\Delta t)-u(t)}{\Delta t}\right)\right| \le C\left\|\frac{u(t+\Delta t)-u(t)}{\Delta t}\right\|_{L_2}\left(\|h\|_{H^4}+\|h\|_{H^2}+\|h\|_{H^2}^3\right).$$

As $u(t+\Delta t)-u(t)\to 0$ in $H^4(\Omega)$ due to (4.1.*l*), we obtain (4.2.f). Therefore, along the trajectory $u(t)$, the values of Φ are monotonously decreasing. Furthermore, if $\bar{u}\in\omega(u_0)$, then

(4.2. g) $$\Phi(\bar{u})=\lim_{n\to\infty}\Phi\big(u(t_n)\big)=\inf_{n\to\infty}\big(u(t_n)\big).$$

In particular, Φ takes a constant value on the ω-limit set $\omega(u_0)$.

It is well known that $\omega(u_0)$ is an invariant set of $S(t)$. Indeed, if $\bar{u}\in\omega(u_0)$, then there exists $t_n\uparrow\infty$ such that $S(t_n)u_0\to\bar{u}$ in $L_2(\Omega)$. Then, $S(t+t_n)u_0=S(t)S(t_n)u_0\to S(t)\bar{u}$; hence $S(t)\bar{u}\in\omega(u_0)$, i.e., $S(t)\omega(u_0)\subset\omega(u_0)$. Conversely, we have $S(t_n)u_0=S(t)S(t_n-t)u_0$ for all t_n such that $t_n\ge t$. Since $S(t_n-t)u_0$ is a relatively compact subset of $L_2(\Omega)$, it is possible to assume that $S(t_n-t)u_0\to\bar{v}\in\omega(u_0)$ in $L_2(\Omega)$, i.e., $\bar{u}=S(t)\bar{v}$. This means that $\omega(u_0)\subset S(t)\omega(u_0)$. For any $\bar{u}\in\omega(u_0)$, consider the trajectory $S(t)\bar{u}$.

As verified, $S(t)\bar{u}\in\omega(u_0)$; therefore, (4.2. g) implies consequently, that $\Phi(S(t)\bar{u})\equiv\Phi(\bar{u})$; $\frac{d}{dt}\Phi(S(t)\,\bar{u})\equiv 0$; in particular, $\frac{d}{dt}\Phi(S(t)\,\bar{u})=0$. Equality (4.2. f) then provides that $A\bar{u}-f(\bar{u})=0$. By virtue of Propositions 4.1, this is equivalent to $\Phi'(\bar{u})=0$. We have

thus verified the following proposition.

Proposition 4.6. *For any* $u_0 \in L_2(\Omega)$, *its* ω*-limit set* $\omega(u_0)$ *consists of critical points of* Φ, *in particular, if* $\bar{u} \in \omega(u_0)$ *then* $\Phi'(\bar{u}) = 0$.

Let us next show that $\Phi(u)$ is twice differentiable.

Proposition 4.7. $\Phi' : H_0^2(\Omega) \to H^{-2}(\Omega)$ *is Fréchet differentiable with the derivative* $\Phi''(u) = \mathcal{A} - \mathcal{F}'(u)$, *where* $\mathcal{F}'(u)$ *is the Fréche derivative of* $\mathcal{F} : H_0^2(\Omega) \to H^{-2}(\Omega)$ *which was introduced above. Precisely, for* $u \in H_0^2(\Omega)$, $\mathcal{F}'(u) \in \mathcal{L}(H_0^2(\Omega), H^{-2}(\Omega))$ *is given by*

$$\mathcal{F}'(u)h = -\mu\nabla \cdot \left(\frac{\nabla u}{1+|\nabla u|^2} - \frac{2(\nabla u \cdot \nabla h)\nabla u}{(1+|\nabla u|^2)^2}\right), \qquad h \in H_0^2(\Omega). \tag{4.2.h}$$

Proof. Noting that ∇ is a bounded linear operator from $L_2(\Omega)$ into $H^{-1}(\Omega)$, let us consider $\frac{\nabla u}{1+|\nabla u|^2}$. For $u,\ h \in H_0^2(\Omega)$,

$$\frac{\nabla(u+h)}{1+|\nabla(u+h)|^2} - \frac{\nabla u}{1+|\nabla u|^2} = \frac{(1+|\nabla u|^2)\nabla h - 2(\nabla u.\nabla h)\nabla u - |\nabla h|^2 \nabla u}{(1+|\nabla(u+h)|^2)(1+|\nabla u|^2)}.$$

And, as seen before,

$$\frac{1}{1+|\nabla(u+h)|^2} = \frac{1}{1+|\nabla u|^2} - \frac{2\nabla u \cdot \nabla h + |\nabla h|^2}{(1+|\nabla(u+h)|^2) + (1+|\nabla u(x)|^2)}.$$

Therefore, it follows that

$$\frac{\nabla(u+h)}{1+|\nabla(u+h)|^2} - \frac{\nabla(u)}{1+|\nabla u|^2} - \frac{(1+|\nabla u|^2)\nabla h - 2(\nabla u.\nabla h)\nabla u}{(1+|\nabla u|^2)^2} \le C(|\nabla h|^2 + |\nabla h|^3),$$

and hence

$$\left\| \frac{\nabla(u+h)}{1+|\nabla(u+h)|^2} - \frac{\nabla(u)}{1+|\nabla u|^2} - \frac{(1+|\nabla u|^2)\nabla h - 2(\nabla u.\nabla h)\nabla u}{(1+|\nabla u|^2)^2} \right\|_{L_2}$$
$$\le C\left(\|\nabla h\|_{L_4}^2 + \|\nabla h\|_{L_6}^3\right) \le C\left(\|h\|_{H^2}^2 + \|h\|_{H^2}^3\right).$$

This shows the operator $u \to \frac{\nabla u}{1+|\nabla u|^2}$ is Frechet differentiable from $H_0^2(\Omega)$ into $L_2(\Omega)$.

4.2.2. Gradient Estimates of $\boldsymbol{\Phi'(u)}$. Let $u_0 \in L_2(\Omega)$ and let $\bar{u} \in \omega(u_0)$. As shown by Proposition 4.3, we know that $\Phi'(\bar{u}) = 0$. The goal of this subsection is to establish the Lojasiwecz-Simon inequality for $\Phi'(u)$ at $\bar{u}$ that plays a crucial role in proving convergence of $u(t)$ to $\bar{u}$. That is, there exists some exponent $0 < \theta \le \frac{1}{2}$ for which it holds true that

$$\|\Phi'(u)\|_{H^{-2}} \ge D\,|\Phi(u) - \Phi(\bar{u})|^{1-\theta}, \qquad u \in U(\bar{u}). \tag{4.2.i}$$

Here, $U(\bar{u})$ denotes a neighborhood of $\bar{u}$ in $H_0^2(\Omega)$ and $D > 0$ is some constant. For this purpose, we will follow the methods devised by Chill [18] in which the underlying space must be divided into a sum of critical manifold and its supplement.

Put $L = \Phi''(\bar{u})$. As a verified by Proposition 4.3, $L = \mathcal{A} - \mathcal{F}'(\bar{u})$ is linear operator

from $H_0^2(\Omega)$ into $H^{-2}(\Omega)$. As a general result of the calculus of variations (see [19, Theorem 5.1.1, p.65]), or as is directly verified from (4.2.h), L is a symmetric operator, i.e.,

(4.2.j) $$\langle Lu, v\rangle_{H^{-2}\times H_0^2} = \langle u, Lv\rangle_{H_0^2\times H^{-2}}, \qquad u, v \in H_0^2(\Omega).$$

In addition, L is observed to be a Fredholm operator. Indeed, writing $L = [I - \mathcal{F}'(\bar{u})A^{-1}]A$, we rather consider the operator $I - K$ acting on $H^{-2}(\Omega)$, where $K = \mathcal{F}'(\bar{u})A^{-1}$. As $\mathcal{R}(K) \subset L_2(\Omega)$, K is a compact operator of $H^{-2}(\Omega)$. Therefore, by virtue of the Riesz-Schauder theory, $\mathcal{K}(I-K)$ is a finite-dimensional subspace of $H^{-2}(\Omega)$. And $\mathcal{R}(I-K)$ is a closed subspace of $H^{-2}(\Omega)$ with finite-dimensional such that $\dim \mathcal{K}(I-K) = \operatorname{codim} \mathcal{R}(I-K) = N$. Since A is an isomorphism from $H_0^2(\Omega)$ onto $H^{-2}(\Omega)$, it follows that $\mathcal{K}(L)$ is a finite-dimensional subspace of $H_0^2(\Omega)$ and $\mathcal{R}(L)$ is a closed subspace of $H^{-2}(\Omega)$ with dim $\mathcal{K}(L)$ = codim $\mathcal{R}(L)$ = N. That is, L satisfies the conditions of Fredholm operator. Since $\mathcal{K}(L)$ is a finite -dimensional space, we can regard it as a closed subspace of any space of triplet $H_0^2(\Omega) \subset L_2(\Omega) \subset H^{-2}(\Omega)$. Furthermore, by the same reason, these topologies are mutually equivalent. In the arguments below, we may not clarify the topology of $\mathcal{K}(L)$ when it is easily presumed by the contexts. We introduce the orthogonal projection $P: L_2(\Omega) \to \mathcal{K}(L)$ in $L_2(\Omega)$. We have a direct sum $L_2(\Omega) = H_0 + \mathcal{K}(L)$, where $H_0 = (I-P)L_2(\Omega)$ is the orthogonal supplement of $\mathcal{K}(L)$ in $L_2(\Omega)$. We notice that P is a bounded operator from $H_0^2(\Omega)$ into itself. So, P induces a projection from $H_0^2(\Omega)$ noto $\mathcal{K}(L)$ and a topological direct sum $H_0^2(\Omega) = H_2 + \mathcal{K}(L)$, where $H_2 = (I-P)H_0^2(\Omega)$ is a topological supplement of $\mathcal{K}(L)$ in $H_0^2(\Omega)$. On the other hand, it is easy to see that $\|Pf\|_{H^{-2}} \le C\|f\|_{H^{-2}}$ for all $f \in L_2(\Omega)$. This means that P can be extend by continuation over the space $H^{-2}(\Omega)$. Clearly, P is a bounded operator from $H^{-2}(\Omega)$ into itself and induces a projection from $H^{-2}(\Omega)$ onto $\mathcal{K}(L)$ which yields another topological direct sum $H^{-2}(\Omega) = H_{-2} + \mathcal{K}(L), H_{-2} = (I-P)H^{-2}(\Omega)$ being a topological supplement of $\mathcal{K}(L)$ in $H^{-2}(\Omega)$.

It is also clear that P is symmetric in the sense that

(4.2.k) $$\langle Pu, \varphi\rangle_{H_0^2, H^{-2}} = \langle u, P\varphi\rangle_{H_0^2, H^{-2}}, \quad u \in H_0^2(\Omega), \varphi \in H^{-2}(\Omega).$$

By definition, $LP = 0$ on $H_0^2(\Omega)$; then, (4.2.j) and (4.2.k) provide that $PL = LP = 0$ on $H_0^2(\Omega)$; in particular, $L = (I-P)L$ on $H_0^2(\Omega)$. This concludes that $\mathcal{R}(L) \subset H_{-2}$ must coincide and consequently

(4.2.*l*) L must be an isomorphism from H_2 onto H_{-2}.

Following [19], we set the critical manifold by

$$S = \{u \in H_0^2(\Omega);\ (I-P)\,\Phi'(u) = 0\}.$$

Then, S is verified to be a $\mathcal{C}^1$-manifold of dimension N in a neighborhood of $\bar{u}$, S can be represented as

$$S = \{(g(u_2), u_2;\ u_2 \in \mathcal{K}(L) \to H_2\},$$

g being a $\mathcal{C}^1$ mapping defined in a neighborhood of $\bar{u}_2 \in \mathcal{K}(L)$, where $\bar{u} = \bar{u}_1 + \bar{u}_2$.

According to [18, Theorem 2], we can state the following proposition.

Proposition 4.8. *Assume that the restriction of* Φ *on* S *satisfies* (4.2.i) *in a subset* $U \cap S$, *where* U *is some neighborhood of* $\bar{u}$ *in* $H_0^2(\Omega)$, *with exponent* $\theta \in \left(0, \frac{1}{2}\right]$. *Then,* Φ *itself satisfies* (4.2.i) *in a neighborhood of* $\bar{u}$ *in* $H_0^2(\Omega)$ *with the same exponent* θ.

The desired inequality (4.2.i) on Scan generally be verified, as mentioned in [18, Corollary 3], from analyticity of the Lyapunov function $\Phi(u)$.

This is, however, not true in the present case, for the correspondence $u \mapsto \int_\Omega \log(1 + |\nabla u|^2)dx$ is not analytic in $H_0^2(\Omega)$ due to the fact that $H^1(\Omega) \not\subset C(\bar{\Omega})$. So, we have to utilize upper shifting of spaces.

Let $0 < \varepsilon < \frac{1}{2}$ be arbitrarily fixed. We introduce the domains $\mathcal{D}(\mathcal{A}^{1+\varepsilon})$ and $\mathcal{D}(\mathcal{A}^{\varepsilon})$. Naturally, $\mathcal{D}(\mathcal{A}^{1+\varepsilon}) \subset \mathcal{D}(\mathcal{A}) = H_0^2(\Omega)$ and $\mathcal{D}(\mathcal{A}^{\varepsilon}) \subset H^{-2}(\Omega)$. And, since $\mathcal{A}^{1+\varepsilon} = \mathcal{A}\mathcal{A}^{\varepsilon}$, $\mathcal{A}$ is an isomorphism from $\mathcal{D}(\mathcal{A}^{1+\varepsilon})$ onto $\mathcal{D}(\mathcal{A}^{\varepsilon})$. Then, by the same reason as before, P is bounded operator from $\mathcal{D}(\mathcal{A}^{1+\varepsilon})$ into itself and induces a topological direct sum $\mathcal{D}(\mathcal{A}^{1+\varepsilon}) = H_{2,\varepsilon} + \mathcal{K}(L)$, where $H_{2,\varepsilon} = (I-P)\mathcal{D}(\mathcal{A}^{1+\varepsilon})$. Similarly, P is a bounded operator from $\mathcal{D}(\mathcal{A}^{\varepsilon})$ into itself and induces a topological direct sum $\mathcal{D}(\mathcal{A}^{\varepsilon}) = H_{-2,\varepsilon} + \mathcal{K}(L)$, where $H_{-2,\varepsilon} = (I-P)\mathcal{D}(\mathcal{A}^{\varepsilon})$. Obviously, $H_{2,\varepsilon} \subset H_2$ and $H_{-2,\varepsilon} \subset H_{-2}$. We can verify that (4.2.*l*) still holds true in the shifted spaces.

Proposition 4.9. *L is an isomorphism form* $H_{2,\varepsilon}$ onto $H_{-2,\varepsilon}$.

Proof. As L is a bounded operator from $\mathcal{D}(\mathcal{A}^{1+\varepsilon})$ into $\mathcal{D}(\mathcal{A}^{\varepsilon})$, so is from $H_{2,\varepsilon}$ into $\mathcal{D}(\mathcal{A}^{\varepsilon})$. So, it suffices to prove that $L\left(H_{2,\varepsilon}\right) = H_{-2,\varepsilon}$. Let $\varphi \in L\left(H_{2,\varepsilon}\right)$; then, $\varphi = Lu$ and $u = (I-P)v$ with some $v \in \mathcal{D}(\mathcal{A}^{1+\varepsilon})$; therefore, $\varphi = (I-P)v = Lu$ with some $u \in \mathcal{D}(\mathcal{A})$; furthermore, $\mathcal{A}u = \mathcal{F}'(\bar{u})u + \varphi \in \mathcal{D}(\mathcal{A}^{\varepsilon})$; therefore, $u \in \mathcal{D}(\mathcal{A}^{1+\varepsilon})$ and $\varphi = (I-P) \in L\left(H_{2,\varepsilon}\right)$. We furthermore verify analyticity of $\Phi(u)$ for $u \in \mathcal{D}(\mathcal{A}^{1+\varepsilon})$.

Proposition 4.10. $\Phi: \mathcal{D}(\mathcal{A}^{1+\varepsilon}) \to \mathbb{R}$ *is analytic.*

Poof. Notice that $\mathcal{D}(\mathcal{A}^{1+\varepsilon}) = \mathcal{D}\left(\mathcal{A}^{\frac{1}{2}+\varepsilon}\right) \subset H^{2+4\varepsilon}(\Omega)$ due to (4.1.e). Hence, $u \in \mathcal{D}(\mathcal{A}^{1+\varepsilon})$ implies $\nabla u \in C(\bar{\Omega})$. Then, for small variable $h \in \mathcal{D}(\mathcal{A}^{1+\varepsilon})$, it is possible to develop

$$\log(1 + |\nabla(u+h)|^2) - \log(1 + |\nabla u|^2) = \log\left(1 + \frac{2\nabla u \cdot \nabla h + |\nabla h|^2}{1 + |\nabla u|^2}\right)$$
$$= \sum_{n=1}^{\infty} \frac{(-1)^{n-1}}{n}\left(\frac{2\nabla u \cdot \nabla h + |\nabla h|^2}{1 + |\nabla u|^2}\right)^n.$$

This directly yields analyticity of $u \to \int_\Omega \log(1 + |\nabla u|^2)\, dx$ on $\mathcal{D}(\mathcal{A}^{1+\varepsilon})$. It is now ready to show the inequality (4.2.i) on S. We first observe that S actually lies in $\mathcal{D}(\mathcal{A}^{1+\varepsilon})$. Indeed, if $u \in S$, then $\Phi'(u) = P\Phi'(u)$; therefore, $\mathcal{A}u = \mathcal{F}(u) + P\Phi'(u) \in L_2(\Omega)$; hence, by

definition, $u \in \mathcal{D}(\mathcal{A}) \subset \mathcal{D}\left(\mathcal{A}^{\frac{3}{2}}\right)$. Thus, $S = \{u \in \mathcal{D}(\mathcal{A}^{1+\varepsilon}); (I-P)\Phi'(u) = 0\}$. As before, S is determined by the operator $G: \mathcal{D}(\mathcal{A}^{1+\varepsilon}) \to H_{-2,\varepsilon}$ given by $G(u_1, u_2) = (I-P)\Phi'(u_1 + u_2)$ for $u_1 \in H_{2,\varepsilon}$ $u_2 \in \mathcal{K}(L)$. As we know that $D_1 G(\bar{u}) = L_{|H_{2,\varepsilon}}$ is an isomorphism, S can be represented in a neighborhood of $\bar{u}$ as

$$S = \{(g(u_2), u_2);\ u_2 \in \mathcal{K}(L), g: \mathcal{K}(L) \to H_{2,\varepsilon}\}.$$

Now, as Φ is analytic, g is also analytic in a neighborhood of $\bar{u}_2$, where $\bar{u} = \bar{u}_1 + \bar{u}_2$, which means that S is an analytic manifold. Remembering that Φ is analytic on $\mathcal{D}(\mathcal{A}^{1+\varepsilon})$, we next apply Lojasiewics's classical result [20] in finite-dimensional spaces to $\Phi_{|S}$. Then, for some exponent $\theta = \left(0, \frac{1}{2}\right]$,

$$\|\Phi'(u)\|_{H^{-2}} \geq C|\Phi(u) - \Phi(\bar{u})|^{1-\theta}$$

for u in a neighborhood of $\bar{u}$ on S.

As stated above, Proposition 4.5 thus provides the desired inequality (4.2.i) in a neighborhood of the whole space $H_0^2(\Omega)$ of $\bar{u}$.

4.3 CONVERGENCE RESULTS

Let $u_0 \in L_2(\Omega)$ and $\bar{u} \in \omega(u_0)$. And let $t_n \uparrow \infty$ be a sequence such that $u(t_n) \to \bar{u}$ in $H_0^2(\Omega)$ due to (4.1.*m*). We can then show that, once the trajectory approaches sufficiently close to $\bar{u}$, it must remain in a neighborhood forever.

Proposition 4.11. *Let $r > 0$ be the radius for which the gradient inequality* (4.2.i) *holds true in the ball $B^{H_0^2}(\bar{u}; r)$ and let t_N be such that $u(t_N) \in B^{H_0^2}(\bar{u}; r)$. Then, if $u(t) \in B^{H_0^2}(\bar{u}; r)$ for every $t \in [t_N, T]$, where $T(\geq t_N)$ is any time, then it holds that*

(4.3.a) $$\|u(t) - u(t_N)\|_{H_0^2} \leq C[\Phi(u(t_N) - \Phi(\bar{u})]^{\frac{\theta}{2}} \quad for\ every\ t \in [t_N, T],$$

here $C > 0$ is a constant independent of T.

Proof. For $0 \leq t \leq T$,

$$\frac{d}{dt}\left[\Phi\left(u(t)\right) - \Phi(\bar{u})\right]^{\theta} = \theta\left[\Phi\left(u(t)\right) - \Phi(\bar{u})\right]^{\theta-1}\frac{du}{dt}\Phi\left(u(t)\right)$$

$$= \theta\left[\Phi\left(u(t)\right) - \Phi(\bar{u})\right]^{\theta-1}\left(\Phi'\left(u(t)\right), \frac{du}{dt}(t)\right)$$

$$= \theta\left[\Phi\left(u(t)\right) - \Phi(\bar{u})\right]^{\theta-1}\left\|\Phi'\left(u(t)\right)\right\|_{L_2}\left\|\frac{du}{dt}(t)\right\|_{L_2}.$$

Here, we used the equality

$$\frac{du}{dt}(t) = -Au(t) + f\left(u(t)\right) = -\Phi'\left(u(t)\right).$$

By virtue of (4.2.i),

$$\frac{d}{dt}\left[\Phi\big(u(t)\big)-\Phi(\bar{u})\right]^{\theta}\geq C\left[\Phi\big(u(t)\big)-\Phi(\bar{u})\right]^{\theta-1}\left\|\Phi'\big(u(t)\big)\right\|_{H^2}\left\|\frac{du}{dt}(t)\right\|_{L_2}\geq C\left\|\frac{du}{dt}(t)\right\|_{L_2}.$$

Integration in $[t_N,t]$ yields that

$$\left[\Phi\big(u(t_N)\big)-\Phi(\bar{u})\right]^{\theta}-\left[\Phi\big(u(t)\big)-\Phi(\bar{u})\right]^{\theta}\geq C\int_{t_N}^{t}\left\|\frac{du}{dt}(t)\right\|_{L_2}ds.$$

Therefore,

(4.3.b)

$$\|u(t)-u(t_N)\|_{L_2}\leq\int_{t_N}^{t}\left\|\frac{d}{dt}(t)\right\|_{L_2}ds\leq C^{-1}\left\{\left[\Phi\big(u(t_N)\big)-\Phi(\bar{u})\right]^{\theta}-\left[\Phi\big(u(t)\big)-\Phi(\bar{u})\right]^{\theta}\right\}.$$

Hence,

$$\|u(t)-u(t_N)\|_{L_2}\leq C^{-1}\left[\Phi\big(u(t_N)\big)-\Phi(\bar{u})\right]^{\theta}.$$

We next apply the estimate

$$\|u\|_{H_0^2}\leq C\|Au\|_{L_2}^{\frac{1}{2}}\|u\|_{L_2}^{\frac{1}{2}},\qquad u\in\mathcal{D}(A),$$

which follows from (4.1.d) to $u(t)-u(t_N)$. Then, in view of(4.1. k), (4.3, a) is obtained.

Choose a time t_N so that $\|u(t_N)-\bar{u}\|_{H_0^2}\leq\frac{r}{3}$ and $C\left[\Phi\big(u(t_N)\big)-\Phi(\bar{u})\right]^{\frac{\theta}{2}}\leq\frac{r}{3}$, here C is the constant obtained in (4.3.a). Then, if $u(t)\in B^{H_0^2}(\bar{u};r)$ for every $t\in[t_N,T],T(\geq t_N)$ being any time, then

$$\begin{aligned}\|u(t)-\bar{u}\|_{H_0^2}&\leq\|u(t)-u(t_N)\|_{H_0^2}+\|u(t_N)-\bar{u}\|_{H_0^2}\\&\leq C\left[\Phi\big(u(t_N)\big)-\Phi(\bar{u})\right]^{\frac{\theta}{2}}+\|u(t_N)-\bar{u}\|_{H_0^2}\leq\frac{2r}{3},\end{aligned}$$

i.e., $u(t)\in\bar{B}^{H_0^2}\left(\bar{u};\frac{2r}{3}\right)$ for $t_N\leq t\leq T$.

This means that the trajectory staring from u_0 is trapped in $B^{H_0^2}(\bar{u};r)$ for all $t\geq t_N$.
We now arrive at the main result.

Theorem 4.1. *Let $u_0\in L_2(\Omega)$ and $\bar{u}\in\omega(u_0)$. Let $t_N$be the time chosen above. Then,*

(4.3.c) $$\|u(t)-\bar{u}\|_{L_2}\leq C\left[\Phi\big(u(t_N)\big)-\Phi(\bar{u})\right]^{\theta}\qquad for\ every\ t\in[t_N,\infty).$$

Proof. We already know that, for all $t_N\leq t<\infty$, $u(t)\in B^{H_0^2}(\bar{u};r)$. So, the same argument as in the proof of Proposition 4.1 is available to $u(t)$ for every $t>t_N$. Let $t_N\leq t<t_n$, where t_n is the sequence introduced above. Then, by the same way as for (4.3.b), we obtain that

$$\|u(t_n)-u(t)\|_{L_2}\leq C^{-1}\left\{\left[\Phi\big(u(t)\big)-\Phi(\bar{u})\right]^{\theta}-\left[\Phi\big(u(t_N)\big)-\Phi(\bar{u})\right]^{\theta}\right\}.$$

Fixing t, let t_n tend to infinity. Then, in view of (4.2. g), (4.3.c) is verified.

5

Homogeneous Stationary Solutions to Epitaxial Growth Model under Dirichlet Conditions

In the previous chapters 3 and 4, we constructed a dynamical system generated by the problem and showed that every trajectory converges to some stationary solution as $t \to \infty$. This chapter is then devoted to investigating stability or instability of the null solution which is a unique homogeneous stationary solution. Indeed, we shall prove that, when the surface diffusion is stronger than roughening, the null solution is globally stable, and in the meantime, when the roughening is stronger than the surface diffusion, the null solution is unstable.

5.1 REVIEWS OF KOWN RESULTS

We assume that Ω is a rectangular domain or a $\mathcal{C}^4$ domain.

In this section, let us review known results obtain in the previous chapters 3, 4. As in chapters 3 and 4, we formulate (1.1) as the Cauchy problem for a semilinear abstract evolution equation

$$\begin{cases} \frac{du}{dt} + Au = f(u), & 0 < t < \infty, \\ u(0) = u_0, \end{cases} \tag{5.1.a}$$

in the underlying space $X = L_2(\Omega)$. Here, A is an associated linear operator in the framework of a triplet $H_0^2(\Omega) \subset L_2(\Omega) \subset H^{-2}(\Omega)\ (= H_0^2(\Omega)')$ with a symmetric sesquilinear from defined by

$$a(u, v) = \int_\Omega \Delta u \cdot \Delta \overline{v}\, dx, \qquad u, v \in H_0^2(\Omega).$$

Then, A is a positive definite self-adjoint operator of X with domain $\mathcal{D}(A) \subset H_0^2(\Omega)$. The operator A is considered as a realization of the fourth order operator $a\Delta^2$ in X under the conditions $u = \frac{\partial u}{\partial n} = 0$ on $\partial\Omega$. As seen by Proposition 4.1, our assumption Ω yields a characterization of $\mathcal{D}(A)$ in such a way that $\mathcal{D}(A) = H^4(\Omega) \cap H_0^2(\Omega)$ with norm equivalence. As the sesquilinear form is symmetric, $\mathcal{D}\left(A^{\frac{1}{2}}\right)$ coincides with the form domain, i.e., $\mathcal{D}\left(A^{\frac{1}{2}}\right) = H_0^2(\Omega)$ with norm equivalence. By interpolation, we can then verify that, for $\frac{1}{2} \le \theta \le 1$,

$$\mathcal{D}(A^\theta) \subset H^{4\theta}(\Omega) \cap H_0^2(\Omega),$$

And for $0 \le \theta \le \frac{1}{2}$,

$$\mathcal{D}\left(A^{\theta}\right) \subset H^{4\theta}(\Omega).$$

In addition, for any $0 \leq \theta \leq 1$, the inequality

(5.1.b) $$\|u\|_{\mathrm{H}^{4\theta}} \leq C\left\|A^{\theta}u\right\|_{L_2}, \quad u \in \mathcal{D}\left(A^{\theta}\right),$$

is satisfied, namely, the embedding described above is continuous. Meanwhile, f is a nonlinear operator defined by

(5.1.c) $$f(u) = \mu\nabla \cdot \frac{\nabla u}{1+|\nabla u|^2}$$

$$= -\mu\left[\frac{\Delta u}{1+|\nabla u|^2} + \frac{\nabla|\nabla u|^2.\nabla u}{(1+|\nabla u|^2)^2}\right], \quad u \in \mathcal{D}\left(A^{\frac{7}{8}}\right).$$

Note that, since $\mathcal{D}\left(A^{\frac{7}{8}}\right) \subset H^{\frac{7}{2}}$ due to (5.1.b) and $H^{\frac{7}{2}} \subset \mathcal{C}^2(\overline{\Omega})$, $u \in \mathcal{D}\left(A^{\frac{7}{8}}\right)$ certainly implies $f(u) \in L_2(\Omega)$. Furthermore, according to (4.1.g), it holds true that

(5.1.d)

$$\|f(u)-f(v)\|_X \leq C\left[\left\|A^{\frac{1}{2}}(u-v)\right\|_X + \left(\left\|A^{\frac{7}{8}}u\right\|_X + \left\|A^{\frac{7}{8}}v\right\|_X\right)\left\|A^{\frac{1}{4}}(u-v)\right\|_X\right],$$

$$u, v \in \mathcal{D}\left(A^{\frac{7}{8}}\right).$$

The general result on abstract semilinear evolution equation (c.f [15, Theoream 4.1]) readily provides local existence of solutions. For any $u_0 \in \mathcal{D}\left(A^{\frac{1}{4}}\right)$, (5.1.a) possesses a unique local solution. As a matter of fact, we can formulate (1.1) even in a larger underlying space $H^{-2}(\Omega)$, there exists a unique local solution. Combining these two existence results, we can claim that, for any $u_0 \in L_2(\Omega) = X$, (5.1.a) possesses a unique local solution in the function space:

(5.1.e) $$u \in \mathcal{C}([0, T_{u_0}]; \mathcal{D}(A)) \cap \mathcal{C}((0, T_{u_0}]; X)) \cap \mathcal{C}^1((0, T_{u_0}]; X),$$

$T_{u_0} > 0$ being determined by the norm $\|u_0\|_X$ alone.

In the subsequent sections, we need to use differentiability of $f(u)$.

Proposition 5.1. $f: \mathcal{D}\left(A^{\frac{7}{8}}\right) \to X$ *is Fréchet differentiable with derivative*

$$f'(u)h = -\mu\nabla.\left(\frac{\nabla h}{1+|\nabla u|^2} - \frac{2(\nabla u.\nabla u)\nabla u}{(1+|\nabla u|^2)^2}\right), \quad u, h \in \mathcal{D}\left(A^{\frac{7}{8}}\right).$$

Proof. Let $u, h \in \mathcal{D}\left(A^{\frac{7}{8}}\right)$. Form (5.1.c) it follows that

$$f(u+h) - f(u) = -\mu\nabla.\left[\left(\frac{1}{1+|\nabla(u+h)|^2} - \frac{1}{1+|\nabla u|^2}\right)\nabla(u+h)\right]$$

$$-\mu\nabla.\left(\frac{\nabla(u+h)-\nabla u}{1+|\nabla(u+h)|^2}\right)$$

$$=-\mu\nabla.\frac{-2\nabla u.\nabla h-|\nabla h|^2\,\nabla(u+h)}{1+\nabla|(u+h)|^2}$$

$$-\mu\nabla.\left[\frac{-2\nabla u.\nabla h-|\nabla h|^2\,\nabla(u+h)}{1+\nabla|(u+h)|^2}\right]-\mu\nabla.\left(\frac{\nabla h}{1+|\nabla u|^2}\right).$$

By the similar calculation as for (5.1.e)

$$\|f(u+h)-f(u)-f'(u)h\|_X\le C\left\|A^{\frac{7}{8}}h\right\|_X^2\left(\left\|A^{\frac{7}{8}}u\right\|_X+\left\|A^{\frac{7}{8}}h\right\|_X\right).$$

This means that $f:\mathcal{D}\left(A^{\frac{7}{8}}\right)\to X$ is Fréchet differentiable at u.

Proposition 5.2. *Let* $u\in\mathcal{D}\left(A^{\frac{7}{8}}\right)$ *vary in a ball* $B^{\mathcal{D}\left(A^{\frac{1}{2}}\right)}(0;1)$. *Then,* $f'(u)$ *satisfies the Lipschitz condition*

$$\|[f'(u)-f'(v)]h\|_X\le C\left\|A^{\frac{1}{2}}(u-v)\right\|_X\left\|A^{\frac{7}{8}}h\right\|_X,$$

$$u,v\in\mathcal{D}\left(A^{\frac{7}{8}}\right)\cap B^{\mathcal{D}\left(A^{\frac{1}{2}}\right)}(0;1);h\in\mathcal{D}\left(A^{\frac{7}{8}}\right).$$

Proof. From the formula giving $f'(u)$, we can estimate directly the difference $f'(u)-f'(v)$. Proposition 4.3 provides *a priori* estimates for local solutions obtained above in the space (5.1.e). Indeed, any local solution to (5.1.a) on interval $[0,T_u]$ satisfies the estimate

$$\|u(t)\|_X^2\le e^{-2\delta t}\|u_0\|_X^2+\mu\delta^{-1},\qquad 0\le t\le,$$

with some fixed exponent $\delta>0$. Then, by standard argument, we conclude that, for any $u_0\in X$, (5.1.a) possesses a unique global solution u in the function space:

(5.1.f) $$u\in\mathcal{C}([0,\infty];X)\cap\mathcal{C}((0,\infty];\mathcal{D}(A))\cap\mathcal{C}^1((0,\infty];X).$$

Furthermore, u also satisfies the same estimate

(5.1.g) $$\|u(t)\|_X^2\le e^{-2\delta t}\|u_0\|_X^2+\mu\delta^{-1},\qquad 0\le t<\infty,$$

which shows dissipation of u. Set a nonlinear semigroup $S(t),0\le t<\infty,$ on X by $S(t)u_0=u(t;u_0)$, using the global solution $u(t;u_0)$ to (5.1.a) with initial data $u_0\in X$. Then, we obtain a dynamical system $(S(t),X)$ generated by (5.1.a). The dissipate estimates yield existence of a finite-dimensional attractor $\mathcal{M}$ which attracts every trajectory $S(t)u_0$ at an exponential rate. Such an attractor is called the exponential attractor. In particular, we know that every trajectory has a nonempty ω-limit set $\omega(u_0)$.

As shown in section 3.4, our system$(S(t),X)$ admits a Lyapunov function of the form

$$\Phi(u) = \frac{1}{2}\int_{\Omega} [a|\Delta u|^2 - \mu \log(1 + |\nabla u|^2)]dx, \qquad u \in H_0^2(\Omega).$$

it is seen that, for $\bar{u} \in \mathcal{D}(A), \Phi'(\bar{u}) = 0$ and $A(\bar{u}) = f(\bar{u})$ (i.e., $\bar{u}$ is a stationary solution) are equivalent. From this equivalence, we see that, if $\bar{u} \in \omega(u_0)$, then $\bar{u}$ must be a stationary solution of (5.1.a). The set $\omega(u_0)$ consists only of stationary solution.

Convergence of Solution. The objective of chapter 4 was then to show that $\omega(u_0)$ is a singleton for every u_0. We proved that$\Phi(u)$ satisfies the Lojasiwicz- Simon inequality

$$\|\Phi'(u)\|_{H^{-2}} \geq D|\Phi(u) - \Phi(\bar{u})|^{1-\theta}$$

in a neighborhood of $\bar{u}$, where $\bar{u} \in \omega(u_0)$, with some exponent $0 < \theta \leq \frac{1}{2}$. This inequality readily implies that

$$\|S(t)u_0 - \bar{u}\|_X \leq C[\Phi(S(t)u_0) - \Phi(\bar{u})]^{\theta}.$$

As $\Phi(S(t)u_0)$ converges to $\Phi(\bar{u})$ as $t \to \infty$, we observe that $S(t)u_0$ converges to $\bar{u}$ in X with some rate of convergence.

5.2 LINEARIZED STABILITY

Let us now investigate stability and instability for the stationary solution (5.1.a). For this purpose, we will employ the general methods for abstract evolution equations, see [1, 13].

Let $\bar{u} \in \mathcal{D}(A)$ be any stationary solution to (5.1.a), i.e., $A(\bar{u}) = f(\bar{u})$. By Propositions 5.1 and 5.2, $f: \mathcal{D}\left(A^{\frac{7}{8}}\right) \to X$ is of class $\mathcal{C}^{1.1}$. It is known that this condition in turn implies Fréchet differentiability of semigroup. Indeed, for $0 < t < t^*$ where $t^* > 0$ is arbitrarily fixed time, $S(t): \mathcal{D}\left(A^{\frac{1}{2}}\right) \to \mathcal{D}\left(A^{\frac{1}{2}}\right)$ is of class $\mathcal{C}^{1.1}$ in a neighborhood $\mathcal{O}'(\bar{u})$ of $\bar{u}$ in $\mathcal{D}\left(A^{\frac{1}{2}}\right)$ together with the estimate

(5.2.a) $$\|S(t)'u - S(t)'v\|_{\mathcal{L}\left(\mathcal{D}\left(A^{\frac{1}{2}}\right)\right)} \leq C\left\|A^{\frac{1}{2}}(u - v)\right\|_X, \qquad u, v \in \mathcal{O}'(\bar{u});\ 0 < t < t^*.$$

For the detailed proof, see the proof of [15, Subsection 6.6.3].

We have to assume a spectral separation condition of the form

$$\sigma\left(A - f'(\bar{u})\right) \cap \{\lambda \in \mathbb{C}; \operatorname{Re}\lambda = 0\} = \emptyset.$$

Then, since $S(t)'\bar{u} = e^{-t\bar{A}}$, where $\bar{A} = A - F'(\bar{u})$, we have in turn a spectral separation for $S(t)'\bar{u}$ of the form

(5.2.b) $$\sigma(S(t)'\bar{u}) \cap \{\lambda \in \mathbb{C};\ |\lambda| = 1\} = \emptyset.$$

According to [15, Theorem 6.9], under (5.2.a) and (5.2.b), a smooth local unstable manifold $\mathcal{M}_+(\bar{u}; \mathcal{O})$ can be constructed in a neighborhood $\mathcal{O}$of $\bar{u}$ in $\mathcal{D}\left(A^{\frac{1}{2}}\right)$.

When

(5.2.c) $$\sigma\big(A-F'(\bar{u})\big) \subset \{\lambda \in \mathbb{C}; \operatorname{Re}\lambda > 0\},$$

we have $\sigma(S(t)'\bar{u}) \subset \{\lambda \in \mathbb{C};\ |\lambda| < 1\}$ and $\mathcal{M}_+(\bar{u};\mathcal{O})$ reduces to a singleton $\{\bar{u}\}$. Whence, if (5.2.c) takes place, $\bar{u}$ is stable. In the meantime, when

(5.2.d) $$\sigma(A - f'(\bar{u})) \cap \{\lambda \in \mathbb{C}; \operatorname{Re}\lambda < 0\} \neq \emptyset,$$

we have $\sigma(S(t)'\bar{u}) \cap \{\lambda \in \mathbb{C};\ |\lambda| > 1\} \neq \emptyset$ and $\mathcal{M}_+(\bar{u};\mathcal{O})$ is not trivial. Whence, if (5.2.d) takes place, $\bar{u}$ is unstable. Let us now apply these discussions to the null solution $\bar{u} \equiv 0$.

We see from Proposition 5.1 that $(A - f'(0) = a\Delta^2 + \mu\Delta$. So, it is necessary to investigation the spectrum of the operator $a\Delta^2 + \mu\Delta$. To this end, we will introduce a normalization of A; indeed, when $a = 1$, we denote $A = A_1$; and, regarding a as a positive parameter, we denote in general $A = aA_1$. Of course, A_1 is a realization of the operator Δ^2 in $L_2(\Omega)$ under the homogenous Dirichlet condition $\partial\Omega$, and is a positive definite self- adjoin operator of X. As verified above, we have $\mathcal{D}(A_1) = H^4(\Omega)\cap H_0^2(\Omega)$ with norm equivalence and $\mathcal{D}\left(A_1^{\frac{1}{2}}\right) = H_0^2(\Omega)$ with norm equivalence. We here notice a fact that the mapping $u \mapsto \frac{\|\nabla u\|_X}{\|\Delta u\|_X}$ is continuers from $H_0^2(\Omega) - \{0\}$ into $\mathbb{R}$ and has a maximum on the sphere $\|A_1 u\|_X = 1$ because of compact embedding,

$$\mathcal{D}(A_1) \subset \mathcal{D}\left(A_1^{\frac{1}{2}}\right).$$

Put

(5.2.e) $$d \equiv \max_{\|A_1 u\|_X = 1} \frac{\|\nabla u\|_X}{\|\Delta u\|_X}.$$

In other words, the d is an optimal coefficient in the inequality

$$\|\nabla u\|_X \leq d\|\Delta u\|_X \qquad u \in \mathcal{D}(A_1).$$

Stability of the null solution is then determined by dominance in magnitude of the two coefficients a and μ to the other but with weight d^{-2} for a.

Theorem 5.1. *If $ad^{-2} > \mu$, then the null solution is stable. If $ad^{-2} < \mu$, then the null solution is unstable.*

Proof. We notice that $a\Delta^2 + \mu\Delta$ is a self-adjoint operator of X whose domain $H^4(\Omega)\cap H_0^2(\Omega)$ is compactly embedded in $L_2(\Omega)$. Therefore, the spectrum set $\sigma(a\Delta^2 + \mu\Delta)$ is contained in the real axis and consists of point spectrum alone. For any $u \in \mathcal{D}(A_1) - \{0\}$, we observe that

$$(a\Delta^2 + \mu\Delta, u) = a\|\Delta u\|_X^2 - \mu\|\nabla u\|_X^2 \geq (ad^{-2} - \mu)\|\nabla u\|_X^2 > 0,$$

provided $ad^{-2} > \mu$. Therefore, if μ is dominated as $\mu < ad^{-2}$, then $\sigma(a\Delta^2 + \mu\Delta) \subset (0, \infty)$ and the null solution is stable. To the contrary, if μ is large enough so that $\mu > ad^{-2}$,i.e., $d > \sqrt{\frac{a}{\mu}}$, then there exists an element $u_0 \in \mathcal{D}(A_1) - \{0\}$ such that $\|\nabla u_0\|_X > \sqrt{\frac{a}{\mu}}\|\Delta u_0\|_X$. Therefore,

$$(a\Delta^2 u_0 + \mu\Delta u_0, u_0) = a\|\Delta u_0\|_X^2 - \mu\|\nabla u_0\|_X^2 < 0.$$

This means that $\sigma(a\Delta^2 + \mu\Delta) \cap (-\infty, 0) \neq \emptyset$. Hence, the null solution is unstable.

As a matter of fact, when $ad^{-2} > \mu$, every trajectory converges to 0, that is, the null solution is globally stable.

Theorem 5.2. *Let $ad^{-2} > \mu$. For any $u_0 \in X, S(t)\,u_0$ converges to 0 as $t \to \infty$ at an exponential rate.*

Proof. Multiply the equation (1.1) by $\overline{u}$ and integrate the product in Ω. Then,

$$\frac{1}{2}\frac{d}{dt}\int_\Omega |u|^2\,dx + a\int_\Omega |\Delta u|^2\,dx = \mu\int_\Omega \frac{|\Delta u|^2}{1+|\nabla u|^2}\,dx \le \mu\int_\Omega |\nabla u|^2\,dx.$$

It then follows from (5.2.e) that

$$\frac{1}{2}\frac{d}{dt}\|u(t)\|_X^2 dx \le -(ad^{-2} - \mu)\|\nabla u(t)\|_X^2 \le -(ad^{-2} - \mu)D^{-1}\|u(t)\|_X^2,$$

where $D > 0$ is a coefficient for the Pincare inequality given by (5.3.a) below. Hence,

$\|u(t)\|_X \le e^{-(ad^{-2}-\mu)D^{-1}}\|u_0\|_X$ for $t \ge 0$.

5.1 ESTIMATION OF *d* FROM ABOVE

The weight constant d can easily be estimated from above from the Poincare inequality

(5.3.a) $$\|u\|_X \le D\|\nabla u\|_X \qquad u \in H_0^2(\Omega).$$

Theorem 5.3. *Let d be the constant determined by* (5.2.e) *and let D be an optimal coefficient for the Poincare inequality* (5.3.a). *Then, it always holds true that $d \le D$.*

Proof. Indeed,

$$\|\nabla u\|_X^2 = (-\Delta u, u) \le \|\Delta u\|_X\|u\|_X \le D\|\Delta u\|_X\|\nabla u\|_X, \qquad u \in H_0^2(\Omega).$$

Therefore, $\|\nabla u\|_X \le D\|\Delta u\|_X$ for $u \in H_0^2(\Omega)$. Of course, it holds that $\|\nabla u\|_X \le D\|\Delta u\|_X$ for $u \in \mathcal{D}(A_1)$.

The coefficient D is usually estimated by the band width of Ω, see [2, Section 4.7].

The rest of this section is devoted to obtaining an optimal estimate of D in the specific case where

$$\Omega = \{(x, y); 0 < x < l_1, 0 < y < l_2\}.$$

Let Λ denotes a realization of $-\Delta$ equipped with the boundary condition $u = 0$ in $L_2(\Omega)$. Then, Λ is a positive definite self-adjoint operator of $L_2(\Omega)$ with domain $\mathcal{D}(\Lambda) = H^2(\Omega) \cap H_0^1(\Omega)$.

Furthermore, since its minimal eigenvalue is $\frac{\pi^2}{l_1^2} + \frac{\pi^2}{l_2^2}$ with eigenfunction $\sin\frac{\pi^2}{l_1^2}x + \frac{\pi^2}{l_2^2}y$, we have $(\Lambda u, u) \ge \frac{\pi^2}{l_1^2} + \frac{\pi^2}{l_2^2}\|u\|_X^2$ for any $u \in \mathcal{D}(\Lambda)$. It then follows that

$$\|\nabla u\|_X^2 = (-\Delta u, u) \ge \left(\frac{\pi^2}{l_1^2} + \frac{\pi^2}{l_2^2}\right)\|u\|_X^2, \qquad u \in \mathcal{D}(\Lambda).$$

Since $\mathcal{D}(\Lambda)$ is dense in $\mathcal{D}\left(\Lambda^{\frac{1}{2}}\right)$ which coincides with $H_0^1(\Omega)$, this inequality holds true for every $u \in H_0^1(\Omega)$. Hence, (5.3.a) takes place with $D = \left(\frac{\pi^2}{l_1^2} + \frac{\pi^2}{l_2^2}\right)^{-\frac{1}{2}}$ and, in fact, this is optimal.

Theorem 5.4. *Let $\Omega = (0, l_1) \times (0, l_2)$. Then, an optimal constant D for the Poincare inequality* (5.3.a) *is given by $D = \frac{l_1 l_2}{\pi\sqrt{l_1^2 + l_2^2}}$. Consequently, the weight constant d is estimated by $d \leq \frac{l_1 l_2}{\pi\sqrt{l_1^2 + l_2^2}}$.*

Corollary 5.1. *Let $\Omega = (0, l_1) \times (0, l_2)$. If $\mu < \frac{\pi^2(l_1^2 + l_2^2)a}{l_1^2 + l_2^2}$, then the null solution is globally stable.*

6

Numerical Results for the Model Equation

In this chapter, first we shall construct a discretization scheme by Finite-Difference Methods for the model equation (1.1). Second we shall illustrate some numerical results.

6.1 FINITE DIFFERENCE METHOS

FDMs are numerical methods for solving partial differential equations by approximating them with difference equations, in which finite differences approximate the derivatives. FDMs are thus discretization methods and involve discretization of the spatial domain, the differential equation, and boundary conditions. In this section we will use FDMs for discretization the problem of the model equation (1.1)

$$\begin{cases} \dfrac{\partial u}{\partial t} = -a\Delta^2 u - \mu\nabla\cdot\left[\dfrac{\nabla u}{1+|\nabla u|^2}\right] & \text{in } \Omega\times(0,\infty), \\ u = \dfrac{\partial u}{\partial n} = 0 & \text{on } \partial\Omega\times(0,\infty), \\ u(x,y,0) = u_0(x,y) & \text{in } \Omega, \end{cases} \qquad (1.1)$$

in a two-dimensional domain Ω.

6.1.1 Finite difference formulation for a one-dimensional problem

***A*- Discretization of time and space in one-dimensional case**

In one dimension the approximate solution is given by $u(x_i, t_n) \approx u_i^n$, *i= 0... I* and *n=0, 1, 2*.... The domain is partitioned in space and in time and approximations of the solution is computed at the space or time points, Therefore the variables step sizes in x direction and step time in t time are labeled by Δx and Δt, respectively. We first perform the time discretization of (1.1):

$$\frac{\partial u}{\partial t} \approx \frac{u(x_i, t_n) - u(x_i, t_{n-1})}{\Delta t} \approx \frac{u_i^n - u_i^{n-1}}{\Delta t}, \qquad (6.1.a)$$

and space discretization of second derivative is given by

$$\frac{\partial^2 u}{\partial x^2} \approx \frac{u(x_{i+1}, t_n) - 2u(x_i, t_n) + u(x_{i-1}, t_n)}{(\Delta x)^2} \approx D^2 u_i^n = \frac{u_{i+1}^n - 2u_i^n + u_{i-1}^n}{(\Delta x)^2}. \qquad (6.1.b)$$

Similarly, on the basis of these relations, for the fourth derivative we have the following approximation

(6.1.c) $$\frac{\partial^4 u}{\partial x^4} \approx \frac{D^2 u_{i+1}^n - 2D^2 u_i^n + D^2 u_{i-1}^n}{(\Delta x)^2}.$$

In the meantime, discretization of $-\mu.\left(\frac{\nabla u}{1+|\nabla u|^2}\right)$ in Eq. (1.1) is given by,

(6.1.d) $$Du_{i+\frac{1}{2}}^n = \frac{u_{i+1}^n - u_i^n}{\Delta x},$$

(6.1.e) $$Du_{i-\frac{1}{2}}^n = \frac{u_i^n - u_{i-1}^n}{\Delta x}.$$

Eventually, the equation (1.1) after discretization becomes as follow

(6.1.f) $$u_i^{n+1} = u_i^n + \Delta t\left[-a\frac{D^2 u_{i+1}^n - 2D^2 u_i^n + D^2 u_{i-1}^n}{(\Delta x)^2} - \mu\frac{1}{\Delta x}\left(\frac{Du_{i+\frac{1}{2}}^n}{1+(Du_{i+\frac{1}{2}}^n)^2} - \frac{Du_{i-\frac{1}{2}}^n}{1+(Du_{i-\frac{1}{2}}^n)^2}\right)\right].$$

***B*- Discretization of boundary conditions in one-dimensional case**

In this study the equation (1.1) is presented under the homogeneous Dirichlet boundary conditions. Therefore, in order to discretization boundary condition in one-dimensional for $u = 0$, we assume that

(6.1.g) $$u_0^n = u_I^n = 0,$$

in which *i=0,…,I* and *n=0, 1, 2...* On the other hand for discretization $\frac{\partial u}{\partial n}$=0, it is assumed that

(6.1.h) $$u_{I+1}^n = u_{I-1}^n,$$

(6.1.i) $$u_{-1}^n = u_1^n.$$

***C*- Applications of MATLAB program in one-dimensional case**

In this study a simulation process for the Eq. (1.1) is shown by MATLAB program. We use the following MATLAB code to illustrate the implementation of Dirichlet boundary condition, and also for simplicity of writing MATLAB code, the equation of (1.1) is shown as the following form: $u_i^{n+1} = u_i^n + \Delta t[-a.part\,1 - \mu\frac{1}{\Delta x}(part\,2 - part\,3)]$,

$$part1: \frac{D^2 u_{i+1}^n - 2D^2 u_i^n + D^2 u_{i-1}^n}{(\Delta x)^2} = \frac{\frac{u_{i+1}^n - 2u_{i+1}^n + u_i^n}{\Delta x^2} - 2\frac{u_{i+1}^n - 2u_i^n + u_{i-1}^n}{\Delta x^2} + \frac{u_i^n - 2u_{i-1}^n + u_{i-2}^n}{\Delta x^2}}{\Delta x^2},$$

$$= \frac{u_{i+2}^n - 4u_{i+1}^n + 6u_i^n - 4u_{i-1}^n + u_{i-2}^n}{\Delta x^4}.$$

$part2-part3$:

$$\frac{\frac{u_{i+1}^n-u_i^n}{\Delta x}}{1+(\frac{u_{i+1}^n-u_i^n}{\Delta x})^2}-\frac{\frac{u_i^n-u_{i-1}^n}{\Delta x}}{1+(\frac{u_i^n-u_{i-1}^n}{\Delta x})^2}=\frac{u_{i+1}^n-u_i^n}{\Delta x}\cdot\frac{(\Delta x)^2}{(\Delta x)^2+(u_{i+1}^n-u_i^n)^2}-\frac{u_i^n-u_{i-1}^n}{\Delta x}\cdot\frac{(\Delta x)^2}{(\Delta x)^2+(u_i^n-u_{i-1}^n)^2}$$

$$=\frac{\Delta x(u_{i+1}^n-u_i^n)}{(\Delta x)^2+(u_{i+1}^n-u_i^n)^2}-\frac{\Delta x(u_i^n-u_{i-1}^n)}{(\Delta x)^2+(u_i^n-u_{i-1}^n)^2}.$$

Boundary condition:

$$u_0^n=u_I^n=0,$$

$$u_{I+1}^n=u_{I-1}^n,\ u_{-1}^n=u_{+1}^n.$$

The MATLAB code to solve this problem is shown below.

```
clc
clear
close all
% a=input('input the constant value, named a:  ');
% miuo=input('input the constant value, named \mu:  ');
% N=input('n=1,2,...,N    input the last value of n (N):  ');
% I=input('i=-1,0,1,...,I+1    input the Penultimate value of i (I):  ');
% dt=input('input the dt value (e.g. 1/1024):  ');
% dx=input('input the dx value:  ');
a=1;
epsilon=0.1
miuo=60;
N=1200;
dx=1/80;
dt=dx.^4;
L=80;
x=(1:L).*dx;
I=length(x);
alpha=2*3.14;
```

Which we specify initial conditions as follows,

```
u (:,1)=a*sin(alpha*x);
```

And we can specify Dirichlet boundary conditions as follows,

```
for n=1:N-1;
    for i=3:I+1;   % play the role of i=1:I-1 without shifting
       u(2,n)=0;   % Boundary condition(6.1.g),play the role of u(0,n)=0 without shifting
       u(1,n)=u(3,n); % B.C(6.1.i),play the role of u(-1,n)=u(1,n) without shifting
```

```
        u(I+2,n)=0;   %B.C(6.1.g),play the role of u(I,n)=0 without shifting
        u(I+3,n)=u(I+1,n);  % B.C(6.1.h), play the role of u(I+1,n)=u(I-1,n) without
```

By using the following routine in this MATLAB code we can compute the numerical solution of an initial value problem with given boundary condition,

```
part1=(u(i+2,n)-4.*u(i+1,n)+6.*u(i,n)-4.*u(i-1,n)+u(i-2,n))./(dx.^4);
   part2=dx.*(u(i+1,n)-u(i,n))./(dx.^2.+(u(i+1,n)-u(i,n)).^2);   %
      part3=dx.*(u(i,n)-u(i-1,n))./(dx.^2.+(u(i,n)-u(i-1,n)).^2);
         u(i,n+1)=u(i,n)+dt.*(-a.*part1-(miuo./dx).*(part2-part3));
           end
       end
```

MATLAB makes plotting functions easy. We can plot our solved function as follows,

```
nn=100;% choose nn from 1 to N
     plot((1:I+3).*dx,u(:,nn))
     xlabel('x')
     ylabel('u');
```

And finally for creating a 3-D graph of the function has been used the following command,

```
set(gcf, 'Renderer', 'zbuffer');
surf(1:N,(1:I+3).*dx,u)
xlabel('n')
ylabel('x')
zlabel('u');
```

-MATLAB code for Lyapunov function

As you remember the Lyapunov function of the dynamical system was presented in chapter 3, such that the values of Lyapunove function are monotone decreasing along trajectories. In this section, in order to illustrate this phenomenon the following MATLAB code is presented.

```
for t=1:N;
    for i=1:I+1;
S(i+1,t)=(a*(u(i+1,t)-2*u(i,t)+u(i-1,t))./dxx.^2)-miuo*log10(1+((u(i+1,t)-u(i,t))/dxx).^2);
    end
    dxx=length(S(:,t));
    SS(t)=inac(dxx,S(:,t));
end
figure
plot(1:N,SS(1:end))
```

And this integral is computed by using the following MATLAB code

```
function [dy]=inac(dx,y)
```

```
for i=1:length(y)
    yy(i)=(y(i)+y(i+1))*dx/2;
end
dy=sum(yy);
```

6.1.2 Finite difference formulation for a two-dimensional problem

***A*- Discretization of time and spaces in two-dimensional case**

In two dimensions the approximate solution is given by $u(x_i, y_j, t_n) \approx u_{ij}^n$ with assume $i = 0, \dots, I$, $j = 0, \dots, J$ and $n = 0,1,2, \dots$.The approximations of solution are computed at the space x, y and time t. The variables step sizes in x and y directions are labeled by $\Delta x, \Delta y$ respectively. And step time in t time is labeled by Δt.

Time discretization is as follows,

$$\frac{\partial u}{\partial t} \approx \frac{u(x_i, y_j, t_n) - u\ (x_i, y_j, t_{n-1})}{\Delta t} \approx \frac{u_{ij}^n - u_{ij}^{n-1}}{\Delta t}. \tag{6.1.j}$$

Space discretization of second derivative in two-dimensional case is given as follows,

$$\left(\frac{\partial^2}{\partial x^2} + \frac{\partial^2}{\partial y^2}\right) u \approx (D_x{}^2 u_{ij}^n + D_y{}^2 u_{ij}^n)$$

$$\Delta u \approx \frac{u_{i+1j}^n - 2u_{ij}^n + u_{i-1j}^n}{(\Delta x)^2} + \frac{u_{ij+1}^n - 2u_{ij}^n + u_{ij-1}^n}{(\Delta y)^2}. \tag{6.1.k}$$

On the basis of these relations, for the fourth derivative we have the approximation

$$\begin{aligned}
&(\frac{\partial^2}{\partial x^2} + \frac{\partial^2}{\partial y^2})^2 = \Delta^2 u \\
&\Delta^2 u \approx \Delta[(D_x{}^2 u_{ij}^n) + (D_y{}^2 u_{ij}^n)] \\
&\quad = \Delta(D_x{}^2 u_{ij}^n) + \Delta(D_y{}^2 u_{ij}^n) \\
&\quad = \left[\frac{(D_x{}^2 u_{i+1j}^n) - 2(D_x{}^2 u_{ij}^n) + (D_x{}^2 u_{i-1j}^n)}{(\Delta x)^2} + \frac{(D_x{}^2 u_{ij+1}^n) - 2(D_x{}^2 u_{ij}^n) + (D_x{}^2 u_{ij-1}^n)}{(\Delta y)^2}\right] + \\
&\quad \left[\frac{(D_y{}^2 u_{i+1j}^n) - 2(D_y{}^2 u_{ij}^n) + (D_y{}^2 u_{i-1j}^n)}{(\Delta x)^2} + \frac{(D_y{}^2 u_{ij+1}^n) - 2(D_y{}^2 u_{ij}^n) + (D_y{}^2 u_{ij-1}^n)}{(\Delta y)^2}\right],
\end{aligned} \tag{6.1.l}$$

with the following definitions

$$D_x{}^2 u_{i+1j}^n = \frac{u_{i+2j}^n - 2u_{i+1j}^n + u_{ij}^n}{(\Delta x)^2}, \qquad D_x{}^2 u_{i-1j}^n = \frac{u_{ij}^n - 2u_{i-1j}^n + u_{i-2j}^n}{(\Delta x)^2},$$

$$D_x{}^2 u_{ij+1}^n = \frac{u_{i+1j+1}^n - 2u_{ij+1}^n + u_{i-1j+1}^n}{(\Delta x)^2}, \quad D_x{}^2 u_{ij-1}^n = \frac{u_{i+1j-1}^n - 2u_{ij-1}^n + u_{i-1j-1}^n}{(\Delta x)^2},$$

$$D_y{}^2 u_{i+1j}^n = \frac{u_{i+1j+1}^n - 2u_{i+1j}^n + u_{i+1j-1}^n}{(\Delta y)^2}, \quad D_y{}^2 u_{i-1j}^n = \frac{u_{i-1j+1}^n - 2u_{i-1j}^n + u_{i-1j-1}^n}{(\Delta y)^2},$$

$$D_y{}^2 u_{ij+1}^n = \frac{u_{ij+2}^n - 2u_{ij+1}^n + u_{ij}^n}{(\Delta y)^2}, \qquad D_y{}^2 u_{ij-1}^n = \frac{u_{ij}^n - 2u_{ij-1}^n + u_{ij-2}^n}{(\Delta y)^2}.$$

In the meantime, discretization of $-\mu.\left(\frac{\nabla u}{1+|\nabla u|^2}\right)$ in Eq. (1.1) is given as follows,

$$-\mu\left(\frac{\partial}{\partial x},\frac{\partial}{\partial y}\right).\left[\frac{\frac{\partial u}{\partial x},\frac{\partial u}{\partial y}}{1+\left(\frac{\partial u}{\partial x}\right)^2,\left(\frac{\partial u}{\partial y}\right)^2}\right]=$$

$$-\mu\frac{\partial}{\partial x}\left[\frac{1}{1+\left(\frac{\partial u}{\partial x}\right)^2,\left(\frac{\partial u}{\partial y}\right)^2}.\frac{\partial u}{\partial x}\right]-\mu\frac{\partial}{\partial y}\left[\frac{1}{1+\left(\frac{\partial u}{\partial x}\right)^2,\left(\frac{\partial u}{\partial y}\right)^2}.\frac{\partial u}{\partial y}\right]\approx$$

$$-\mu\frac{1}{\Delta x}\left[\frac{D_x u^n_{i+\frac{1}{2}\,j}}{1+\left(D_x u^n_{i+\frac{1}{2}\,j}\right)^2+\left(D_y u^n_{i+\frac{1}{2}\,j}\right)^2}-\frac{D_x u^n_{i-\frac{1}{2}\,j}}{1+\left(D_x u^n_{i-\frac{1}{2}\,j}\right)^2+\left(D_y u^n_{i-\frac{1}{2}\,j}\right)^2}\right]$$

$$-\mu\frac{1}{\Delta y}\left[\frac{D_y u^n_{i\,j+\frac{1}{2}}}{1+\left(D_x u^n_{i\,j+\frac{1}{2}}\right)^2+\left(D_y u^n_{i\,j+\frac{1}{2}}\right)^2}-\frac{D_y u^n_{i\,j-\frac{1}{2}}}{1+\left(D_x u^n_{i\,j-\frac{1}{2}}\right)^2+\left(D_y u^n_{i\,j-\frac{1}{2}}\right)^2}\right], \quad \text{(6.1.m)}$$

all relations in (6.1.m) are defined as follow,

$$\left(\frac{\partial u}{\partial x}\right)_{i+\frac{1}{2}\,j}\approx D_x u^n_{i+\frac{1}{2}\,j}=\frac{u^n_{i+1\,j}-u^n_{ij}}{\Delta x},$$

$$\left(\frac{\partial u}{\partial x}\right)^n_{i-\frac{1}{2}\,j}\approx D_x u^n_{i-\frac{1}{2}\,j}=\frac{u^n_{ij}-u^n_{i-1\,j}}{\Delta x},$$

$$\left(\frac{\partial u}{\partial x}\right)_{i\,j+\frac{1}{2}}\approx D_x u^n_{i\,j+\frac{1}{2}}=\frac{u^n_{i+1\,j}-u^n_{i-1,\;j}+u_{i+1,\;j+1}-u_{i-1,\,j+1}}{4\Delta x}$$

$$\left(\frac{\partial u}{\partial x}\right)^n_{i\,j-\frac{1}{2}}\approx D_x u^n_{i\,j-\frac{1}{2}}=\frac{u^n_{i+1\,j}-u^n_{i-1,\;j}+u_{i+1,\;j-1}-u_{i-1,\,j-1}}{4\Delta x},$$

$$\left(\frac{\partial u}{\partial y}\right)_{i\,j+\frac{1}{2}}\approx D_y u^n_{i\,j+\frac{1}{2}}=\frac{u^n_{ij+1}-u^n_{ij}}{\Delta y}\quad and\ \left(\frac{\partial u}{\partial y}\right)^n_{i\,j-\frac{1}{2}}\approx D_y u^n_{i\,j-\frac{1}{2}}=\frac{u^n_{ij}-u^n_{i\,j-1}}{\Delta y},$$

$$\left(\frac{\partial u}{\partial y}\right)_{i+\frac{1}{2}j}\approx D_y u^n_{i+\frac{1}{2}j}=\frac{u^n_{i\,j+1}-u^n_{i,\;j-1}+u_{i+1,\;j+1}-u_{i+1,\,j-1}}{4\Delta y}\quad and$$

$$\left(\frac{\partial u}{\partial y}\right)^n_{i-\frac{1}{2}j}\approx D_y u^n_{i-\frac{1}{2}j}=\frac{u^n_{i\,j+1}-u^n_{i,\;j-1}+u_{i-1,\;j+1}-u_{i-1,\,j-1}}{4\Delta y}.$$

Eventually, the equation (1.1) after above discretization becomes as follow

$$\frac{u_{ij}^{n+1}-u_{ij}^{n}}{\Delta t}=-a\left[\frac{(D_x{}^2u_{i+1\,j}^{n})-2(D_x{}^2u_{i\,j}^{n})+(D_x{}^2u_{i-1\,j}^{n})}{(\Delta x)^2}+\frac{(D_x{}^2u_{i\,j+1}^{n})-2(D_x{}^2u_{i\,j}^{n})+(D_x{}^2u_{i\,j-1}^{n})}{(\Delta y)^2}+\right.$$
$$\left.\frac{(D_y{}^2u_{i+1\,j}^{n})-2(D_y{}^2u_{i\,j}^{n})+(D_y{}^2u_{i-1\,j}^{n})}{(\Delta x)^2}+\frac{(D_y{}^2u_{i\,j+1}^{n})-2(D_y{}^2u_{i\,j}^{n})+(D_y{}^2u_{i\,j-1}^{n})}{(\Delta y)^2}\right]$$
$$-\mu\frac{1}{\Delta x}\left[\frac{D_xu^n_{i+\frac{1}{2}\,j}}{1+\left(D_xu^n_{i+\frac{1}{2}\,j}\right)^2+\left(D_yu^n_{i+\frac{1}{2}\,j}\right)^2}-\frac{D_xu^n_{i-\frac{1}{2}\,j}}{1+\left(D_xu^n_{i-\frac{1}{2}\,j}\right)^2+\left(D_yu^n_{i-\frac{1}{2}\,j}\right)^2}\right]$$
$$-\mu\frac{1}{\Delta y}\left[\frac{D_yu^n_{i\,j+\frac{1}{2}}}{1+\left(D_xu^n_{i\,j+\frac{1}{2}}\right)^2+\left(D_yu^n_{i\,j+\frac{1}{2}}\right)^2}-\frac{D_yu^n_{i\,j-\frac{1}{2}}}{1+\left(D_xu^n_{i\,j-\frac{1}{2}}\right)^2+\left(D_yu^n_{i\,j-\frac{1}{2}}\right)^2}\right]. \qquad (6.1.n)$$

***B*- Discretization of boundary conditions in two-dimensional case**

In order to discretization boundary conditions for $u=0$ we assume that

$$\begin{cases} u^n_{0\,j}=0 & 0\le j\le J,\\ u^n_{I\,j}=0 & 0\le j\le J,\\ u^n_{i\,J}=0 & 0\le i\le I,\\ u^n_{i0}=0 & 0\le i\le I. \end{cases} \qquad (6.1.o)$$

In addition, for discretization $\frac{\partial u}{\partial n}$=0, it is assumed that

$$\begin{cases} u^n_{-1\,j}=u^n_{+1\,j} & 0\le j\le J,\\ u^n_{I+1\,j}=u^n_{I-1\,j} & 0\le j\le J,\\ u^n_{i\,-1}=u^n_{i\,+1} & 0\le i\le I,\\ u^n_{i\,J+1}=u^n_{i\,J-1} & 0\le i\le I. \end{cases} \qquad (6.1.p)$$

6.2 Numerical Example in 1D

In this section, we present numerical examples for the problem of equation (1.1)

$$\begin{cases} \dfrac{\partial u}{\partial t}=-a\Delta^2u-\mu\nabla\cdot\left[\dfrac{\nabla u}{1+|\nabla u|^2}\right] & \text{in } \Omega\times(0,\infty),\\ u=\dfrac{\partial u}{\partial n}=0 & \text{on } \partial\Omega\times(0,\infty),\\ u(x,0)=u_0(x) & \text{in } \Omega, \end{cases} \qquad (1.1)$$

in one-dimensional case to illustrate the critical point in roughening coefficient μ.

And also we investigate stability and instability of null solution by controlling roughening coefficient μ. (cf. [chapter 5, Theorem 5.1]). For this purpose, we consider (1.1) in the interval $\Omega = (0, l)$, where $l = 1$. In this section the coefficient a is fixed as $a = 1$ but $\mu > 0$ is treated as a control parameter. We also specify the initial function as

$$u_0(x) = 0.1[\sin(2 \times 3.14\, x)], \qquad x \in \Omega,$$

which is a perturbation of the null solution $u \equiv 0$. Clearly, the null solution is a unique homogeneous stationary solution.

A- Investigation critical point by roughening coefficient μ in 1D

Critical point is equivalency point .In this study the critical point is observed about μ=13, see Figure 6.1.Notice that after the critical point any profiles with increased μ become inhomogeneous stationary solution.

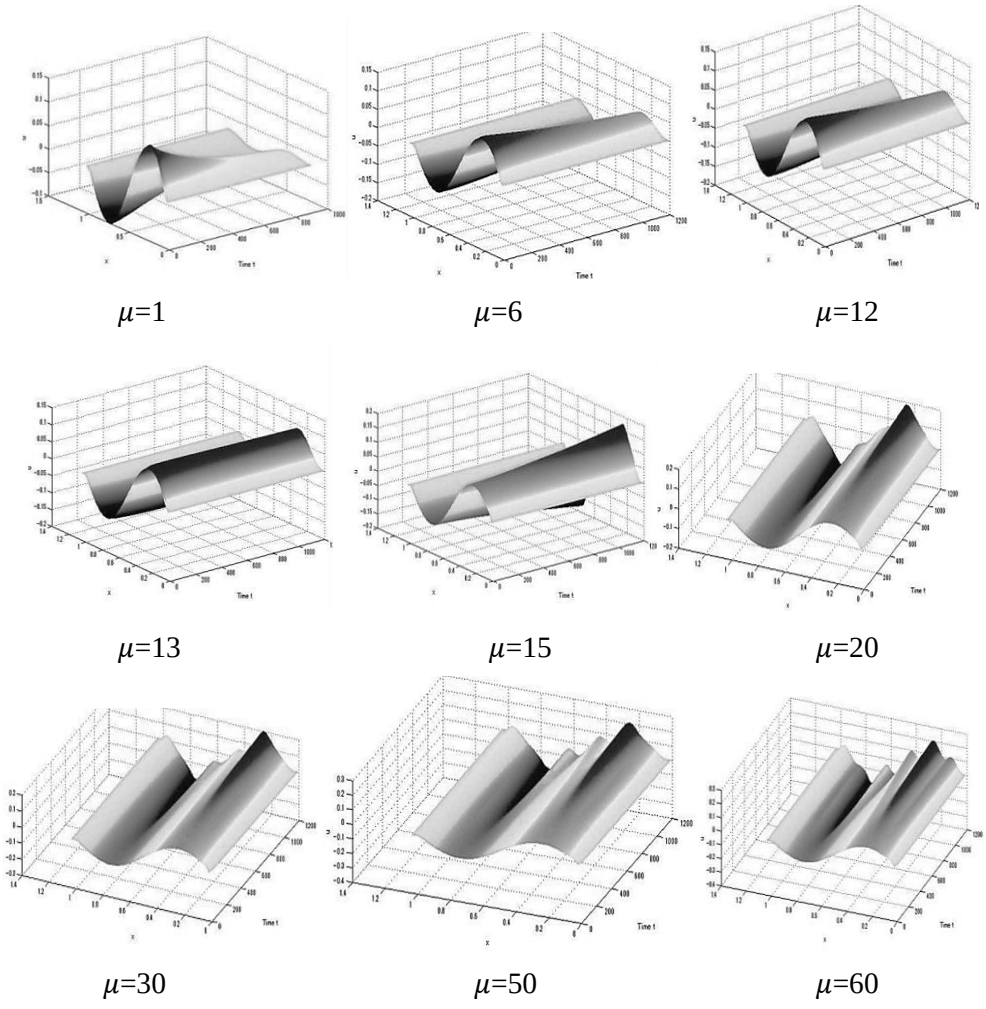

μ=1 μ=6 μ=12

μ=13 μ=15 μ=20

μ=30 μ=50 μ=60

Figure.6.1: Dynamics for several μ at the same time $t = 150$

B- Investigation of stability and instability of null solution by controlling roughening coefficient in 1D

We illustrate some numerical examples which show stability or instability of null solution by controlling roughening coefficient μ.

Set first $\mu = 12$. As seen by Figure 6.2, the solution tends to the null solution as $t \to \infty$, and the Lyapunov function along this trajectory is given by Figure 6.2(d).

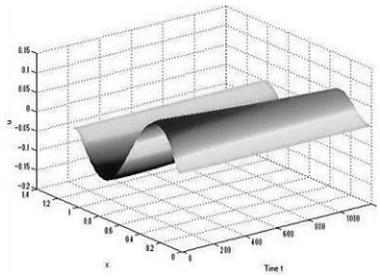

(a) $t = 0$

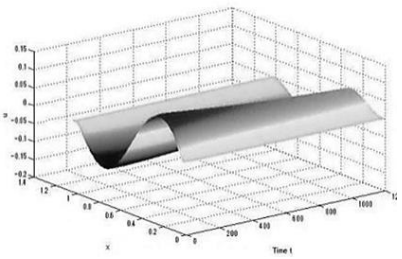

(b) $t = 35$

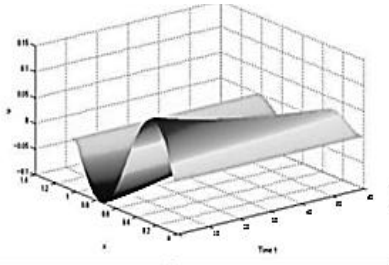

(c) $t = 65$

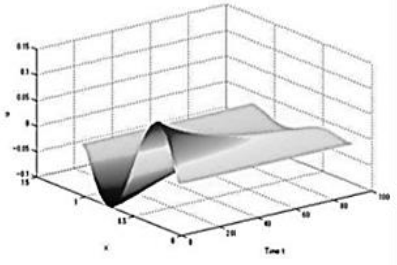

(d) $t = 100$

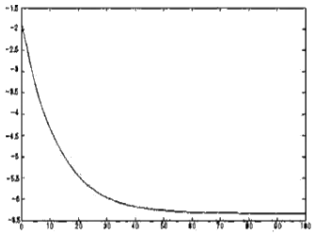

(d) Lyapunov function

Figure.6.2: Dynamics for $\mu = 12$ in 1D.

Take next $\mu = 30$. As seen by Figure 6.3, the solution no longer tends to null solution. Instead, as time increases, the small perturbation grows into shallow ridges. The graph of Lyapunov function along the trajectory is given by Figure 6.3(i).

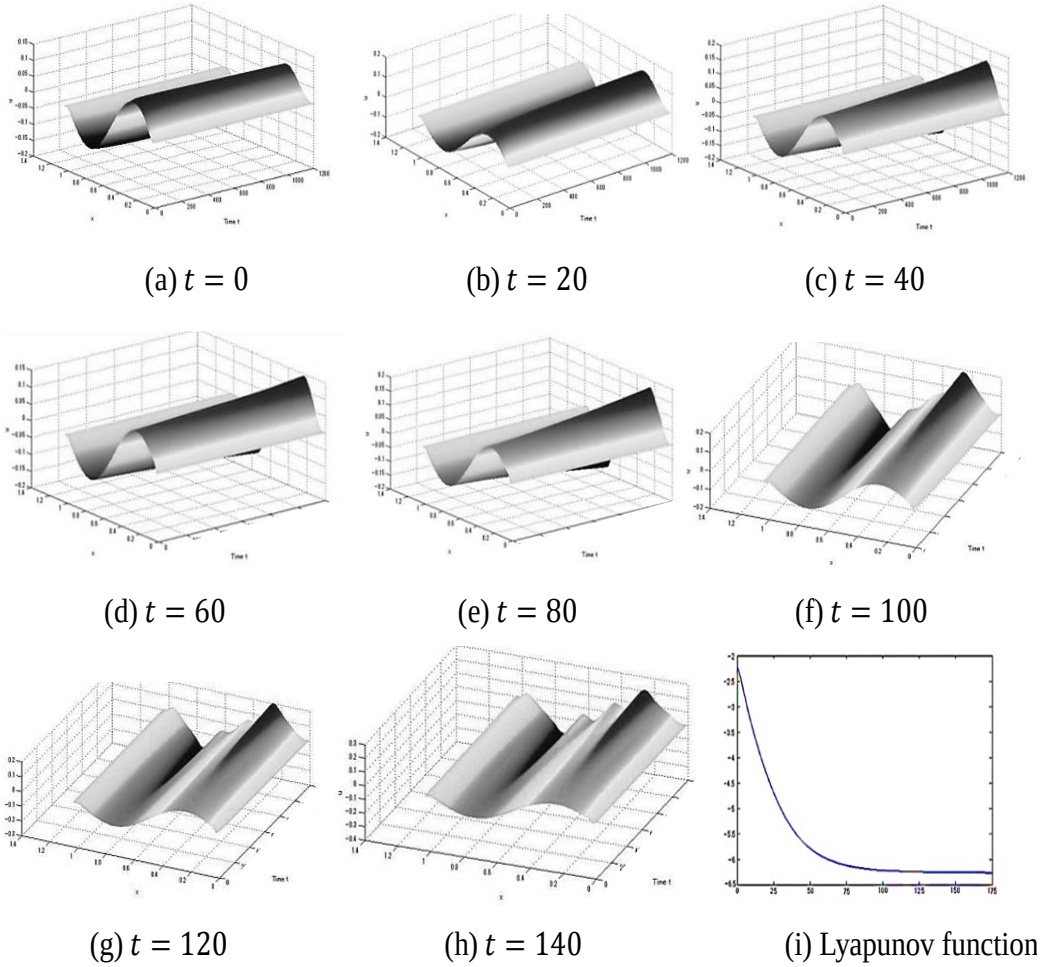

(a) $t = 0$ (b) $t = 20$ (c) $t = 40$

(d) $t = 60$ (e) $t = 80$ (f) $t = 100$

(g) $t = 120$ (h) $t = 140$ (i) Lyapunov function

Figure.6.3: Dynamics for $\mu = 30$ in 1D.

Finally, take a sufficiently large μ, say $\mu = 60$. As seen by Figure 6.4, as time increases, the perturbation grows into deep ridges. Therefore, the solution again converges to non-null stationary solution. This means that the null stationary solution is unstable. The graph of Lyapunov function along the trajectory is given by Figure 6.4(i).

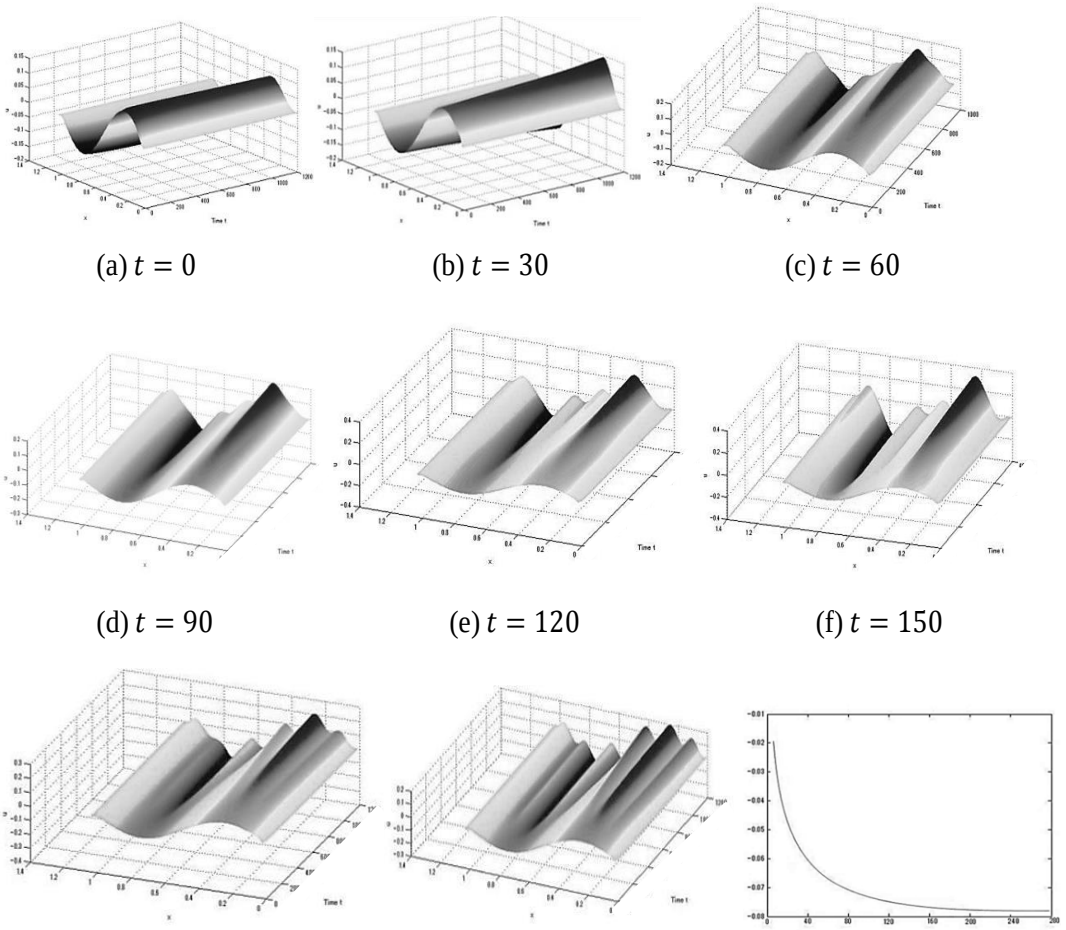

(a) $t = 0$ (b) $t = 30$ (c) $t = 60$

(d) $t = 90$ (e) $t = 120$ (f) $t = 150$

(g) $t = 180$ (h) $t = 210$ (i) Lyapunov function

Figure.6.4: Dynamics for $\mu = 60$ in 1D.

6.3 Numerical Example in 2D

In this section, we present some numerical examples for the problem of equation (1.1)

$$\begin{cases} \dfrac{\partial u}{\partial t} = -a\Delta^2 u - \mu\nabla\cdot\left[\dfrac{\nabla u}{1+|\nabla u|^2}\right] & \text{in } \Omega\times(0,\infty), \\ u = \dfrac{\partial u}{\partial n} = 0 & \text{on } \partial\Omega\times(0,\infty), \\ u(x,y,0) = u_0(x,y) & \text{in } \Omega, \end{cases} \qquad (1.1)$$

in a tow-dimensional domain Ω.

A- Investigation of stability and instability of null solution by controlling roughening coefficient

As first results for 2D, we illustrate some numerical examples which show agreements to theorem (5.1) in chapter 5 (*if* $ad^{-2} > \mu$*, then the null solution is stable. If* $ad^{-2} < \mu$*, then the null solution is unstable*).

Stability and instability of the null solution is determined by dominance in magnitude of the two coefficients a and μ to the other but with weight d^{-2} for a. For this purpose, we consider (1.1) in the square domain $\Omega = (0,1)\times(0,1)$. The coefficients a is fixed as $a = 1$ but $\mu > 0$ is treated control parameter. In this section constant d is computed as $d \approx \frac{1}{\sqrt{2\pi}}$ (cf. [chapter 5, Theorem 5.4]). We also set the initial function as

$$u_0(x,y) = 0.1[\sin(2\cdot 3.14x)\times\sin(2\cdot 3.14y)], \qquad (x,y)\in\Omega,$$

which is a perturbation of the null solution $u \equiv 0$. Clearly, the null solution is a unique homogeneous stationary solution.

Set first $\mu = 12$, such that $ad^{-2} > 12$, then the null solution is stable. In this case, as seen by Figure 6.5, the solution tends to the null solution as $t \to \infty$. This means that the null stationary solution is stable.

The Lyapunov function along this trajectory is given by Figure 6.5(e).

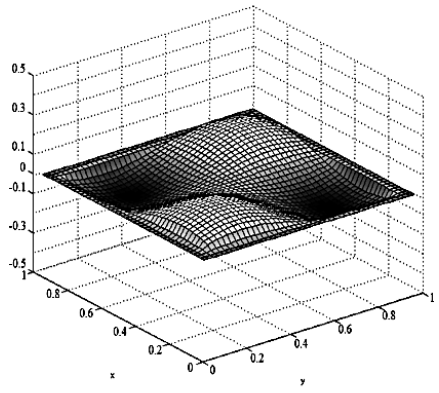

(a) $t = 0$

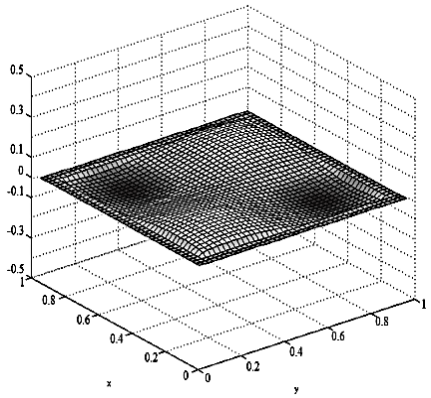

(b) $t = 20$

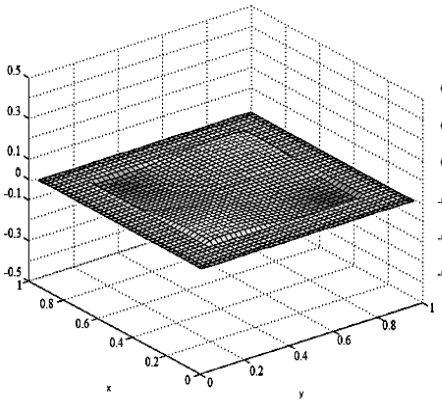

(c) $t = 40$

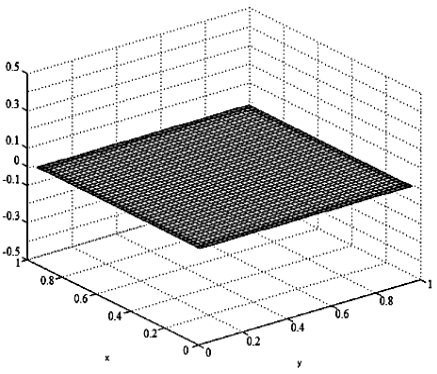

(d) $t = 60$

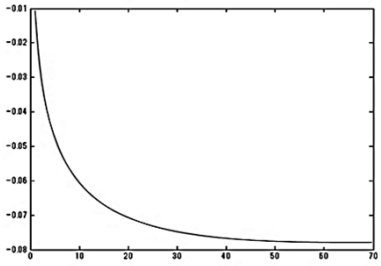

(e) Lyapunov function

Figure 6.5: Dynamics for $\mu = 12$

Take next $\mu = 40$, such that $ad^{-2} < 40$, then the null solution is unstable. As seen by Figure 6.6, in this case the solution no longer tends to the null solution. Instead; the perturbation grows into two columns of ridges. This means that the null stationary solution is unstable. The Lyapunov function along this trajectory is given by Figure 6.6(f).

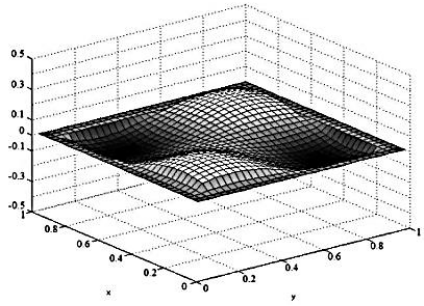

(a) $t = 0$

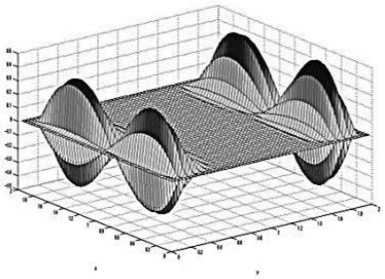

(b) $t = 40$

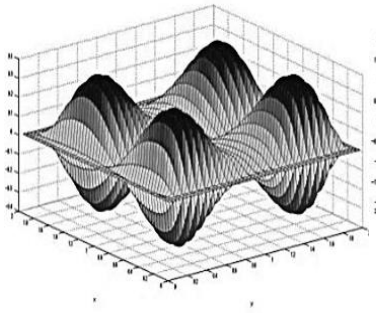

(c) $t = 80$

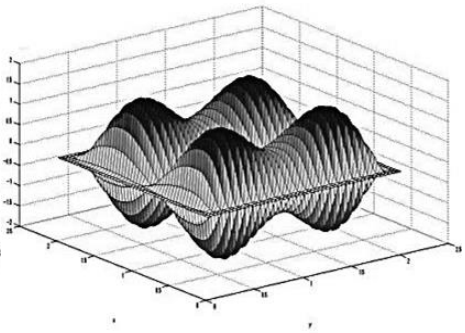

(d) $t = 120$

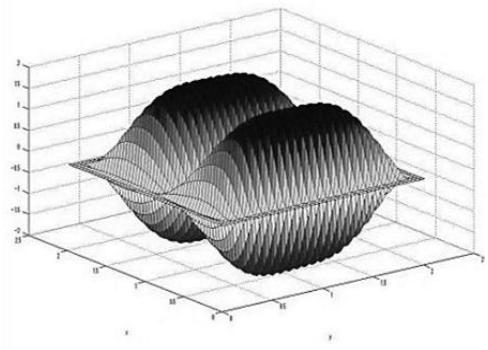

(e) $t = 160$

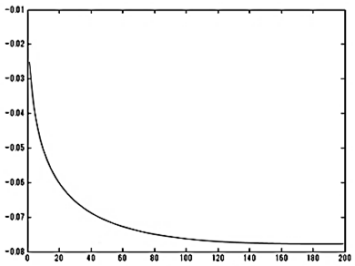

(f) Lyapunov function

Figure.6.6: Dynamics for $\mu = 40$ in Δx =1/256 and $\Delta t = \Delta x.\hat{}4$

With respect to symmetric initial function, theoretically the profiles of solutions must also be symmetric. According of figure 6.7, as expected, in the small time the perturbation growth of *x* and *y* directions are in the symmetric state, however, with increasing time the perturbation growth of *x* direction is dominant to perturbation growth of *y* direction. Also note that this symmetric growth in very small value of Δx and Δt can be observed (e.g. Δx =1/1024 and $\Delta t = \Delta x.\text{^}5$). This means that the symmetric solution is unstable.

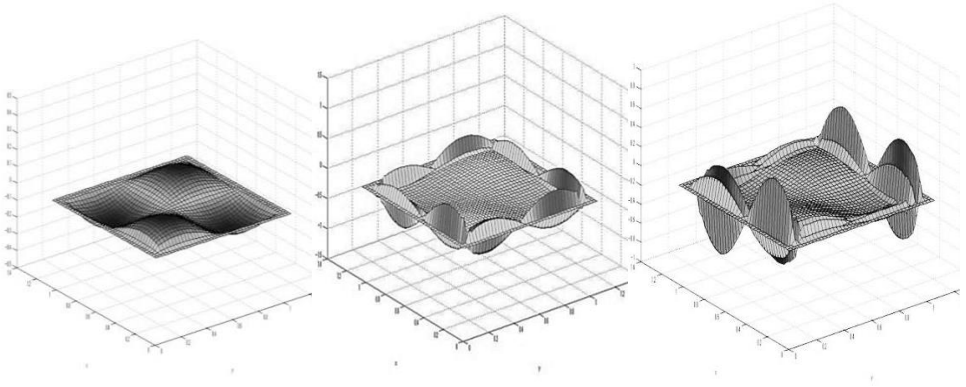

(a) $t = 0$ (b) *t*=20 (c) $t = 40$

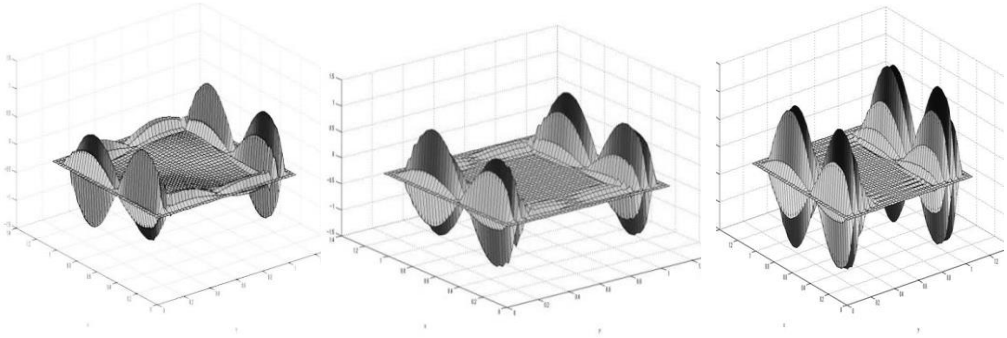

(d) $t = 60$ (e) $t = 80$ (f) $t = 100$

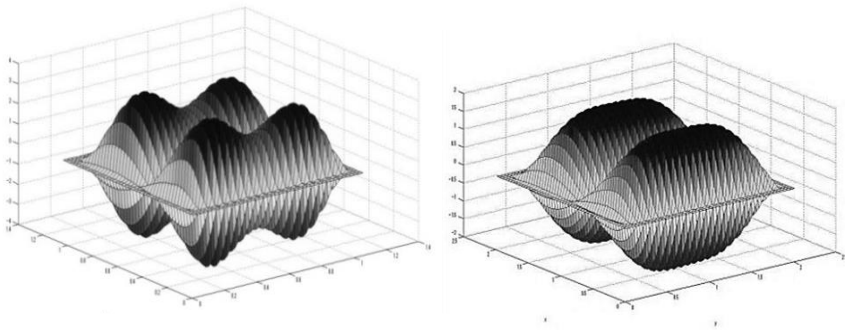

(g) *t*=120 (h) *t*= 140

Figure.6.7: Dynamics for $\mu = 40$ in Δx =1/1024 and $\Delta t = \Delta x.\text{^}5$

***B*- Change of profiles by enhancement of roughening coefficient**

In this section, we shall illustrate some numerical results to observe how change the profile of stationary solution by enhancement of roughening coefficient. Therefore, in order to justify this section by numerical examples, we consider (1.1) with one of the roughening coefficient $\mu = 13, 30, 40$. The coefficient a is fixed as $a = 1$. In addition, the square domain is specified in $\Omega = (0,1) \times (0,1)$. We choose initial function as

$$u_0(x, y) = 0.1[\sin(2 \cdot 3.14x) \times \sin(2 \cdot 3.14y)], \qquad (x, y) \in \Omega .$$

When $\mu = 13$ the solution tends to non-null stationary solution and the perturbation grows into two columns of ridges. In the meantime, as seen by Figure 6.8 in each column there are 12 ridges. Also, the Lyapunov function along this trajectory is given by Figure 6.8(e).

Set secondly $\mu = 30$. In this case as before, the solution tends to non-null stationary solution and the perturbation grows into two columns of ridges, with the exception that the number of ridges in a column increases more than that of the case of $\mu = 13$. In each column there are 18 ridges, as shown in Figure 6.9. Also, the Lyapunov function along this trajectory is given by Figure 6.9(e). Finally, set $\mu = 90$. As noted above, in this case, the solution tends to non-null stationary solution and the perturbation grows into two columns of ridges and the numbers of ridges in each column are more than those of other cases, as shown in Figure 6.10. Also, the Lyapunov function along this trajectory is given by Figure 6.10(g).

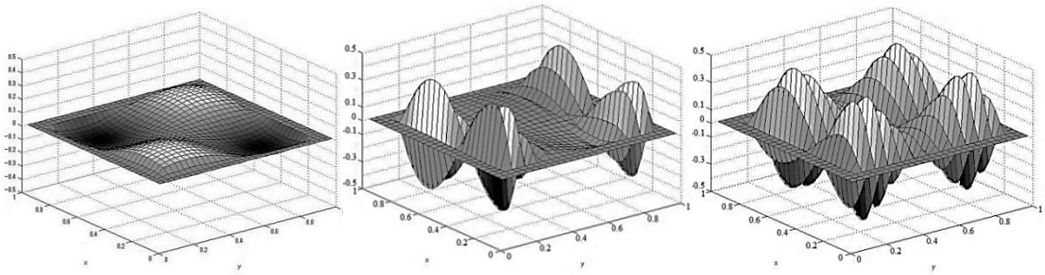

(a) $t = 0$ (b) $t = 30$ (c) t=60

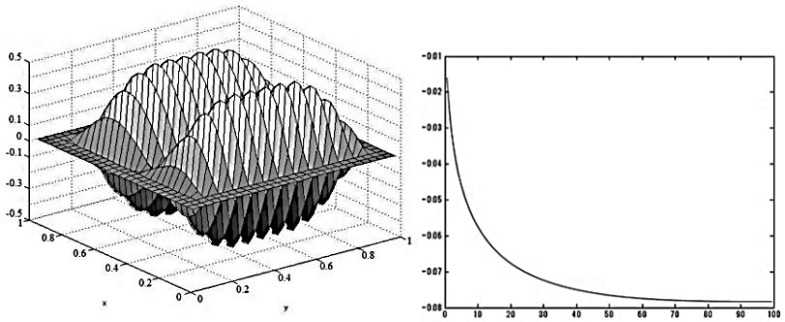

(f) t=90 (e) Lyapunov function

Figure.6.8: Dynamics for $\mu = 13$

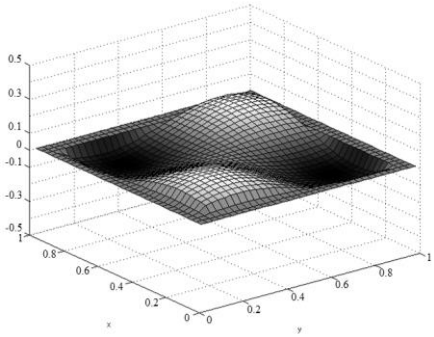

(a) $t = 0$

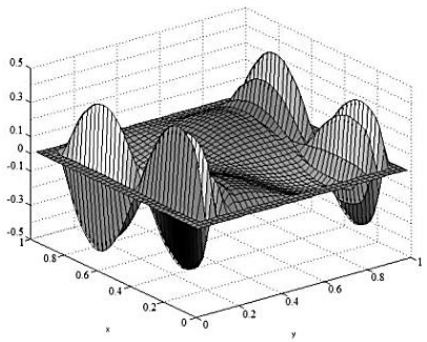

(b) $t = 40$

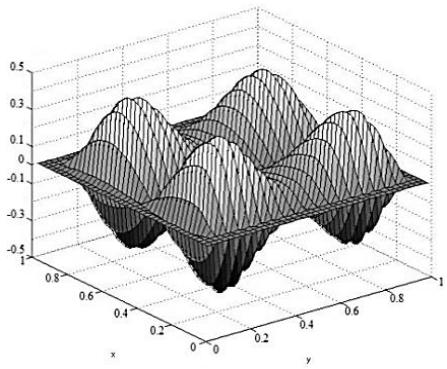

(c) $t = 80$

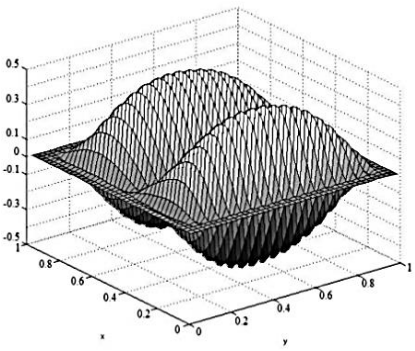

(d) $t = 120$

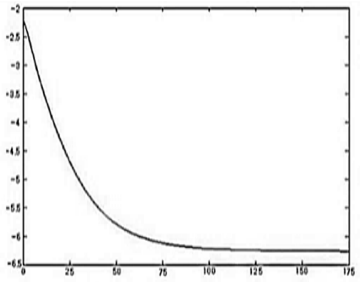

(e) Lyapunov function

Figure.6.9: Dynamics for $\mu = 30$

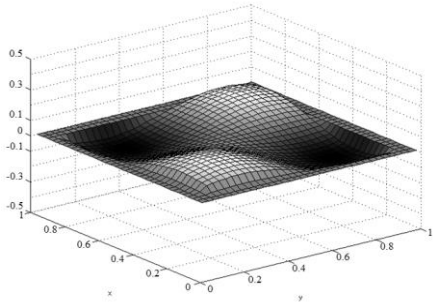

(a) $t = 0$

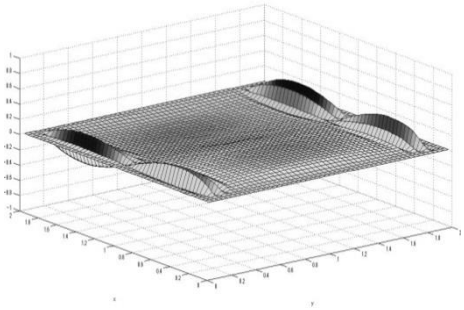

(b) $t = 50$

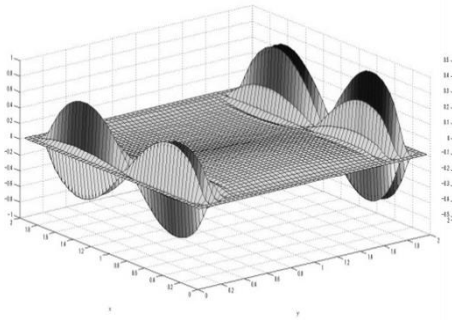

(c) $t = 100$

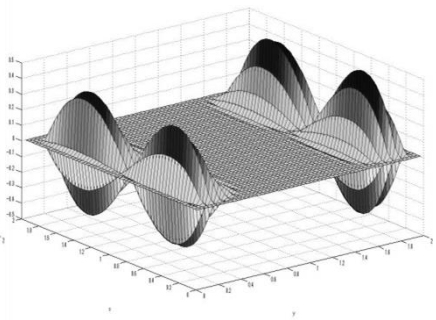

(d) $t = 150$

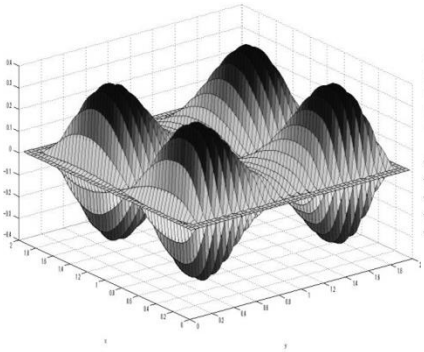

(e) $t = 200$

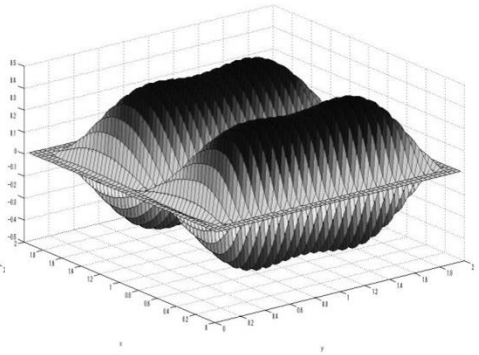

(f) $t = 250$

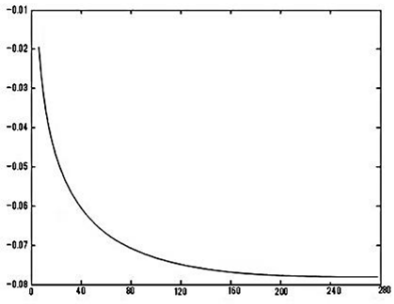

(g) Lyapunov function

Figure.6.10: Dynamics for $\mu = 90$

***C*- Change of profiles by initial functions at $\mu = 40$**

In this section, we shall illustrate some numerical results to observe how change the profile of stationary solution by initial functions. Therefore, in order to justify this section by numerical examples, we treat (1.1) in the square domain $\Omega = (0,1) \times (0,1)$. The coefficients a and μ are fixed as $a = 1$ and $\mu = 40$, respectively. We shall choose initial function as

$$u_0(x,y) = 0.1[\sin(3.14kx) \times \sin(3.14y)], \qquad (x,y) \in \Omega,$$

where k is a positive integer varying from 1 to 5. These are a perturbation of the null stationary solution to $u \equiv 0$. First, let $k = 1$ in initial function. The dynamics for the solution is illustrated by Figure 6.11. The small initial perturbation grows into a single column of ridges. The graph of the Lypunove function is given by Figure 6.11(f). At time about $t = 120$, the values of the Lyapunov function are stabilized. In view of Theorem 4.0 in chapter 4, this suggests that a final profile of the trajectory may be given by that of time $t = 120$.

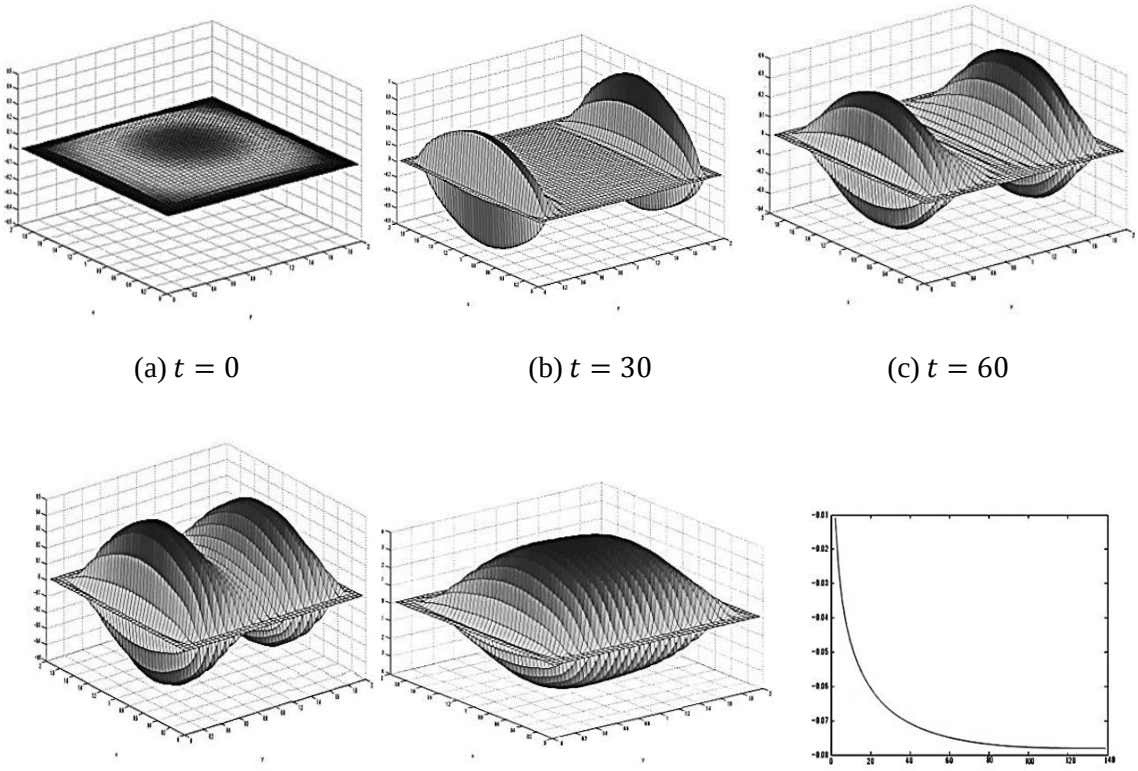

(a) $t = 0$ (b) $t = 30$ (c) $t = 60$

(d) $t = 90$ (e) $t = 120$ (f) Lyapunov function

Figure.6.11: Dynamics for $k = 1$

Secondly, let $k = 2$ in initial function. As Figure 6.12 shows, the perturbation grows in this case into double columns of ridges. The profile of the solution is stabilized about time $t = 180$. The graph of Lyapunov function is given by Figure 6.12(f).

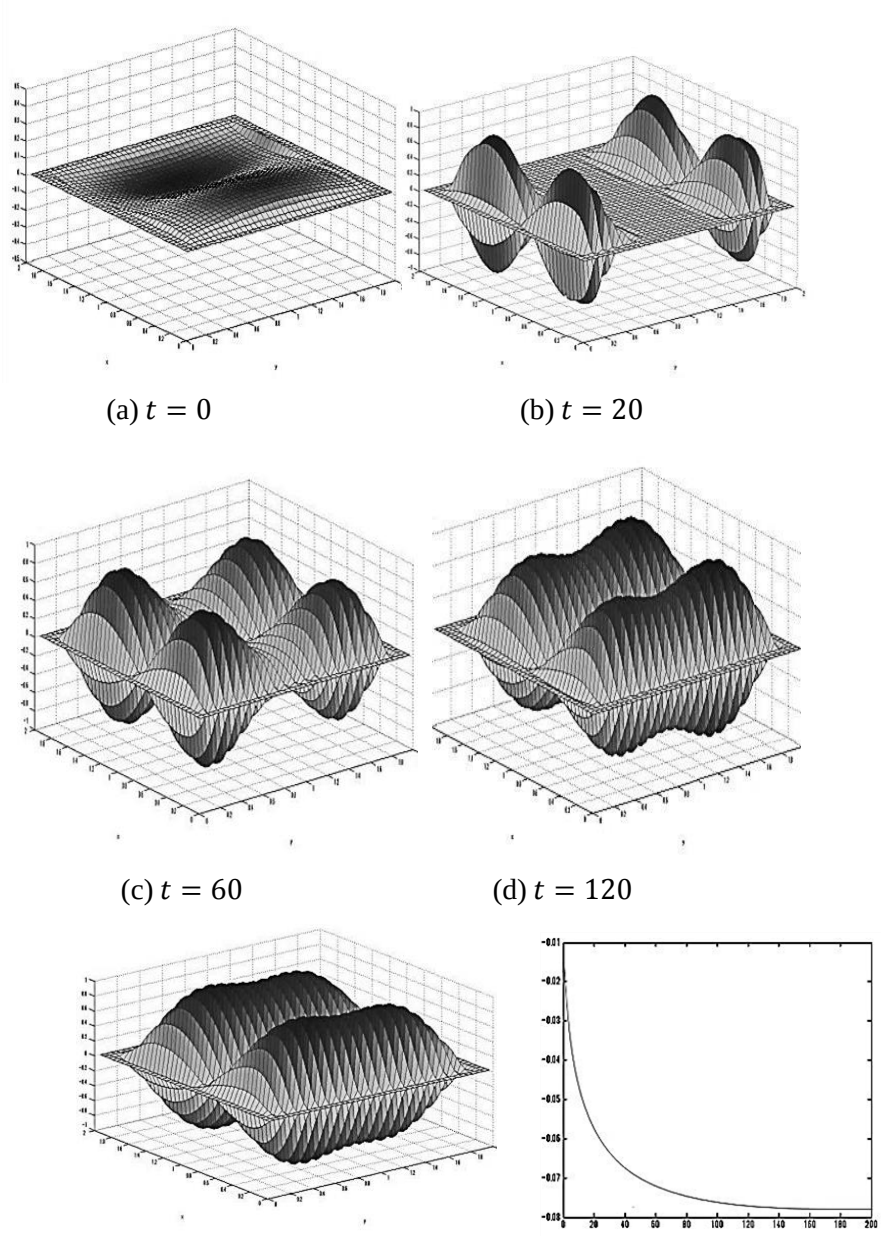

(a) $t = 0$ (b) $t = 20$

(c) $t = 60$ (d) $t = 120$

(e) $t = 180$ (f) Lyapunov function

Figure.12: Dynamics for $k = 2$

Thirdly, consider the case where $k = 3$. As seen by figure 6.13, the initial perturbation grows into triple columns of ridges. Figure 6.13(f) illustrates the graph of the Lyapunov function of trajectory.

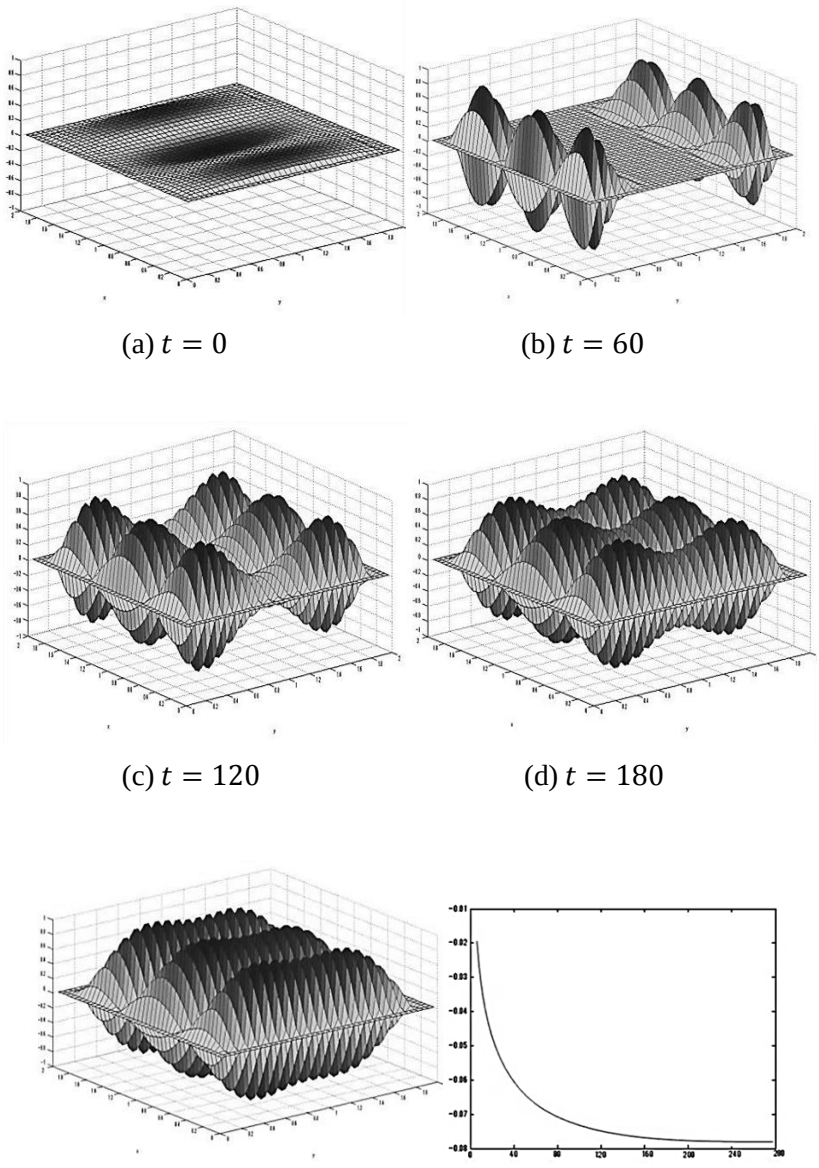

(a) $t = 0$ (b) $t = 60$

(c) $t = 120$ (d) $t = 180$

(e) $t = 240$ (f) Lyaponuv function

Figure.6.13: Dynamics for $k = 3$

Next, consider the case where $k = 4$ in initial function. For a while, the small perturbation grows into four columns of ridges. Gradually, the state of fourth column becomes unstable. Ultimately, one column of ridges disappears and the trajectory converges to a stationary solution whose profile is the same as that of the case where $k = 3$, see Figure 6.14. Numerical results indicate that the total number of the stationary solution at μ=40 is 3. Also was shown that the stationary solutions to which trajectory convergence are dependent on initial functions.

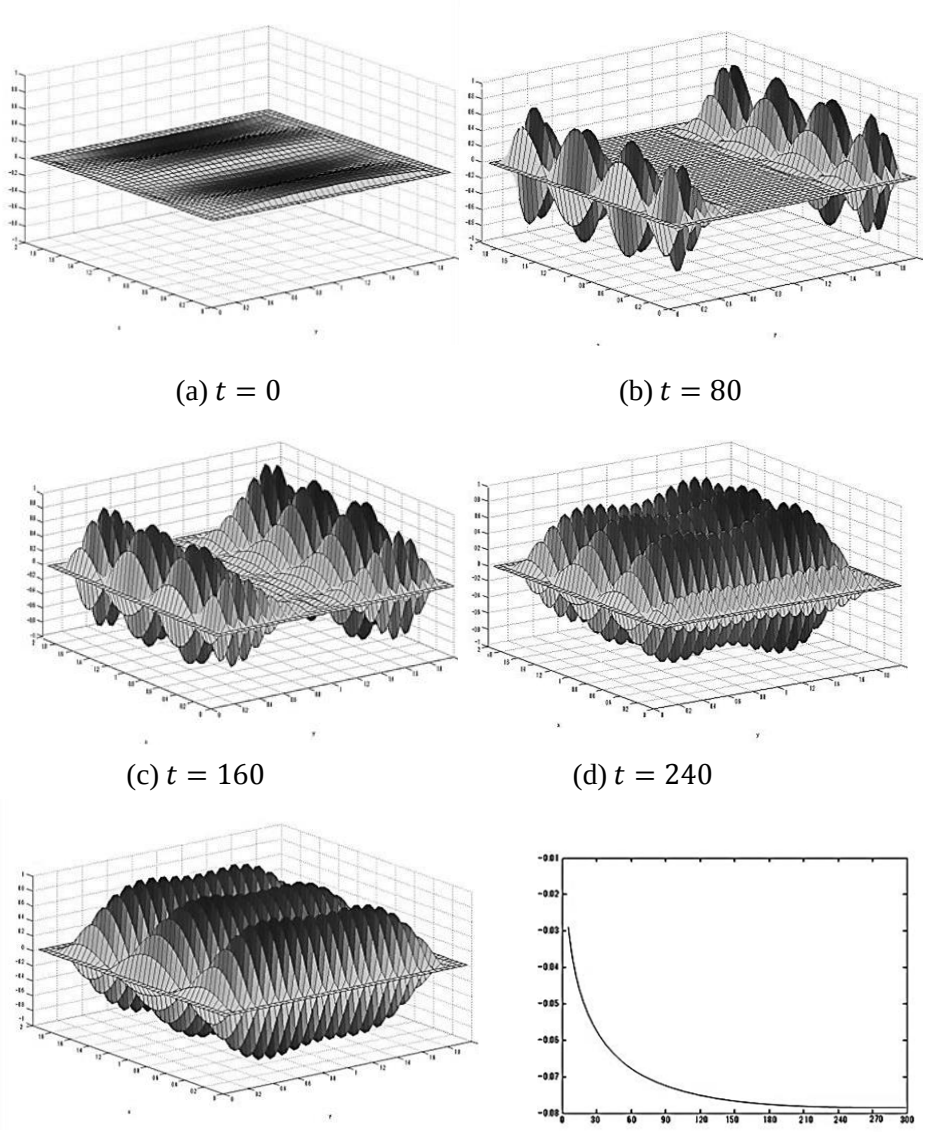

(a) $t = 0$ (b) $t = 80$

(c) $t = 160$ (d) $t = 240$

(e) $t = 300$ (f) Lyapunov function

Figure6.14: Dynamics for $k = 4$

Finally, consider the case where $k = 5$ in the initial function. Two columns of ridges disappear and the trajectory converges to a stationary solution whose profile is the same as that of the case where $k = 3$, see Figure 6. 15.

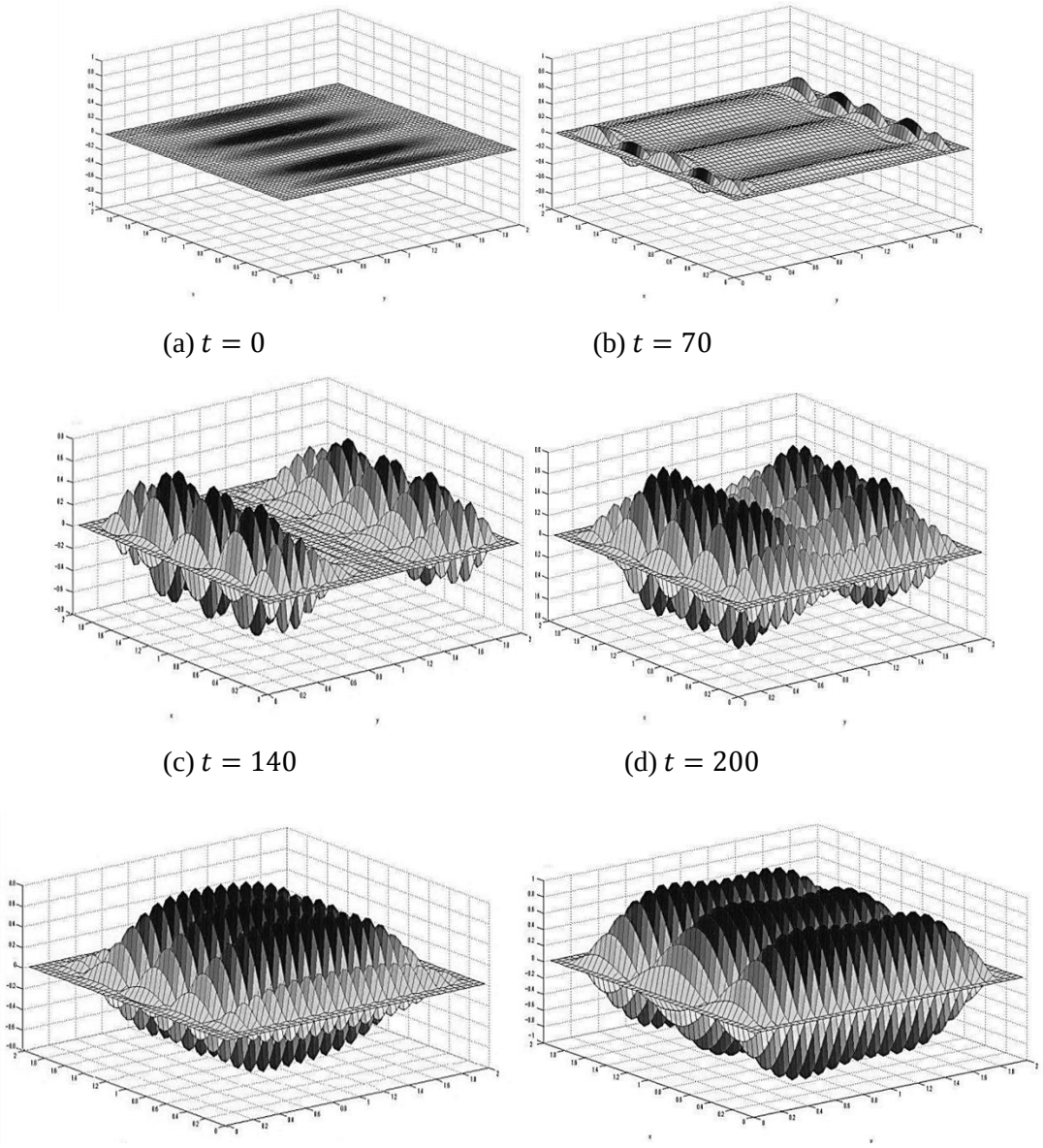

(a) $t = 0$ (b) $t = 70$

(c) $t = 140$ (d) $t = 200$

(e) $t = 270$ (f) $t = 340$

Figure.6.15: Dynamics for $k = 5$

***D*- Change of profiles by initial functions at $\mu = 90$**

In this section, as before we shall illustrate some numerical results to observe how change the profile of stationary solution by initial functions with $\mu = 90$. We treat (1.1) in the square domain $\Omega = (0,1) \times (0,1)$. We shall choose initial function as

$$u_0(x,y) = 0.1[\sin(3.14x) \times \sin(3.14ky)], \qquad (x,y) \in \Omega,$$

where k is a positive integer varying from 1 to5.

First, we apply $k = 1$ in initial function. The dynamics for the solution is illustrated by Figure 6.16. The small initial perturbation grows into a single column of ridges. The final profile of the trajectory is stabilized about time $t = 150$.

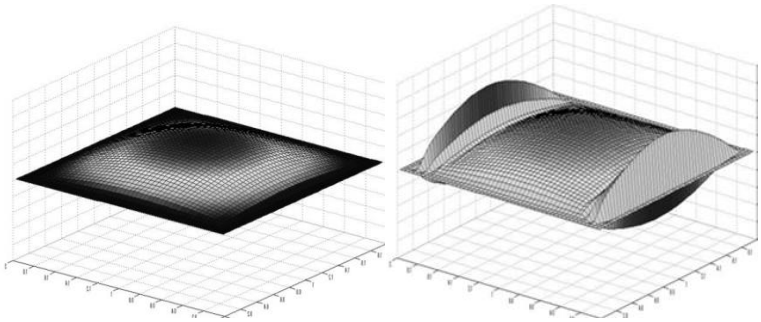

(a) $t = 0$ (b) $t = 50$

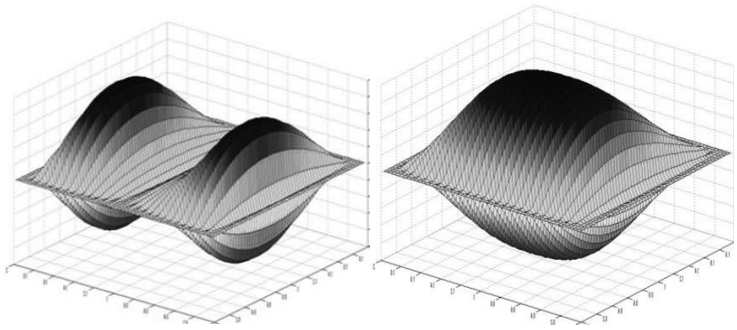

(c) $t = 100$ (d) $t = 150$

Figure.6.16: Dynamics for $k = 1$ in $\mu = 90$.

Secondly, we consider $k = 2$ in initial function. The small initial perturbation grows into a double column of ridges. The profile of the solution is stabilized about time $t = 200$. the dynamics for the solution is illustrated by Figure 6.17

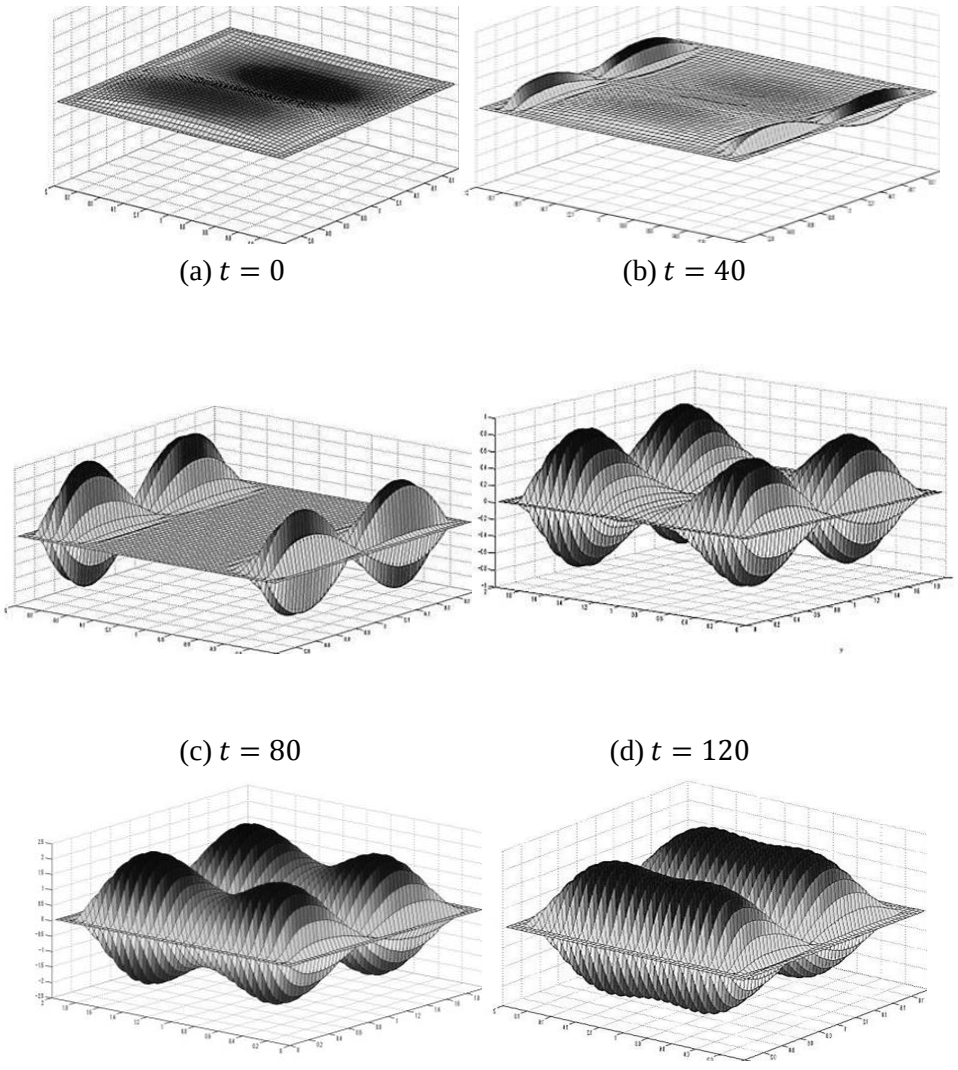

(a) $t = 0$ (b) $t = 40$

(c) $t = 80$ (d) $t = 120$

(e) $t = 160$ (f) $t = 200$

Figure.6.17: Dynamics for $k = 2$ in $\mu = 90$.

Thirdly, consider the case where $k = 3$. As seen by figure 6.18, the initial perturbation grows into triple columns of ridges. The profile of the solution is stabilized about time $t = 260$.

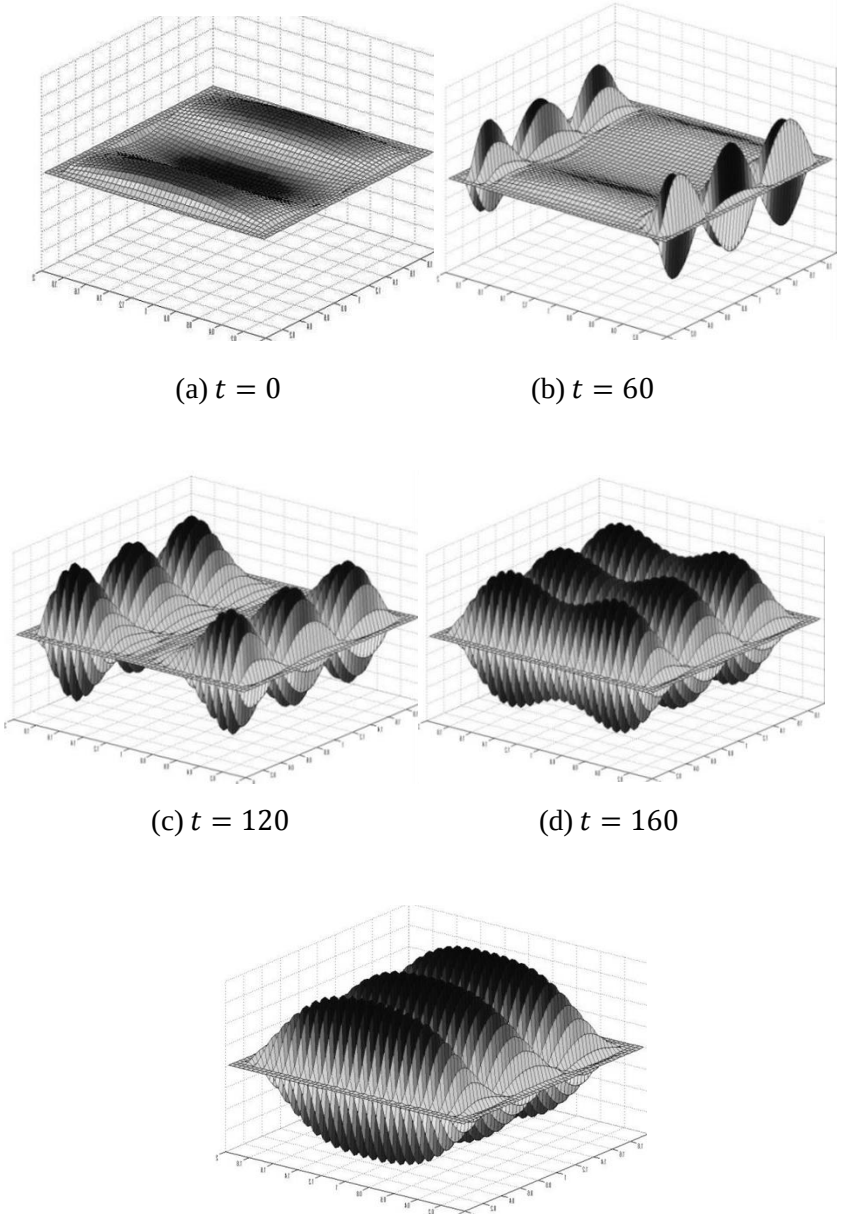

(a) $t = 0$ (b) $t = 60$

(c) $t = 120$ (d) $t = 160$

(e) $t = 260$

Figure.6.18: Dynamics for $k = 3$ in $\mu = 90$.

Next, we consider the case where $k = 4$ in the initial function. The initial perturbation grows into four columns of ridges. Notice that the profile is not the same as of the case where $k = 4$, in $\mu = 40$. In this case the state of fourth column becomes stable see Figure 6.19.

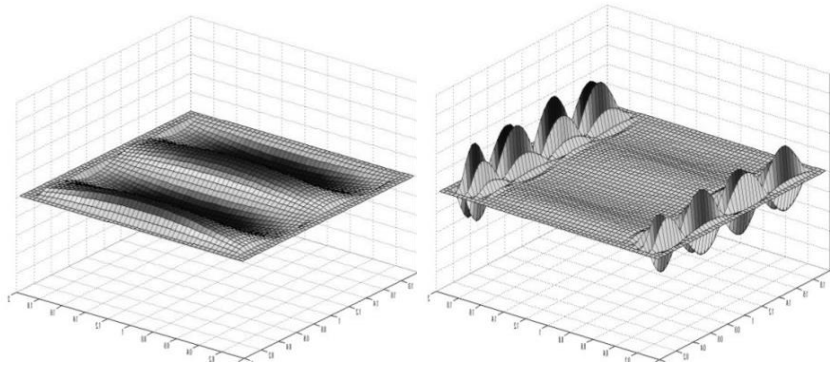

(a) $t = 0$ (b) $t = 80$

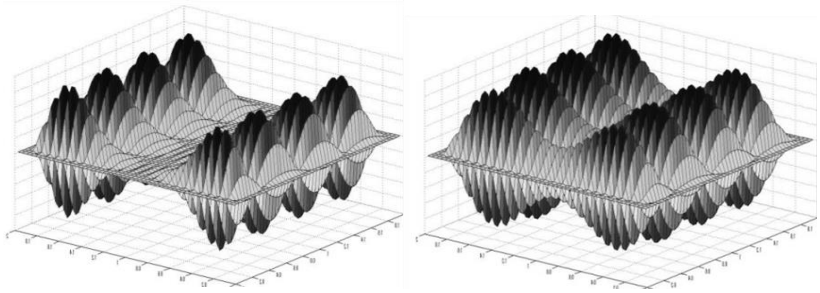

(c) $t = 160$ (d) $t = 250$

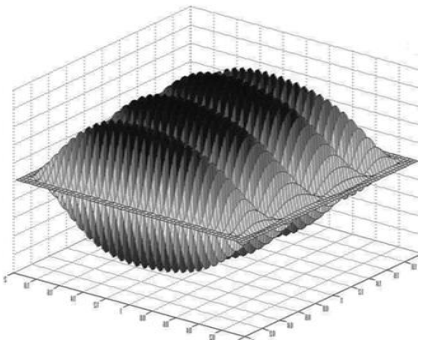

(e) $t = 330$

Figure.6.19: Dynamics for $k = 4$ in $\mu = 90$.

Finally, consider the case where $k = 5$ in the initial function. For a while, the small perturbation grows into five columns of ridges. Gradually, the state of fifth column becomes unstable. Ultimately, one column of ridges disappears and the trajectory converges to a stationary solution whose profile is the same as that of the case where $k = 4$, see Figure 6.20. The profile of the solution is stabilized about time $t = 360$. Numerical results of this indicate that the total number of the stationary solution at μ=90 is 4, and is more than of μ=40.

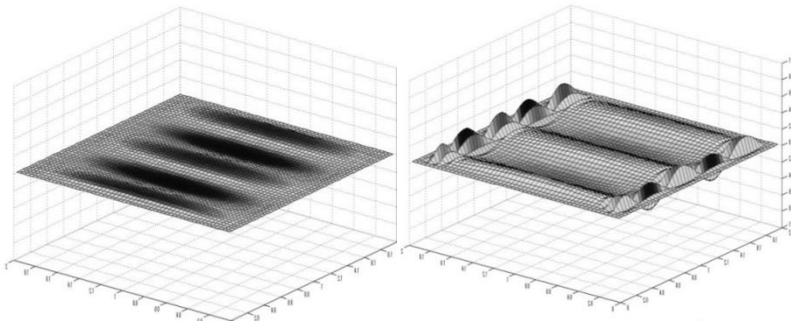

(a) $t = 0$ (b) $t = 90$

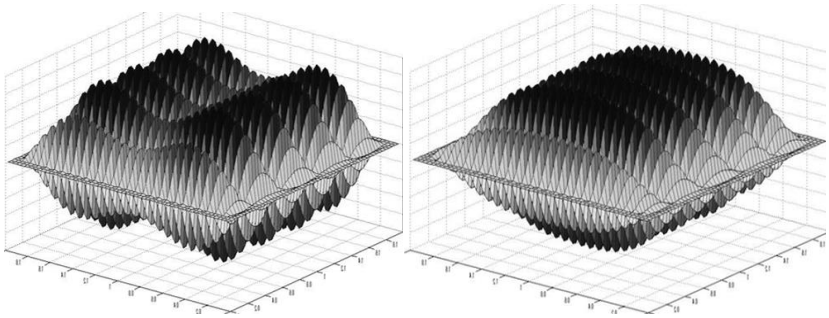

(c) $t = 180$ (d) $t = 270$

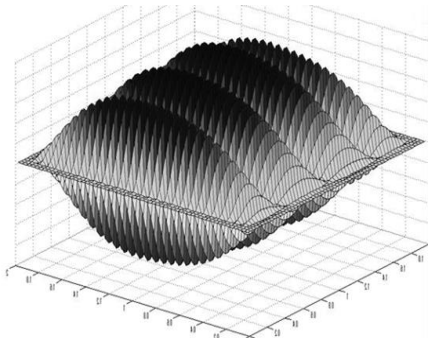

(e) $t = 360$

Figure.6.20: Dynamics for $k = 5$ in $\mu = 90$.

***E*- Change of profiles by initial function in rectangular domain**

In this section, we shall illustrate some numerical results to observe how change the profile of stationary solution by initial function in rectangular domain. For this, we consider (1.1) in the rectangular domain

$$\Omega = (0,1) \times (0,2).$$

The coefficients a and μ are fixed as $a = 1$ and $\mu = 90$, respectively. we shall choose initial function as

$$u_0(x,y) = 0.1[\sin(3.14kx) \times \sin(3.14y)], \qquad (x,y) \epsilon\, \Omega\,,$$

where k is a positive integer varying from 1 to 4.

First, we apply $k = 1$ in initial function. The dynamics for the solution is illustrated by Figure 6.21. The small initial perturbation grows into a single column of ridges. The final profile of the trajectory is stabilized about time $t = 200$.

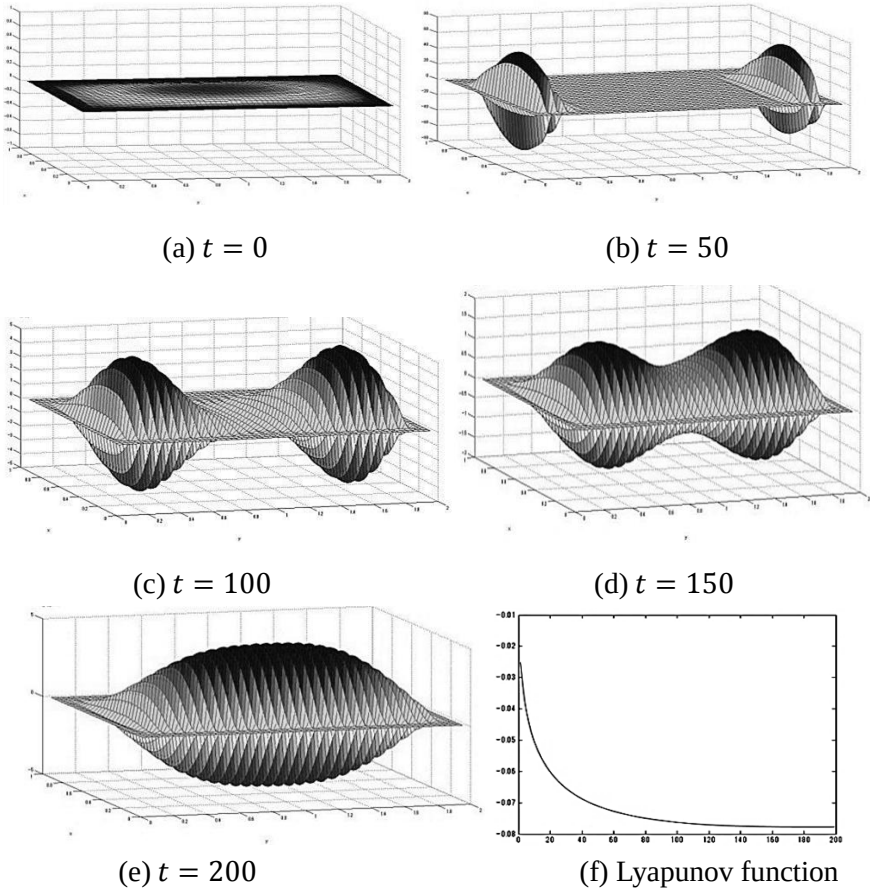

(a) $t = 0$ (b) $t = 50$

(c) $t = 100$ (d) $t = 150$

(e) $t = 200$ (f) Lyapunov function

Figure.6.21: Dynamics for $k = 1$ in rectangular domain.

Secondly, we consider $k = 2$ in initial function. The small initial perturbation grows into a double column of ridges. The profile of the solution is stabilized about time $t = 280$. The dynamics for the solution is illustrated by Figure 6.22. Figure 6.22(g) illustrates the graph of the Lyapunov function of trajectory.

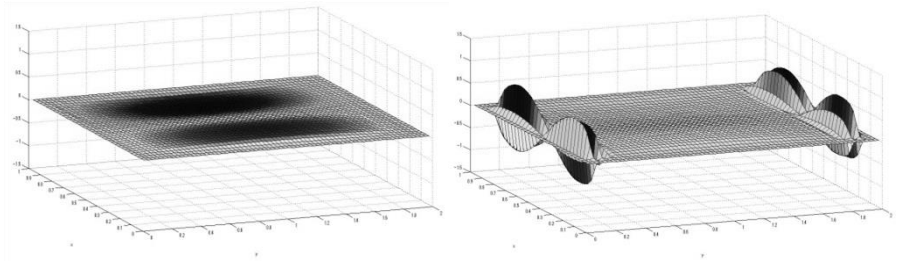

(a) $t = 0$ (b) $t = 40$

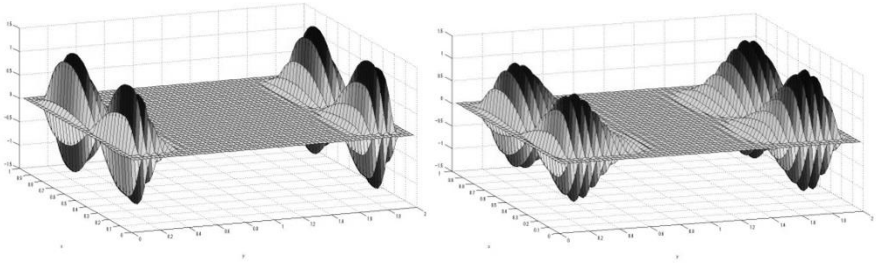

(c) $t = 80$ (d) $t = 160$

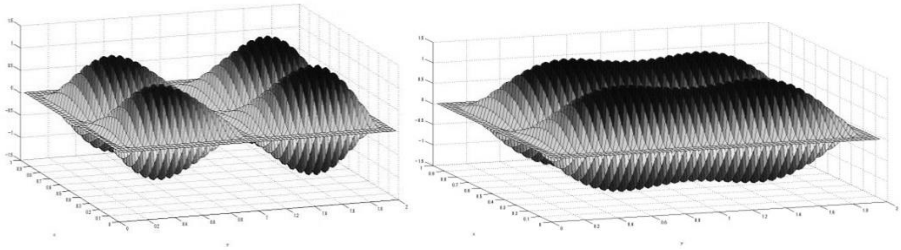

(e) $t = 240$ (f) $t = 280$

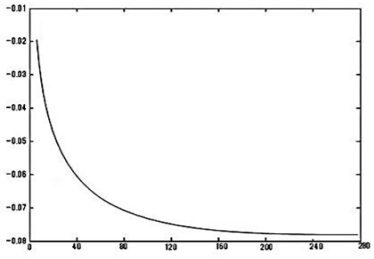

(g) Lyapunov function

Figure.6.22: Dynamics for $k = 2$ in rectangular domain.

Next, consider the case where $k = 3$ in initial function. For a while, the small perturbation grows into triple columns of ridges. Gradually, the state of third column becomes unstable. Ultimately, one column of ridges disappear and the trajectory converges to a stationary solution whose profile is the same as that of the case where $k = 2$, see Figure 6.23. The profile of the solution is stabilized about time $t = 350$. The graph of Lyapunov function is given by Figure 6.23(f).

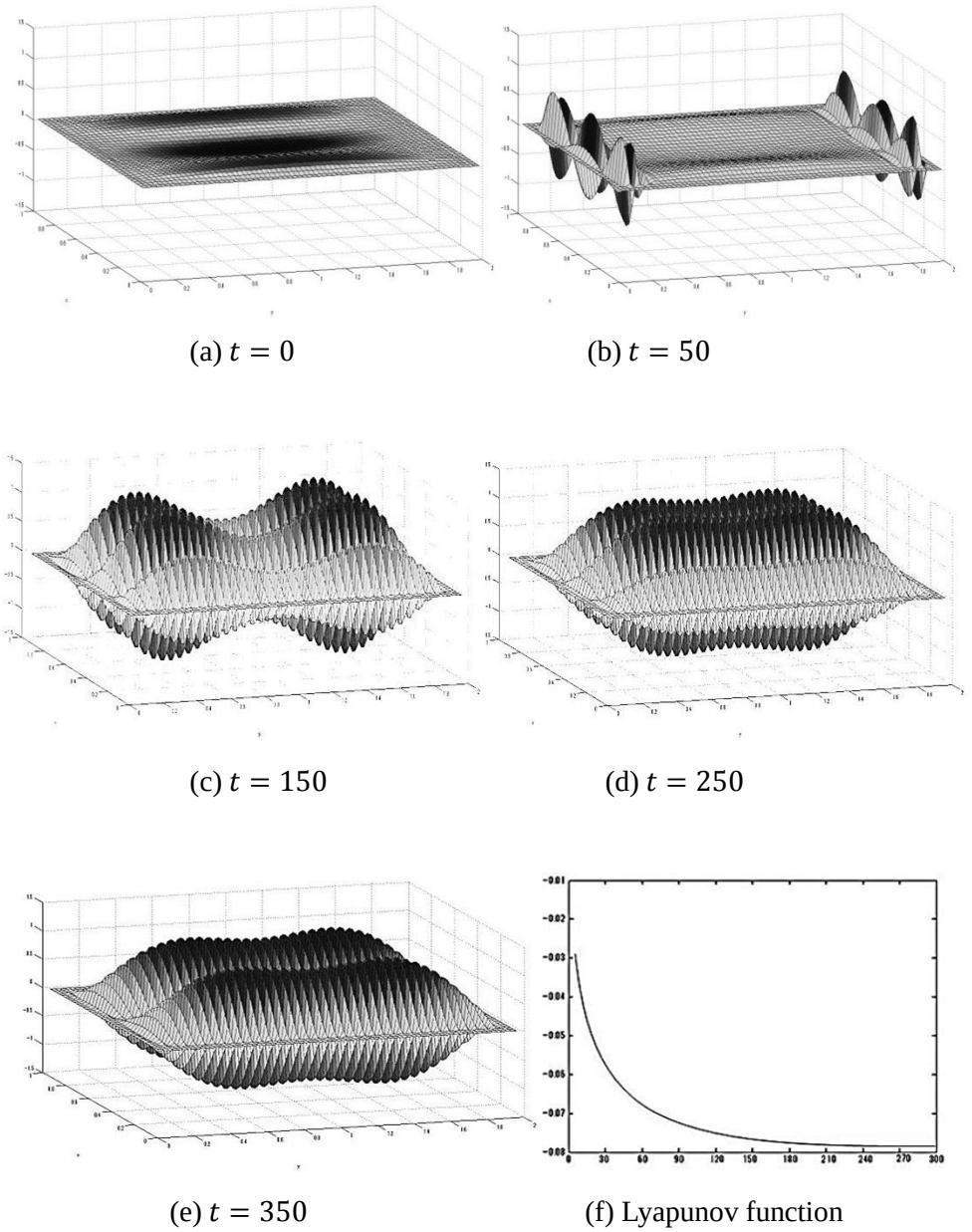

(a) $t = 0$ (b) $t = 50$

(c) $t = 150$ (d) $t = 250$

(e) $t = 350$ (f) Lyapunov function

Figure.6.23: Dynamics for $k = 3$ in rectangular domain.

Finally, consider the case where $k = 4$ in the initial function. Two columns of ridges disappear and the trajectory converges to a stationary solution whose profile is the same as that of the case where $k = 2$, see Figure 6. 24. Numerical results of this section indicate that the total number of the stationary solution at μ=90 in rectangular domain is 2.

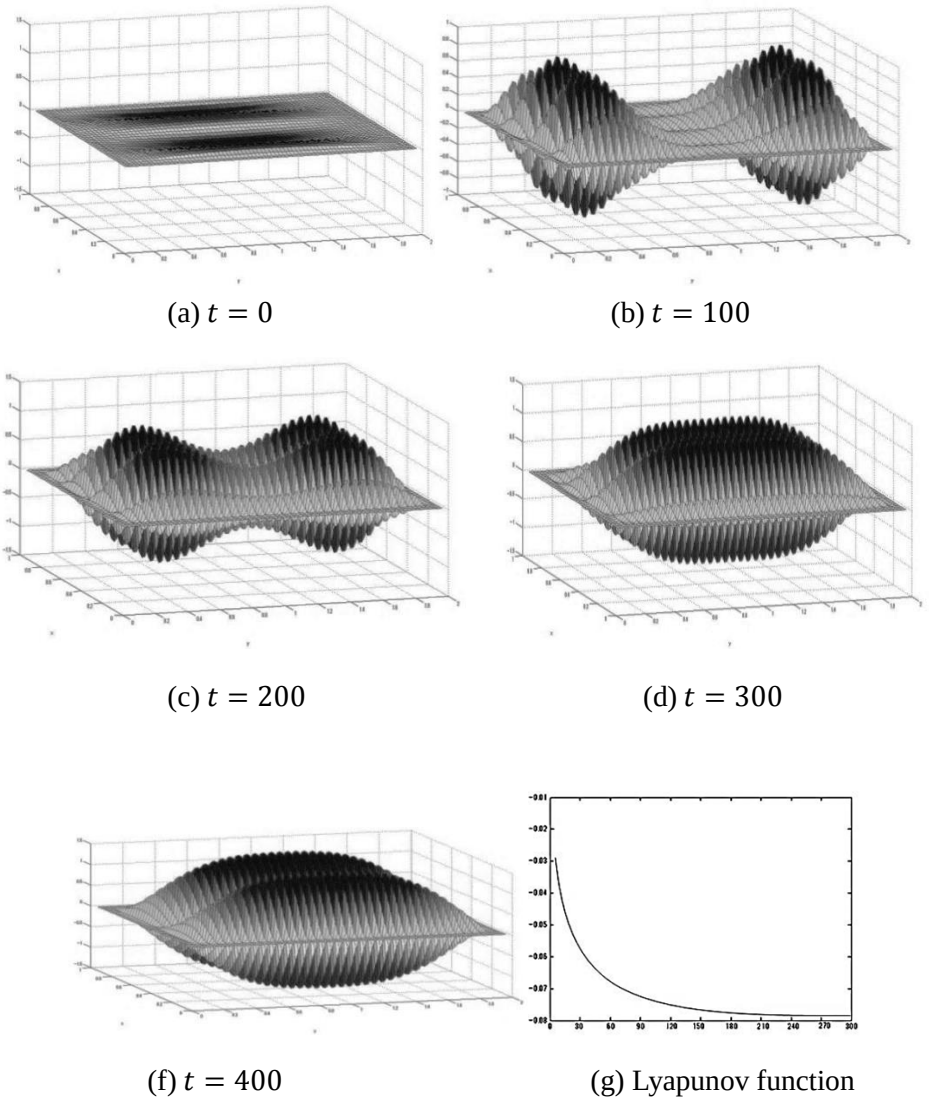

(a) $t = 0$ (b) $t = 100$

(c) $t = 200$ (d) $t = 300$

(f) $t = 400$ (g) Lyapunov function

Figure.6.24: Dynamics for $k = 4$ in rectangular domain.

***F*- Change of profiles by decreasing of rectangular domain**

In this section, we shall illustrate some numerical results to observe how change the profile of stationary solution by decrease domain in rectangular space. For this, we consider (1.1) in the one of the following rectangular domains

$$\Omega = (0, l) \times (0,2), \quad \text{where } l \text{ is } \frac{1}{2} \text{ or } 1.$$

The coefficients a and μ are fixed as $a = 1$ and $\mu = 90$, respectively.

Set first $\Omega = \left(0, \frac{1}{2}\right) \times (0,2)$. We also set the initial function as

$$u_0(x, y) = 0.1[\sin(3.14kx) \times \sin(3.14y)], \qquad (x, y) \epsilon\, \Omega\,,$$

where k is positive integer varying from 1 to 3. First, let $k = 1$ in the initial function. The dynamics of the solution is illustrated by Figure 6.25. The small initial perturbation grows into a single column of ridges. The final profile of the trajectory is stabilized about time $t = 240$. The graph of the Lyapunov function is given by Figure 6.25(f).

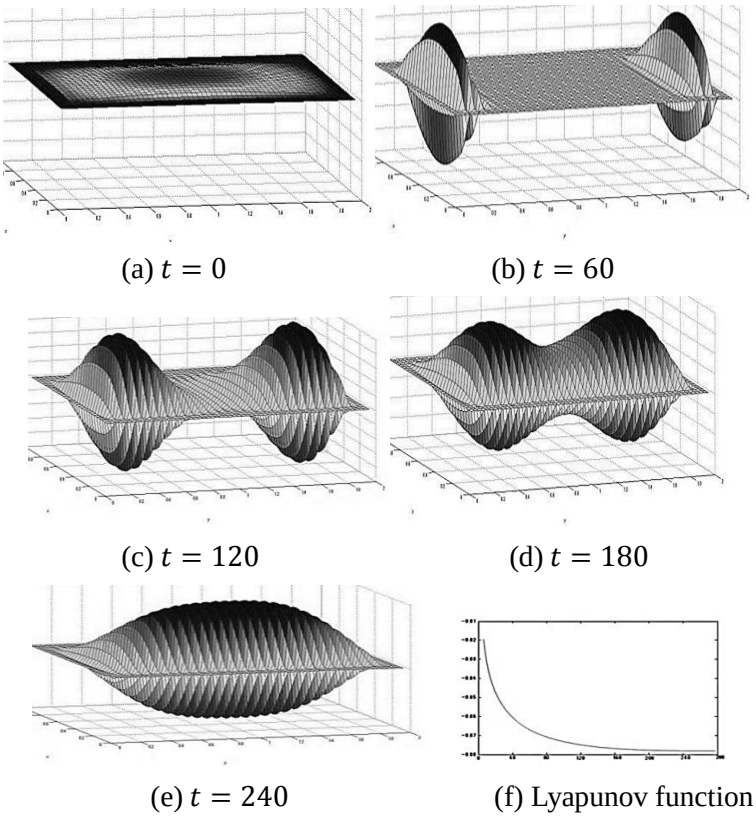

(a) $t = 0$ (b) $t = 60$

(c) $t = 120$ (d) $t = 180$

(e) $t = 240$ (f) Lyapunov function

Figure.6.25: Dynamics for $k = 1$ in $\Omega = \left(0, \frac{1}{2}\right) \times (0,2)$.

Secondly, let $k = 2$ in the initial function. As Figure 6.26 shows, for a while, the small initial perturbation grows into a double column of ridges. Gradually, the states of two columns become unstable. Ultimately, one column of ridges disappears and the trajectory converges to a stationary solution whose profile is the same as that of the case where $k = 1$. The final profile of the trajectory is stabilized about time $t = 300$.

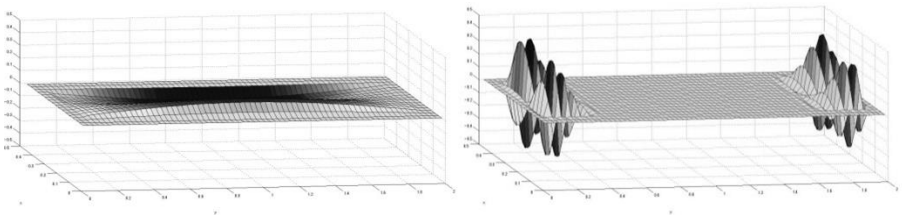

(a) $t = 0$ (b) $t = 60$

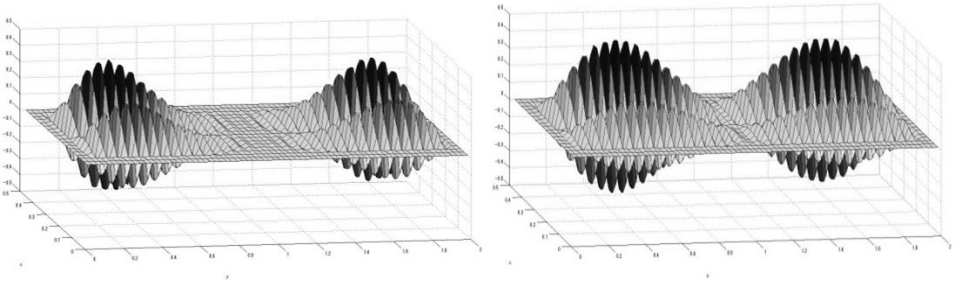

(c) $t = 120$ (d) $t = 180$

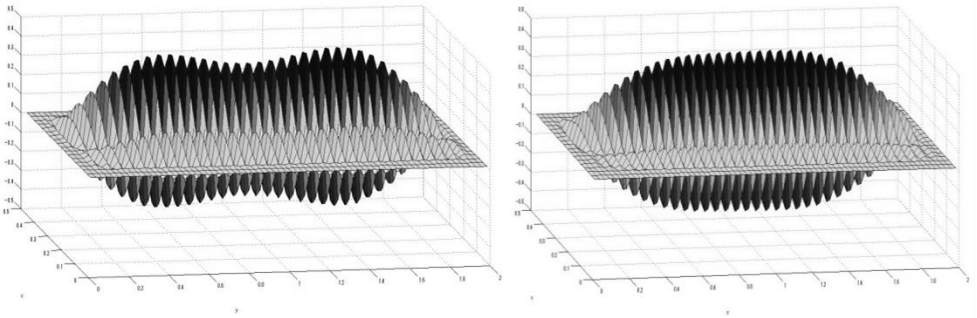

(d) $t = 240$ (b) $t = 280$

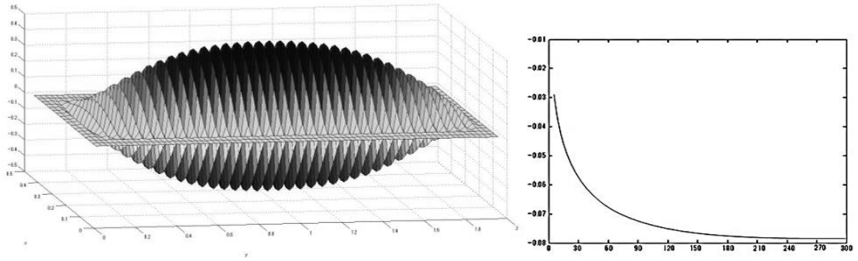

(e) $t = 300$ (f) Lyapunov function

Figure.6.26: Dynamics for $k = 2$ in $\Omega = \left(0, \frac{1}{2}\right) \times (0,2)$.

Thirdly, let $k = 3$ in the initial function. As Figure 6.27 shows, for a while, the small initial perturbation grows into a triple column of ridges. Gradually, the states of first and two columns become unstable. Ultimately, two columns of ridges disappear and the trajectory converges to a stationary solution whose profile is the same as that of the case where $k = 1$. The final profile of the trajectory is stabilized about time $t = 350$.

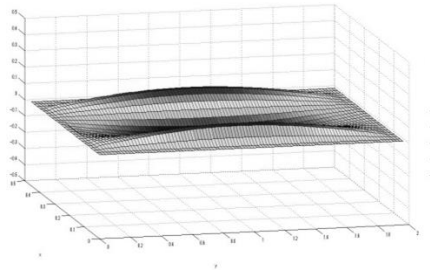

(a) $t = 0$

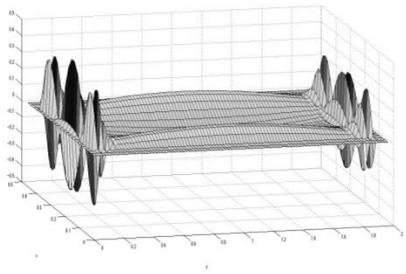

(b) $t = 70$

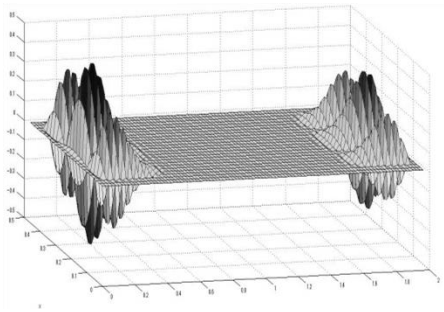

(c) $t = 140$

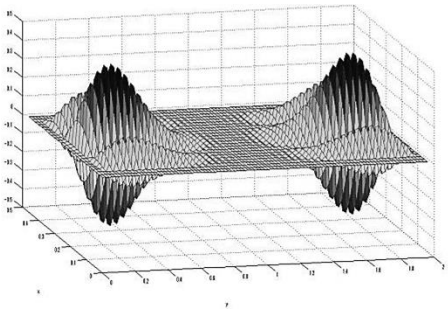

(d) $t = 210$

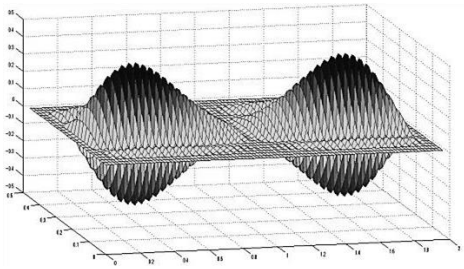

(e) $t = 250$

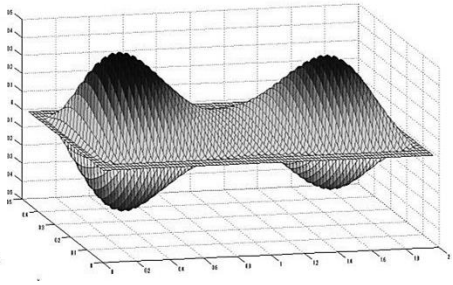

(f) $t = 270$

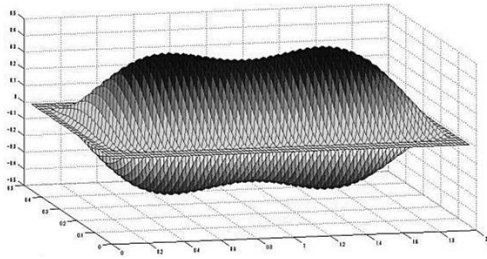

(g) $t = 300$

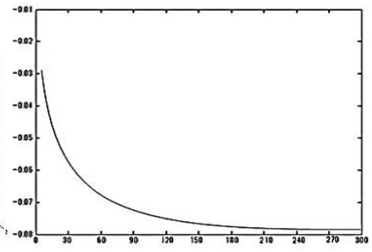

(h) Lyapunov function

Figure.6.27: Dynamics for $k = 3$ in $\Omega = \left(0, \frac{1}{2}\right) \times (0,2)$.

Set secondly $\Omega = (0,1) \times (0,2)$. We also set the initial function as

$$u_0(x,y) = 0.1[\sin(3.14kx) \times \sin(3.14y)], \qquad (x,y) \epsilon \Omega,$$

where k is a positive integer varying from 1 to 4.

First, let $k = 1$ in the initial function. The dynamics of the solution is illustrated by Figure 6. 28. The small initial perturbation grows into a single column of ridges.

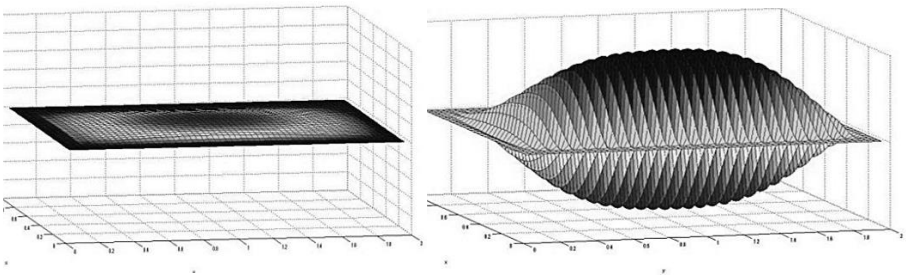

(a) $t = 0$ (b) $t = 240$

Figure.6.28: Dynamics for $k = 1$ in $\Omega = (0,1) \times (0,2)$.

Secondly, we consider $k = 2$ in initial function. The small initial perturbation grows into a double column of ridges. The profile of the solution is stabilized about time $t = 280$. The dynamics for the solution is illustrated by Figure 6. 29.

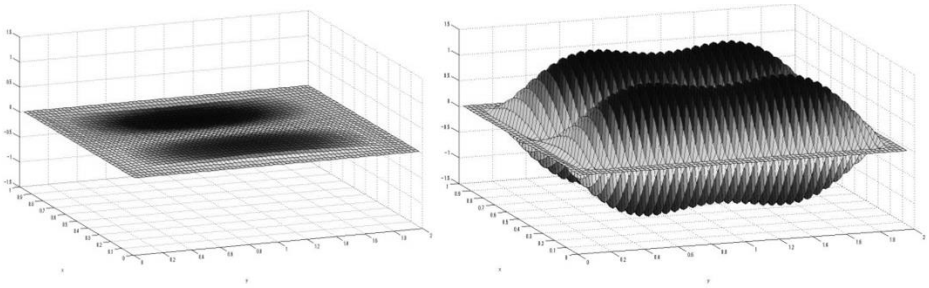

(a) $t = 0$ (b) $t = 280$

Figure.6.29: Dynamics for $k = 2$ in $\Omega = (0,1) \times (0,2)$.

Next, consider the case where $k = 3$ in initial function. For a while, the small perturbation grows into triple column of ridges. Gradually, the state of third column becomes unstable. Ultimately, one column of ridges disappears and the trajectory converges to a stationary solution whose profile is the same as that of the case where $k = 2,$ see Figure 6.30. The profile of the solution is stabilized about time $t = 350.$

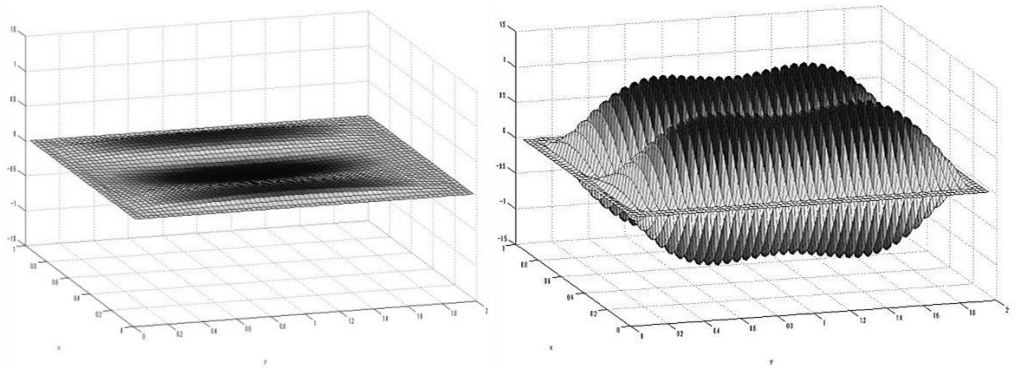

(a) $t = 0$ (b) $t = 350$

Figure.6.30: Dynamics for $k = 3$ in $\Omega = (0,1) \times (0,2)$.

Finally, consider the case where $k = 4$ in the initial function. Two columns of ridges disappear and the trajectory converges to a stationary solution whose profile is the same as that of the case where $k = 2,$ see Figure 6.31.

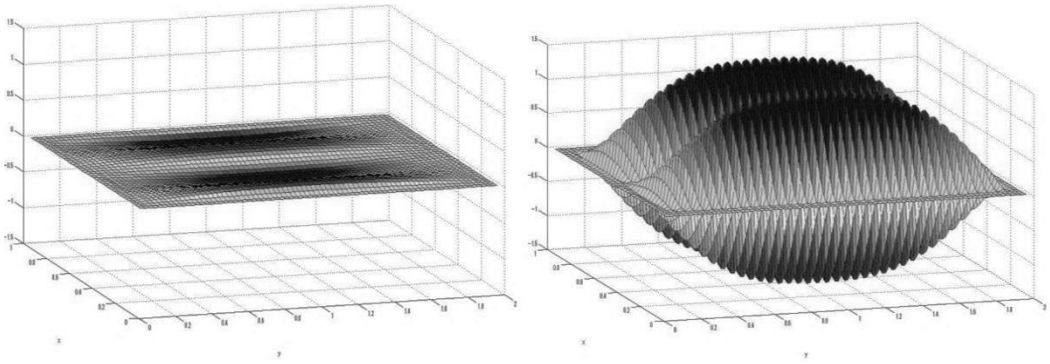

(a) $t = 0$ (b)$t = 400$

Figure.6.31: Dynamics for $k = 4$ in $\Omega = (0,1) \times (0,2)$.

Numerical results of this section indicate that the total number of the stationary solution in rectangular domain at μ=90 decreases.

***G*- Investigation of stability or instability of the null solution by controlling slenderness of domain**

In this section, we illustrate some numerical examples which show some agreements to corollary 5.1 in chapter 5. For this, we consider (1.1) in one of the following rectangular domains

$$\Omega = \left(0, \frac{1}{l}\right) \times (0, l), \quad \text{where } l \text{ is } 1,2 \text{ or } 4.$$

When $l = 1$, Ω is square. Otherwise, Ω is strictly rectangular. The area of Ω is constantly equal to 1. The coefficients a and μ are fixed as $a = 1$ and $\mu = 40$. Also the constant d is computed as $d \approx \frac{1}{\sqrt{2}\pi}$ (by. [Chapter 5, Theorem 5.4]).

Set first $\Omega = (0,1) \times (0,1)$. We also set the initial function as

$$u_0(x, y) = 0.1[\sin(3.14x) \times \sin(3.14y)], \qquad (x, y) \epsilon\, \Omega,$$

see Figure 6.32. This is a small perturbation of the null solution. The solution then converges to some non-null stationary solution as $t \to \infty$. Its profile is given by Figure 6.32 (d). This means that the null stationary solution is unstable.

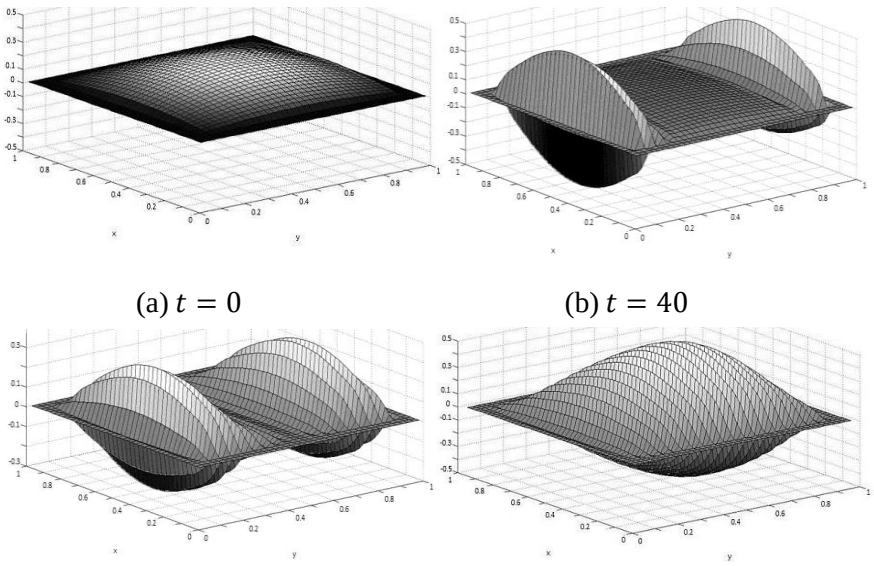

(a) $t = 0$ (b) $t = 40$

(c) $t = 80$ (d) $t = 120$

Figure.6.32: Case where $\Omega = (0,1) \times (0,1)$

Set secondly $\Omega = \left(0, \frac{1}{2}\right) \times (0,2)$, and the constant d is computed as $d \approx \frac{2}{\sqrt{17}\pi}$. We accordingly replace the initial function with

$$u_0(x, y) = 0.1[\sin(2 \cdot 3.14x) \times \sin(3.14y)], \qquad (x, y) \in \Omega,$$

see Figure 6.33. The solution again converges to some non-null stationary solution as $t \to \infty$ whose profile is given by Figure 6.33(e). This means that the null solution is still unstable.

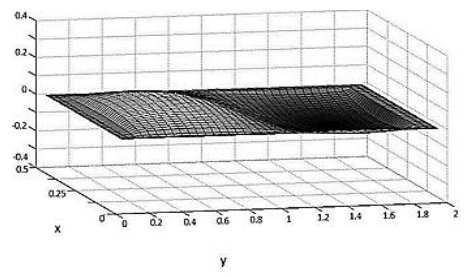

(a) $t = 0$

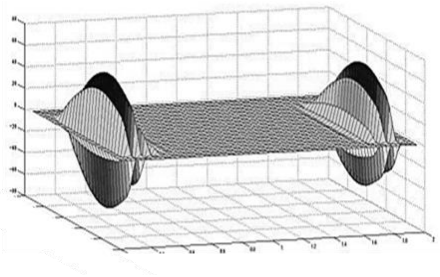

(b) $t = 20$

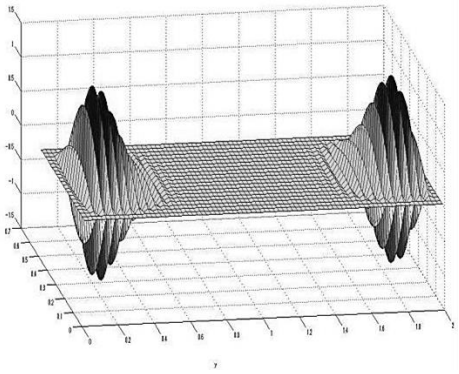

(c) $t = 40$

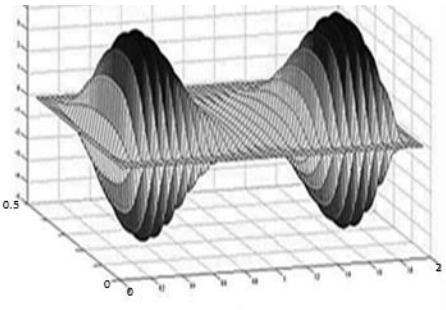

(d) $t = 80$

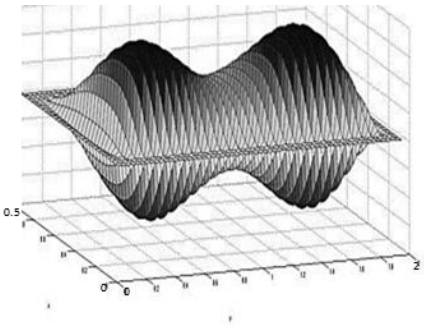

(d) $t = 120$

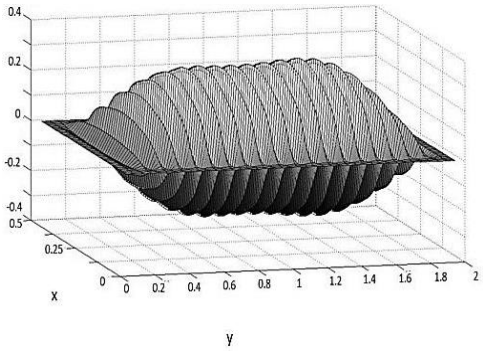

(e) $t = 180$

Figure.6.33: Case where $\Omega = \left(0, \frac{1}{2}\right) \times (0,2)$

Finally, set $\Omega = \left(0, \frac{1}{4}\right) \times (0,4)$. The constant d is computed as $d \approx \frac{4}{\sqrt{257}\pi}$ and replace the initial function with

$$u_0(x, y) = 0.1[\sin(4 \cdot 3.14x) \times \sin(3.14y)], \qquad (x, y) \epsilon\, \Omega,$$

see Figure 6.34. As seen by Figure 6.34(d), the solution now converges to the null solution. The domain Ω is slender enough to reduce the weight constant d in such a way that $d \leq \frac{l_1 l_2}{\pi \sqrt{l_1^2 + l_2^2}}$ (by [chapter 5, Theorem 5.4]) and to globally stabilized the null solution as ensured by Corollary 5.1 in chapter 5.

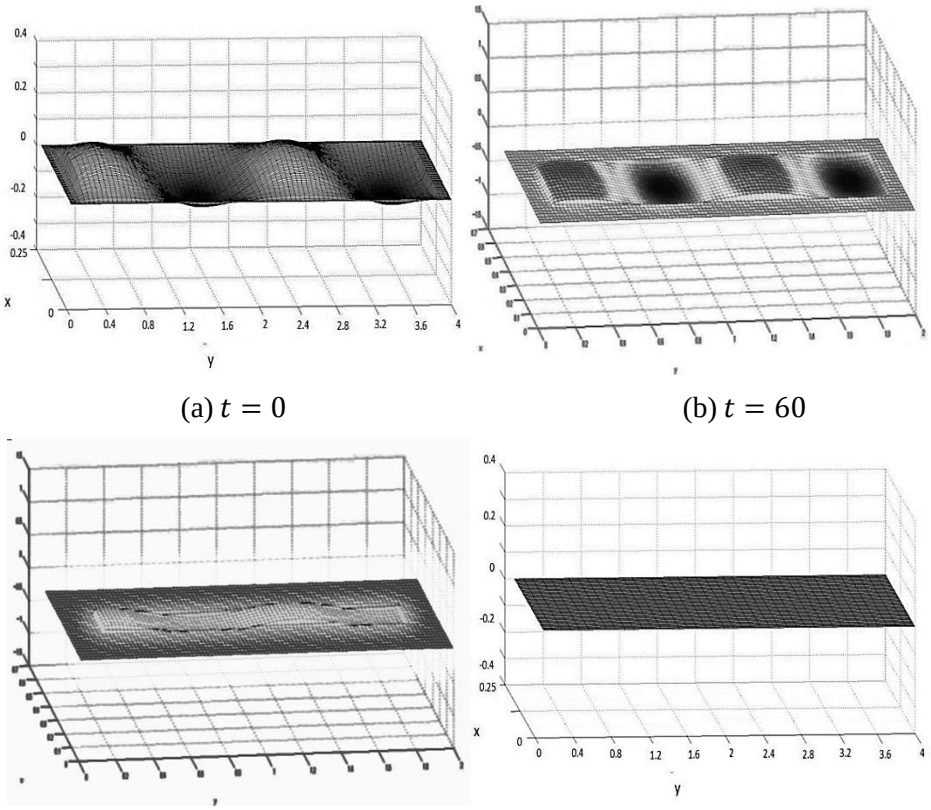

(a) $t = 0$ (b) $t = 60$

(c)$t = 120$ (d) $t = 240$

Figure.6.34: Case where $\Omega = \left(0, \frac{1}{4}\right) \times (0,4)$.

7

Conclusions

In the present thesis, we are concerned with the initial-boundary value problem for a nonlinear parabolic equation of fourth order in a two-dimensional bounded domain $\Omega \subset R^2$, Ω being a substrate domain. Such a problem has been presented by Johnson-Orme-Hunt-Graff-Sudijono-Sauder-Orr, in order to describe the process of growing crystal surface under Molecular Beam Epitaxy. MBE is one of useful techniques that enable us to grow structures with very high precision in the vertical direction. The model equation contains two terms describing a surface diffusion and a roughening effect caused from the Schwoebel barrier. Equipping the homogeneous Dirichlet boundary conditions, we studied the model equation analytically and numerically.

We have obtained the follow results:

- For any initial value $u_0 \in L_2(\Omega)$, there exists a unique global solution. For showing this, we used the general theory of abstract parabolic equations in infinite-dimensional spaces. The theory is available to the higher order semilinear parabolic equations, too. After providing global existence of solutions, we constructed a dynamical system generated by the problem and showed that the dynamical system possesses a Lyapunov function.

- Using the Lyapunov function, we succeeded in showing that every trajectory converges to some stationary solution as $t \to \infty$. Also, stationary solutions to which trajectories converge are dependent on initial functions.

- We investigated stability and instability of the null solution which is a unique homogenous stationary solution. When the surface diffusion is stronger than the roughening, the null solution is globally stable. In the meantime, when the roughening is stronger than the surface diffusion, the null solution becomes unstable.

- We made many numerical simulations to find that, when the null solution is unstable, non-null stationary solutions have a certain number of columns of ridges. When the roughening becomes stronger, the number of columns and the number of ridges in a column both increase.

References

[1] A. V. Babin and M. I. Vishik, *Attractors of evalution Equations*, North- Holland, Amsterdam, 1992.

[2] R. Dautray and J. L. Lions, *Mathematical Analaysis and Numerical Methods for Science and Technology*, Vol. 2, Springer- Verlag, Berlin, 1988.

[3] G. Ehrlich and F. G. Hudda, *Atomic view of surface self- diffusion: tungesten on tungesten*, J. Chem. Phys. 44(1966), 1039-1049.

[4] H. Fujimura and A. Yagi, *Dynamical system for BCF model describing crystal surface growth*, Vestnik Chelyabinsk Univ. Ser. 3 Mat. Mekh. Inform. 10 (2008), 75-88.

[5] H. Fujimura and A. Yagi, *Asymptotic behavior of solutions for BCF model describing crystal surface growth*, Int. Math. Forum 3 (2008), 1803– 1812.

[6] H. Fujimura and A. Yagi, *Homogeneous stationary solution for BCF model describing crystal surface growth*, Sci. Math. Jpn. 69(2009), 295-302.

[7] M. Grasselli, G. M. Mola and A. Yagi, *On the longtime behavior of solutions to a model for epitaxial growth*, Osaka J. Math. 48(2011), 987- 1004.

[8] M. D. Johnson, C. Orme, A.W. Hunt, D. Graff, J. Sudijono, L. M. Sauder and B. G. Orr, *Stable and unstable growth in molecular beam epitaxy*, Phys. Rev. Letter 72(1994), 116- 119.

[9] S. G. Krein, *Linear Differential Equations in Banach Space*, AMS, 1971.

[10] W. Mullins, *Theory of thermal grooving*, J. Applied Phys. 28 (1957), 333-339.

[11] R. L Schwoebel and E. J. Shipsey, *Step motion on crystal surface*, J. Appl. Phys. 37 (1966), 3682-3686.

[12] H. Tanaba, *Equations of Evaluation*, Iwanami Shoten, 1975 (in Japanese); English translation: Pitman, (1979).

[13] R. Temen, Infinite- *Dimensional Dynamical System in Mechanics and Physics*, 2nd ed., Springer- Verlag, Berlin, 1997.

[14] M. Uwaha, *Study on Mechanism of Crystal Growth*, Kyotisu Publisher, 2002 (in Japanese).

[15] A. Yagi, *Abstract Parabolic Evolution Equation and their Applications*, Springer, 2010.

[16] S.Azizi and A.Yagi, *Dynamical system for epitaxial growth model under Dirichlet conditions*, sci. Math. Jpn. (2015) .

[17] H. Tanabe, *Functional Analytic Methods for Partial Differential Equations*, Marcel Dekker, 1997.

[18] R. Chill, *TheLojasiewicz- Simon gradient inequality on Hibert space*, Proc, 5th European Maghrebian Workshop on Semigroup Theory, Evolution Equations and Applications, 2006, 25-36.

[19] H. Cartan, *Course de calcul Differential*, Herman 1967.

[20] S.Azizi, G. Mola, and A. Yagi, *Longtime convergence for epitaxial growth model under Dirichlet conditions,*sci. to appear .

[21] A .W. Hunt, *Instability in MBE growth,* A. W. [Hunt]. Europhys. Lett. 1994, Vol. 27. P. 611-616.

[22] R.A. Swalin, *Thermodynamics of solids*. New York: John Wiley & Sons, 1972.

[23] W. K. Burton , *The growth of crystals and the equilibrium structure of their surface,* Royal Soc. London 1951. Vol. 27. P. 299-358.

[24] O. Pierre- Louis, *New nonlinear evolution equation for steps during molecular beam epitaxy on vicional surface*. Phys. Rev. Lett. Vol.80. P. 4221-4224.

[25] M. Rost, *Coarsening of surface structures in unstable epitaxial growth.* Phys. Rev. Lett. E.1997. Vol. 55. P. 3952-3957.

[26] M. Rost, Unstable epitaxy on vicinal surface science. 1996. Vol. 369. P. 393-402.

[27] K. Osaki, A. Yagi, *Global existence for a chemotaxis- growth system in* $\mathbb{R}^2$, Adv. Math. Sci. Appl. 2002. Vol. 12. P. 587-606.

[28] P. Grisvard, *Eliptic Problems in Nonsmooth Domains*, London : Pitman, 1985.

[29] H.Trieble, *Interpolation Theory, Function spaces, Differential Operators*, Amestrdam: North- Holland, 1978.

[30] H. Brezis, *Analyse founctionnell, theorie at applications*, Paris: Masson, 1983.

[31] M. Aida, T. Tsujikawa, M. Efendiev, A. Yagi and M. Mimura, *Lower estimate of attractor dimension for chemotaxis growth system*, J. London Math. Soc. 74 (2006). P. 453-474.

[32] A. Yagi, $\mathcal{H}_\infty$ *functional calculus and charactrization of domain of functional power*, Proc. 17th Conference on " Operator Theory and Applications", Brikhauser, Basel, 2008, 217-235.

[33] F.A. Kroger, *The Chemistry of Imperfect Crystals*, vol. 1. Amsterdam, Netherlands: North Holland Publishing Company, 1973.

[34] S. Gonda and Y. Matsushima, *Molecular beam epitaxy of GaP and GaAsP,* Jap. J. Appl. Phys., vol. 15, no. 11, pp. 2093{2101, 1976.

[35] P.S. Kop'ev and N.N. Ledentsov, *Molecular beam epitaxy of heterostructures made of III/V compounds,* Sov. Phys. Semicond., vol. 22, no. 10, 1093 pp. 1101, 1988.

[36] H. Amann, *Linear and Quasilinear Parabolic Problems* , BirkhÄauser, Basel, 1995.

[37] E. BÄansch, P. Morin, R. Nochetto, *Surface diffusion of graphs: Variational formulation, error analysis, and simulation*, SIAM J. Numer. Anal. 42 (2004), 773-799.

[38] E. BÄansch, P. Morin, R. Nochetto, *Finite element methods for surface diffusion*, in: P.Colli, C.Verdi, A.Visinti, eds., Free boundary problems, Int. Ser. Num. Math. 147 BirkhÄauser, Basel, 2003, 5363.

[39] P. Baras, J. Duchon, R. Robert, *Evolution d'une interface par diffusionde surface*, Comm. Partial Diff. Eq. 9 (1984), 313-335.

[40] A.J. Bernoff, A. L. Bertozzi, T.P. Witelski, *Axisymmetric surface diffusion: Dynamics and stability of self-similar pinchoff*, J. Stat. Phys. 93(1998), 725-776.

[41] B. D. Coleman, R.S. Falk, M. Moakher, *Space-time finite element methods for surface diffusion with applications to the theory of the stability of cylinders*, SIAM J. Sci. Comp. 17 (1996), 1434-1448.

[42] F. Davi, M.E. Gurtin, *On the motion of a phase interface by surface diffusion*, J. Appl.Math. Phys. 41 (1990), 782-811.

[43] K. Deckelnick, G. Dziuk, C.M. Elliott, *Fully discrete semi-implicit second order splitting for anisotropic surface diffusion of graphs*, Preprint (Isaac Newton Institute, Cambridge, 2003).

[44] K. Deimling, *Nonlinear Functional Analysis* (Springer, Berlin, 1985).

[45] C.M. Elliott, H. Garcke, *Existence results for diffusive surface motion laws*, Adv. Math. Sci. Appl. 7 (1997), 465488.

[46] V.Lods, A.Pietrus, J.M.Rakotoson, *Mathematical study of the equation describing the evolution of the surface of a film*, Asymptotic Analysis 33 (2003), 67-91.

[47] U.F. Mayer, *Numerical solutions for the surface diffusion flow in three space dimensions*, Comput. Appl. Math. 20 (2001), 361-379.

[48] J.E. Taylor, *Some mathematical challenges in materials science*, Bull. Amer. Math. Soc. 40 (2002), 69-87.

[49] H. Gao, W. D. Nix, *Surface roughening of heteroepitaxial thin films* 29 (1999), 173-209.

[50] R. L. Schwoebel, J. Appl. Phys. 40(1969)614.

[51] Y. Saito, *Statistical Physics of Crystal Growth*, World Scientific, 1996.

[52] N. Ohtani, M. Katsuno, T. Aigo, T. Fujimoto, H. Tsuge et. al., J. *Crystal Growth* 210 (2000) 613.

[53] T. Michely and Krug J 2003 Islands, Mounds, and Atoms: *Patterns and Processes in Crystal Growth Far from Equilibrium* (Berlin: SpringerVerlag).

[54] M. C. Bartelt, *Kinetic modelling of epitaxial fillm growth* , Surface Science 1999, 423, 189207.

[55] X. Guoliang, Q. Pan, and C. Bajaj, *Discrete surface modelling using partial differential equations. Computer Aided Geometric Design*, 23(2):125–145, 2006.

[55] G. Wheeler, *Fourth order geometric evolution equations*, Bulletin of the Australian Mathematical Society, 82(03):523–524, 2010.

[56] M. Bloor and M. Wilson, *Using partial differential equations to generate free-form surfaces*. Computer-Aided Design, 22(4):202–212, 1990.

[57] G. Wheeler. *Gap phenomena for a class of fourth-order geometric differential operators on surfaces with boundary*. arXiv preprint arXiv:1302.4165, 2013.

Publications

1. **Somayyeh Azizi**, AtsushiYagi: *Dynamical system for epitaxial growth model under Dirichlet conditions,* Sci. Math. Jpn., accepted for publication.
2. **Somayyeh Azizi**, G. M. Mola and Atsushi Yagi, *Longtime convergence for epitaxial growth model under Dirichlet conditions,* to appear.
3. **Somayyeh Azizi**, Atsushi Yagi: *Homogeneous stationary solution to epitaxial growth model under Dirichlet conditions,* Sci. Math. Jpn., accepted for publication.

Conferences

1. **S. Azizi**, *A mathematical model for surface dynamic of growing crystal*: International conference on atomically controlled fabrication technology, February 5-6 2014, Osaka, japan.
2. **S. Azizi**, *One dimensional simulation of growing crystal under molecular beam epitaxy*: 3rd international conference on Advances in mathematical applications in Engineering, September 23-25 -2014, Kuala lumpur, Malaysia
3. **S. Azizi**, *Mathematical Analysis and Numerical Computation for Describing Crystal Surface Growth*: 7th International Symposium on Surface Science, November 2-6. 2014, , Matsue, Shimane, Japan
4. **S. Azizi**, *Evolutionary distance in the yeast genome*. ICCBGES 2013: international conference on genome evolution and speciation. 14-15 Jan. 2013, Zurich, Switzerland

Award

International conference on atomically controlled fabrication technology, February 5-6 2014, Osaka, japan. (Top First Poster Presentation Award)

Acknowledgements

I would like to express my sincere gratitude to my advisor Prof. Atsushi Yagi for the continuous support of my Ph.D. study and related research, for his patience, motivation, and immense knowledge and for his constant encouragement. His guidance helped me in all the time of research and writing of this thesis. I owe him more gratitude than I can express. I have learned a lot of things in various phases from him.

I would also like to express my thanks to professors Yoshitada Morikawa, Yuji Kuwahara and Yoshitaka Yamamoto for carefully reading this thesis, and I am gratefully indebted to them for their very valuable comments and suggestions.

Finally, I must express my very profound gratitude to my husband for unconditional support in all time of my Ph.D. study.